INSTITUTO NACIONAL DE TECNICA AEROESPACIAL

"ESTEBAN TERRADAS"

MADRID, SPAIN

O P E N F I R E S

A N D

T R A N S P O R T O F F I R E B R A N D S

Principal Investigator

C. Sánchez Tarifa

Colaborators:

P. Pérez del Notario

F. García Moreno

A. Liñán Martínez

A. Bollain Sánchez

MAY 31, 1963 - MAY 31, 1964

OPEN FIRES AND TRANSPORTS OF FIREBRANDS

- - -- - - - -

SUMMARY

a) Open Fires

During the report period the research work on Open Fires has been dedicated to the continuation of the experimental and theoretical studies on burning rates, and to the development of a new model of the fire.

Normal heptane and a mixture of dioxane and water have been used as fuels and pools of 25 and 50 cm in diameter have been utilized.

Variables of the process have been the overflow rate for the case of the normal heptane and the proportion of water for the case of dioxane.

It is shown that the experimental and theoretical results, obtained according to the fire model developed in Second Annual Report are in a better agreement when the pool of 50 cm is used, for small overflow rates and when the proportions of water in dioxane are small. These results are explained by considering that in the model only heat transferred through radiation was considered which is the dominant heat transfer mechanism as the flame size increases.

A new model of the fire has been developed, which consists in assuming that the flame behaves as a fixed volume of gas at uniform temperature. It is expected that this model will permit a quantitative study of the distribution of the heat transferred to the fuel surface between radiant and conductive heats. It will also be used to establish a general balance of energy of the fire.

b) Transport of Firebrands

During the report period the research work on transport of firebrands has been dedicated to the continuation of the theoretical and experimental studies on flight paths and burning lifetimes of firebrands.

Spherical and cylindrical firebrands have been studied for five kinds of wood and for several initial

sizes. Terminal velocities of fall have been directly measured by using two wind tunnels. From their values the flight paths and burning-out times of the firebrands have been calculated for several convection columns models and for different wind conditions.

Several interesting conclusions have been drawn regarding to the most dangerous types of firebrands according to size, shape, kind of wood and moisture content.

A new type of strain-gauges balance has been designed and constructed for the large wind tunnel.

A study has been recently initiated directed to the attainments of the laws governing combustion of wood particles under forced convection conditions.

From these laws it is expected to derive general expressions giving the flight paths and lifetimes of the firebrands as well as the scaling laws of these process.

= = = = = = = = =

I - OPEN FIRES

I.1 Introduction

The research work performed on Open Fires during the report period may be divided as follows:

a) Continuation of the theoretical and experimental studies along the lines shown in Second Annual Report.

b) Study and development of a model of the fire.

The research work on Open Fires is being conducted by using the pool-fire technique with overflow system. The model of the process which is being utilized is as follows:

1 - A certain amount of heat $\dot{Q}_s$ is transmitted from the flame to the fuel surface per unit area and per unit time.

2 - An energy balance is established in the liquid phase which gives the burning rate and the temperature profiles within the fuel, once the overflow rate is given.

No assumption was made on the value of $\dot{Q}_s$ or on the heat transfer mechanism. Afterwards, $\dot{Q}_s$ was roughly measured by placing radiometers around the fire and by assuming that the heat was transmitted to the fuel exclusively through radiation.

From this value of $\dot{Q}_s$ it is possible to calculate the burning rate of fuel, which in turn can be measured directly. A comparison of both values was made and results shown in Second Annual Report were in fair agreement.

The research work has been continued along this lines. Results have been obtained using as fuels n-heptane, dioxane and a mixture of dioxane and 25% - 50% of water. Two pools have been used of 25 and 50 cm in diameter and results for several values of the overflow rate have been obtained. Theoretical calculations have been also continued as well as comparisons between theoretical and experimental results.

Furthermore, a model of the fire is being developed which gives the value of this heat transferred $\dot{Q}_s$ as well as its distribution between radiant and convective heat.

The model is essentially based in assuming that the flame behaves as a certain volume of gas of uniform temperature, which has a fixed geometrical shape.

This model seems to be very promising because it also gives some interesting relations among several of the more important variables of the process.

I-2 Theoretical Studies on Burning Rates

In Seoond Annual Report expressions were derived giving the stationary values of the dimensionless burning rate:

$$\dot{\nu} = a^2 X_s V \qquad (1)$$

and of the temperature profiles $\theta = f(\delta)$

$$\theta = \frac{T}{T_s} \qquad (2)$$

$$\delta = \frac{X}{X_s} \qquad (3)$$

as functions of the dimensionless heat χ_s received by the fuel per unit time and per unit surface:

$$\chi_s = \frac{Q_s X_s}{\lambda T_s} \qquad (4)$$

and as a function of the dimensionless latent heat of evaporation χ_1 :

$$\chi_1 = \frac{q_1}{T_s c} \qquad (5)$$

Such expressions were:

$$\nu = \frac{1}{\xi \chi_1}\left(\chi_s - \nu_e{}^{\nu} \frac{1 - \theta_o}{e^{\nu} - 1}\right) \qquad (6)$$

and:

$$\theta = 1 - (1 - \theta_o) \frac{e^{\nu} - e^{\nu\delta}}{e^{\nu} - 1} \qquad (7)$$

in which,

$$\theta_o = \frac{T_o}{T_s} \qquad (8)$$

$$\xi = \frac{\dot{m}_b}{\dot{m}} \qquad (9)$$

Since the values of ν and θ will have to be used very frequently and compared with experimental results for different values of the parameters, a series of diagrams were prepared giving the values of $\nu = f(\chi_s)$ and $\theta = f(\delta)$ for the following values of the parameters:

$$\xi \chi_1 = 0.15,\ 0.30,\ 0.45,\ 0.60,\ 0.75$$

$$\theta_o = 0.2\ ,\ 0.4\ ,\ 0.6\ ,\ 0.8\ ,\ 1.0$$

Results have been resumed in six figures (1 through 6) and from them the actual dimensional values of the burning rate and of the temperature may be readily obtained.

I-3. Experimental Results

The experimental investigation on Open Fires is being conducted according to the procedures exposed in Second Annual Report.

Burning rates, fuel temperatures, radiant heat emitted by the flame, flame length, flame lateral surface and flame temperatures have been measured for n-heptane and different values of ξ (ξ = 0.25, 0.69, 0.71, 0.89, 0.91 and 1.0) using vessels of 25 and 50 cm in diameter. The same measurements have been performed with dioxane with 25 and 50% of water (ξ = 0.059, 0.118, 0.22, 0.35 and 1.0).

Until now, the main purpose of this research program has been to verify the theoretical values of the burning rates obtained according to the method described in Second Annual Report.

By changing the overflow rate, it is possible to vary in a continuous way the properties of the flame, specially its size. In the same form, by modifying the amount of water mixed with dioxane, it is also possible to vary continuously the properties of the dioxane flame, specially the ratio q_r/q_l which is a fundamental parameter in connection with flame properties.

By utilizing the model of the fire described in I-4, these measurements will be also used to study the energy balance of a fire and to calculate the total heat transferred to the fuel surface as well as its distribution between radiant and conductive heat.

also explained by considering that the flame becomes smaller as the proportion of water mixed with the dioxane increases.

Results are now being obtained for proportions of water of 15% , 35% and 50% for $\xi = 1$, which will be analized by using the theoretical model described in the following paragraph.

I.4 Open Fires. A Model of the Fire

In order to estimate the over-all thermal balance of a fire and the distribution of heat transfer between convective and radiant heat, a model of the fire has been developed based upon the following assumptions:

a) Turbulent flame
b) Stationary conditions (mean values)
c) The flame (luminous region) is assumed to be constituted by a volume of gases of uniform temperature.
d) The flame, for a circular burner, is assumed to be of conical or cylindrical shape, as shown in Fig. 12 with a conical mass of fuel vapors in its lower region. The geometrical configuration of the flame depends on four parameters which are experimentally determined.

From direct observations of pool fires it has been concluded that the flames have an inner core of fuel vapors immediately above the fuel surface which has approximately a conical shape[3] . The temperature within

that zone is small as compared to the flame temperature and its absortion coefficient is practically negligeable.

The inner core exists in both laminar and turbulent flames. In the laminar flame produced by a small burner, the inner core is large and the ratio $Z_{v,max}/D$ of its height to the burner diameter may reach considerable values[4].

On the other hand, for large burners the flame is turbulent, the air is entrained towards the center of the burner and the ratio $Z_{v,max}/D$ reduces considerably.

The situation changes considerably for the case of the flame produced by a gas jet. In this case the fuel is forced towards the combustion region and that inner core, which also exists, is very large [4].

Temperature profiles across a turbulent flame may be approximated by means of "top hat" profiles, since temperature changes abruptly in the boundaries of the luminous region and it does not change very much within the flame. Furthermore, in the longitudinal direction the temperature of a turbulent flame changes little also. Therefore the flame will be considered as a volume of gas at uniform temperature.

This model allows the calculation of the heat transferred through conduction $\dot{Q}_{cf}$ and through radiation $\dot{Q}_{rf}$ from the flame to the fuel. It also relates the mean flame temperature with the burning rate, once the air entrainment coefficient is given.

I.5 Heat Transfer through Conduction

The value $\dot{q}_{cf}$ of the heat reaching the fuel surface per unit area and per unit time through conduction will be calculated by assuming that the motion of the fuel vapors within the inner cone is one-dimensional and that the heat transferred towards the Y direction is negligeable as compared to the heat transferred towards the Z direction.

The equation of energy which governs the heat transport phenomenon is:

$$v \frac{dT}{dZ} = \frac{\lambda}{\rho c} \frac{d^2 T}{dZ^2} \qquad (10)$$

Introducing dimensionless variables and using subscript v to denote fuel vapor or inner cone region, we have:

$$\frac{d^2 \theta_v}{d \delta_v} - \nu_v \frac{d \theta_v}{d \delta_v} = 0 \qquad (11)$$

in which:

$$\nu_v = \frac{Z_v \theta_v}{\lambda_v} \dot{m}_b \quad , \qquad (12)$$

$$\delta_v = \frac{Z}{Z_v} \qquad (13)$$

Boundary conditions are as follows:

$$\begin{aligned} \delta_v &= 0 \qquad \theta_v = 1 \\ \delta_v &= 1 \qquad \theta_v = \theta_f \end{aligned} \qquad (14)$$

The integration of Eq. (11) with boundary conditions (14) gives:

$$\theta_v = 1 + \frac{\theta_f - 1}{e^{\nu_v} - 1}\left(e^{\nu_v \delta_v} - 1\right) \qquad (15)$$

The heat received through conduction per unit area by the fuel surface is:

$$\dot{q}_{cf} = \lambda_v \left(\frac{dT}{dZ}\right)_{Z=0} = \lambda_v \frac{T_s}{Z_v} (\theta_f - 1) \frac{\nu_v}{e^{\nu_v} - 1} \qquad (16)$$

This heat transferred depends on Z_v, and, therefore, it varies along a burner radius. The total heat $\dot{Q}_{cf}$ received through conduction by the burner is given by:

$$\dot{Q}_{cf} = \int_0^{D/2} \dot{q}_{cf}\, 2\pi r\, dr = 2\pi \lambda_v T_s (\theta_f - 1) \int_0^{D/2} \frac{\nu_v}{Z_v} \frac{1}{e^{\nu_v} - 1} r\, dr \qquad (17)$$

For the case shown in Fig.12, it results:

$$\frac{Z_v}{Z_{v,min}} = 1 + (\beta - 1)\left(1 - \frac{2r}{D}\right) \qquad (18)$$

in which:

$$\beta = \frac{Z_{v,max}}{Z_{v,min}} \qquad (19)$$

Taking (18) into (17), it results:

$$\dot{Q}_{cf} = \frac{\pi D^2}{4} \frac{T_s \lambda_v}{Z_{v,min}} (\theta_f - 1) \varphi_v \qquad (20)$$

in which:

$$\varphi_v = \frac{2}{\beta - 1}\left[- 2 \ln \left(1 - e^{-\nu_{v,min}}\right) - \frac{1}{\nu_{v,min}\,(\beta - 1)} \, x \right.$$

$$\left. x \sum_{n=1}^{\infty} \frac{\left(1 - e^{-\nu_{v,max}}\right)^n - \left(1 - e^{-\nu_{v,min}}\right)^n}{n^2} \right] \qquad (21)$$

The mean value $\bar{\dot{q}}_{cf}$ of the heat received per unit area is:

$$\bar{\dot{q}}_{cf} = \frac{4\,\dot{Q}_{cf}}{\pi D^2} = \frac{T_s \lambda_v}{Z_{v,min}} (\Theta_f - 1)\,\varphi_v \qquad (22)$$

The value of φ_v is shown in Fig.13. It may be seen in the figure how φ_v decreases rapidly as ν_v (that is to say $\dot{m}_b$ or $Z_{f,min}$) increases.

For large values of $\nu_{v,min}$ ($\nu_{v,min} \gg 1$) , it results:

$$\varphi_v \approx 2\, e^{-\nu_{v,min}} \left[\frac{1}{\beta - 1} + \frac{1}{\nu_{v,min}\,(\beta - 1)^2} \right] \qquad (23)$$

On the other hand, for small values of $\nu_{v,min}$ ($\nu_{v,min} \ll 1$) , we obtain:

$$\varphi_v \approx \frac{2}{\beta - 1} \left[\frac{\beta}{\beta - 1} \ln \beta - 1 \right] \qquad (24)$$

I.6 Heat Transferred through Radiation

a) Flame emissivity

The radiant heat received by the fuel surface depends on the size, shape, temperature and on the emission coefficient of the flame.

The heat received per unit area is given by:

$$\dot{q}_{rf} = \mathcal{E}_f \sigma T_f^4 - \mathcal{E}_l \sigma T_s^4 \approx \mathcal{E}_f \sigma T_s^4 \varphi_f^4 \qquad (25)$$

since $T_s \ll T_f$.

The value of $\mathcal{E}_f$ depends on the point considered on the fuel surface. An average value of $\mathcal{E}_f$ on the whole surface may be estimated by assuming, as far as radiation is concerned, that the flame occupies not only its own volume, but also the volume of the inner core of fuel vapors, which is very small as compared with the volume of the flame, and by taking the equivalent radiant hemisphere approximation.

The average emissivity is, then, given by:

$$\bar{\mathcal{E}}_f = 1 - e^{-\alpha_f L_h} \qquad (26)$$

in which α is the absortion coefficient, and L_h is the radius of the equivalent radiant hemisphere or mean beam lenght. The value of L_h may be obtained by means of numerical integrations, but a very approximated value of it is given by the expression:

$$L_h = 4 \frac{\text{Flame Volume}}{\text{Total Flame Surface}} = 4 \text{ x hydraulic radius} \quad (27)$$

For the case of a conical flame, we obtain:

$$L_h = \frac{2}{3} \frac{D}{\frac{D}{2L} + \sqrt{1 + 4\left(\frac{D}{L}\right)^2}} \quad (28)$$

and for a cylindrical flame:

$$L_h = \frac{D}{\frac{D}{2L} + 1} \quad (29)$$

Mean beam lenght L_h may be approximately measured in a flame by means of the expression:

$$L_h = \frac{L}{1 + \left(\frac{L \cdot D}{A_f}\right)^2 + 4 \frac{L^2}{A_f}} \quad (30)$$

where A_f is the cross-section area of the flame as seen in a photograph.

Fig. 14 shows the average emissivity $\bar{\epsilon}_f$ for conical and cylindrical flames of several sizes and shapes. It may be observed how $\bar{\epsilon}_f$ increases as the flame size also increases.

b) Radiant heat balance

An important parameter in the balance of energy of a fire is the ratio φ_r of the radiant heat received by the fuel to the total radiant heat emitted by the flame.

The calculation of φ_r is very complicated because the flame emissivity depends on the flame thickness, and therefore, it results from the numerical calculation of very complicated integrals.

For conical and cylindrical flames approximated values of φ_r are given by the expressions:

$$\varphi_r \text{ (conical)} = \frac{\int_0^{D/2} \left(1 - e^{-\alpha Z}\right) 2\pi r \, dr}{2\int_0^{D/2} \left(1 - e^{-\alpha Z}\right) 2\pi r \, dr + \int_0^{L} \left(1 - e^{-2Y\alpha}\right) 2\pi Y dz} =$$

$$= \frac{1}{2 + 2\left(\frac{L}{D}\right)^3 \frac{\frac{(\alpha D)^2}{2} + \alpha D\, e^{-\alpha D} + e^{-\alpha D} - 1}{1 - e^{-\alpha L} + \frac{(L\alpha)^2}{2} - L\alpha}} \qquad (31)$$

$$\text{(cylindrical) } \varphi_r = \frac{1}{2 + 4\,\frac{L}{D}\left(\frac{1 - e^{-\alpha D}}{1 - e^{-\alpha L}}\right)} \qquad (32)$$

When the flame is very large it behaves as a opaque body. For this case we have:

$$\varphi_r = \frac{\pi D^2/4}{A_{ft}} \qquad (33)$$

or:

$$\varphi_{r\ (\text{conical})} = \frac{1}{1 + 2\frac{L}{D}\sqrt{1 + \frac{D^2}{4L^2}}} \qquad (34)$$

$$(\text{cylindrical})\ \varphi_r = \frac{1}{2 + 4\frac{L}{D}} \qquad (35)$$

I.7 Energy Balance

The energy balance of a fire is governed by the two following equations:

a) Energy Balance at the Fuel Surface

Assuming that the surface reflectivity is equal to zero and that the radiant heat is absorbed by the fuel in a zero thickness layer, we have:

$$\bar{\dot{q}}_{cf} + \bar{\dot{q}}_{rf} = q_1 \dot{m}_b + \bar{\dot{q}}_{c1} \qquad (36)$$

which expresses that the total heat reaching the fuel surface is equal to the heat consumed in evaporating the fuel plus the heat transmitted through conduction into the fuel.

The value of $\bar{\dot{q}}_{c1}$ was determined in Second Annual Report and its value is given by:

$$\bar{\dot{q}}_{c1} = \frac{\lambda_1 T_s}{X_s} (1 - \theta_o) \frac{\nu_1 e^{\nu_1}}{e^{\nu_1} - 1} \qquad (37)$$

in which:

$$\nu_1 = \frac{c_1 X_s \dot{m}}{\lambda_1} \qquad (38)$$

The heat $\bar{\dot{q}}_{c_1}$ may be expressed in the form:

$$\bar{\dot{q}}_{c_1} = \frac{\lambda_1 T_s (1 - \theta_o) \varphi_{c1}}{X_s} \qquad (39)$$

where:

$$\varphi_{c_1} = \frac{\nu_1 e^{\nu_1}}{e^{\nu_1} - 1} , \qquad (40)$$

is the ratio between the heat transmitted to the interior of the fuel and the heat which would be transmitted if the fuel were at rest.

Coefficients φ_{c1} is shown in Fig.13, as a function of ν_1. It may be observed how φ_{c1} increases as the mass flow $\dot{m}$ augments.

Taking into (36) the values of $\bar{\dot{q}}_{cf}$, $\bar{\dot{q}}_{rf}$ and $\bar{\dot{q}}_{cl}$ given by (22), (25) and (39) we obtain:

$$\dot{m}_b = \frac{1}{q_1} \left[\bar{\varepsilon}_f \sigma T_{ss}^4 \theta_f^4 + \frac{T_s \lambda_v}{Z_{v,min}} (\theta_f - 1) \varphi_v - \frac{T_s \lambda_1}{X_s} (1-\theta_o) \varphi_{c_1} \right] \qquad (41)$$

which gives the burning rate $\dot{m}_b$ as a function of flame size and shape, through parameters $\bar{\varepsilon}_f$, φ_v and φ_{c_1}.

b) Over-all Energy Balance

Disregarding kinetic energies, which are always very small in a fire, the equation giving the over-all balance of

energy in a fire is:

$$\left(\frac{\pi D^2}{4}\dot{m}_b + \dot{M}_a\right) c_f (T_f - T_o) + \frac{\pi D^2}{4}\frac{1}{\varphi_r}\bar{\epsilon}_f \sigma T_f^4 +$$

$$+ \frac{\pi D^2}{4}\frac{T_s \lambda_v}{Z_{v,min}}(\Theta_f - 1)\varphi_v = \frac{\pi D^2}{4}\dot{m}_b q_r + \frac{\pi D^2}{4}\dot{m}_b c_v (T_s - T_o) \quad (42)$$

In this expression $\dot{M}_a$ is the air mass flow entrained by the fire and entering into the flame:

Let:

$$\frac{\dot{M}_a}{\frac{\pi D^2}{4}\dot{m}_b} = K_s K_d \quad (43)$$

being K_s the stoichiometric air/fuel ratio and K_d the dilution coefficient, which has a value close to unity for laminar flames and a value of 2 or 3 for turbulent flames.

Equation (41) gives the burning rate m_b as function of the properties of flame and fuel and as function of the geometrical flame configuration.

Equation (42) relates the burning rate with the flame temperature once the dilution coefficient is known as well as the flame properties and configuration. Therefore, these two equations relate the main variables and parameters of the process.

From the research program it is expected to obtain information on the values of these parameters, which will permit to study the relative influence of several important variables and to explain some experimental facts, such as: influence of the fuel properties (q_r and q_l); relative influence on the burning rate of the radiant and conductive heat transfer, influence of flame emissivity, scaling laws, etc.

II - TRANSPORT OF FIREBRANDS

II-1 Introduction

During the report period the following work has been performed on the problem of transport of firebrands:

a) Continuation of the experimental and theoretical studies on flight paths and burning lifetimes of firebrands.

b) Design and construction of new research facilities.

c) Studies on the basic laws governing combustion of wood particles under forced convection conditions, and calculations of flight paths and lifetimes from the results obtained.

According to the program exposed in Second Annual Report a series of experiments are being carried out by burning firebrands of several kinds of wood, of different initial size and shape and for several values of the moisture content.

From these tests and fixing a certain model of the convection column above a fire and for given wind conditions, the flight paths and flight lifetimes of the firebrands are being calculated.

The objectives of the research program are to establish what are the most dangerous types of firebrands for different convection columns and wind conditions and to calculate the maximum distances that the firebrands may reach while still burning.

In order to carry out these tests two suction-intakes wind tunnels are being utilized. A wind tunnel is the small one described in First Annual Report, but it has been placed in vertical position. In this way direct measurements of the terminal velocities of fall of the firebrands are more easily made. The other wind tunnel is the one described in Second Annual Raport, but a new type of strain-gauges balance has been designed and constructed which gives more accurate readings than the strain-gauges balance previously utilized.

Finally, a new study has been recently initiated which is directed to the attainment of the basic laws controlling combustion of wood particles with forced convection. From this study it is expected to derive general expressions giving the burning rates of wood particles when they fly at their therminal velocity of fall, and it is also expected to derive general scaling laws of the process.

II.2 Experimental Results

The complete program comprises the study of the properties of different sized spherical, cylindrical and plate-shaped firebrands of five kinds of wood: pine (pinus pinaster); spruce (picea excelsa); oak (quercus rubra); aspen (populus tremuloides) and balsa (ochroma lagopus) with moisture contents of 2% and 25%. Afterwards, natural firebrands will also be investigated.

Spherical firebrans of 10; 15; 17.5; 22 and 50 mm in diameter have been studied and cylinders of 6 x 18, 8x 24, 10 x 30 and 12 x 36 mm in diameter and length respectively.

The study of plate-shaped firebrands have also been very recently initiated.

Most results have been obtained with moistures contents of 25%, although some results are also available for a 2% of moisture content. The results obtained till now show that the moisture content exerts a not important influence on the process. However, a detailed study of the influence of the moisture content is presently under study.

The experimental studies consist in the direct measurements of the terminal velocities of fall of the firebrands according to the procedure exposed in Second Annual Report.

Most of these measurements have been performed in the small wind tunnel described in First Annual Report, but placed in a vertical position with the intake section down. The firebrands are held by means of a thin piece of wire, which is kept in a horizontal position by continuously reducing the wind speed as the firebrands burns. In this way, the aerodynamic drag of the firebrand is kept equal to the its weight throughout the combustion process.

Large firebrands are tested in the large horizontal wind tunnel. In this tunnel it is also possible to determine directly the terminal velocity of fall of firebrands, by equalizing the recorded values of the weight and the aerodynamic drag of the firebrand by adjusting continuously the tunnel wind speed.

A new type of strain-gauges balance for this wind

tunnel has been designed and constructed, which will be described in Section II.4.

A total number of about four hundred measurements have been performed till now. This great number of tests is due to the very large number of parameters of the process and to the heterogeneous properties of wood, which makes necessary that four or five tests have to be made for each case in order to obtain average values.

The experimental values of the terminal velocities of fall are shown in Figs. 16 to 20. In order to calculate the flight paths and the flight burning times it is now necessary to specify the convection column model and the horizontal wind conditions.

II.3 Convection Columns and Flight Paths

According to the method described in Second Annual Report, the flight paths of the firebrands are calculated by assuming that they always fly at their terminal velocity of fall, characterized by:

$$w_{xf} = o \tag{44}$$

$$w_{yf} = w_f = \sqrt{\frac{2 g m}{\rho C_D A}} \tag{45}$$

Therefore, the flight paths are calculated with the expressions:

$$X = \int_o^t u_x \, dt \tag{46}$$

$$Y = \int_0^t (u_y - w_f)\, dt \qquad (47)$$

Functions X (t) and Y (t) are immediately calculated from the experimental values of w_f (t) once the components of the velocity u_x and u_y are given within and out of the convection column.

Wind conditions above a forest fire can be very different as shown in Fig. 47 . However, it has been observed than in most major forest fires a low jet wind exists [5] for which the maximum intensity of wind occurs at the ground or near the ground, as shown in several wind profiles of Fig. 47

Convection columns always exists above a well developed forest fire. They are of different types, which are determined by the prevailing wind conditions.

When there is a jet wind, and the wind decreases or has a small value aloft a vertical or almost vertical convection column appears, which is called a tower convection column [5] . If the wind aloft increases, the convection column curves gradually towards the direction of the wind.

When there exists a strong wind-gradient aloft, the convection column bends sharply originating which is called a fractured convection column [5].

There are almost no data on the values of the convective speeds within the convection columns although vertical velocities up to 100-130 km/hour have been observed in some high-intensity fires.

Flight paths and flight lifetimes of the firebrands can be immediately calculated for any type of convection column. However, for simplicity, and because of the lack of actual data, two very simplified models of convection columns were considered in Second Annual Report.

First model considers a vertical convection column of constant speed. The firebrands leave at random the convection column thrown out by turbulence, and then they are picked up by a constant horizontal wind.

Second model assumes an inclined convection column of a given width. The velocity within the convection column is constant and it is the resultant of a constant horizontal wind and of a constant vertical convective velocity.

The firebrands are picked up from the ground and they leave the convection column at a point determined by the initial position of the firebrand.

These two models are oversimplified. For example, constant horizontal winds do not exist, and if an inclined convection column exists is because there is a strong wind aloft. However, these two models are very useful because they give an actual order of magnitude of the distances reached by the firebrands while still burning, and they are also very useful for the calculations of comparative results, which would be very lenghty using more realistic models.

However, some examples will be given using actual wind conditions and more realistic convection columns models and it is intended to study the most adverse possible wind

conditions as far as maximum range of the firebrands is concerned.

Most results have been till now obtained with the vertical convection column model. These results have been obtained for an extense range of the vertical velocity u_y and they have been expressed as fuction of the horizontal component of the wind u_x .

Figs. 21 to 30 show the values of the critical height Y_m as function of velocity u_y for all kinds of firebrands. If the firebrand leaves the convection column at this critical height it reaches a maximum horizontal distance while still burning.

In those figures the values of $t_f - t_v$, time of flight out of the convection column are also shown. These times are proportional to the horizontal distance, and therefore, for a given value of the horizontal wind component u_x the maximum range X_m corresponding to each value of Y_m is immediately calculated.

In order to obtain comparative results Figs. 31 through 40 show the same variables Y_m and $t_f - t_v$ as functions of the initial diameter of the spherical or cylindrical firebrands.

From these curves it may be observed:

a) There is a critical size for each speed u_y which gives the maximum range. This critical size increases as the vertical wind component u_y increases.

b) There is not a great difference between the flight and burning characteristics of spherical and cylindrical firebrands.

Measuring the potential danger of fire spread by the maximum horizontal distance that may be reached by the firebrands while still burning, it may be observed that, in general, cylindrical firebrands are more dangerous than spherical firebrands of equal initial diameter.

c) The influence of the kind of wood on the flight paths and lifetimes of firebrands depends on the value of the convective velocity u_x and on the initial size of the firebrands.

Aspen firebrands are the most dangerous ones for low values of the convective velocity u_y and when the firebrands are large.

Pine wood firebrands may reach approximately, the same horizontal distances as those of aspen firebrands, provided that the velocity u_y is large.

Spruce firebrands behave similarly as pine firebrands, but, in general, they are less dangerous.

Large oak firebrands are less dangerous than pine or aspen firebrands of similar size. However, small oak firebrands are the most dangerous ones, specially for high values of velocity u_y.

Finally, balsa firebrands are less dangerous than any other kind of firebrands among the fire types of wood investigated. Balsa wood has a very small density but it burns very rapidly, and therefore, balsa firebrands cannot fly till very ~~great~~ distances.

Results have also been obtained for inclined convection columns. The program is not yet finished and some results obtained until now are shown in Figs. 41 to 46. In these figures critical height Y_m and total flight time t_f are represented as functions of the vertical convective component u_y. Y_m and t_f are the values which correpond to maximum range of the firebrand (maximum horizontal distance reached while still burning).

Results depend, essentially, on the initial position of the firebrand with respect to the convection column border line. Therefore, in the same figures ratio L/u_x has been also represented, in which L is the aforementioned initial distance of the firebrand to the convection column border line and u_x is the horizontal wind component. The value of L/u_x is obtained by expressing the condition of maximum range and it has a maximum, and sometimes a minimum value, as function of u_y.

For small values of the convective velocity u_y, the firebrands may have initial values of their terminal velocities of fall w_f larger than u_y, and therefore, they

cannot fly. It has been assumed that the firebrands burn at rest until their terminal velocity of fall becomes equal to u_y, and then they start flying. These especial conditions are represented by segments a-b in the abovementioned figures.

Because of the form in which the experimental data have been obtained, the period of combustion at rest of the firebrands has been taken at velocity w_f and not at u_y. It may introduce some errors in the results, and therefore, these special cases will be studied by burning firebrands at constant wind speed until a certain size at which $w_f = u_y$, and from then onwards keeping the wind speed continually equal to the terminal velocity of fall.

From the results included in Figs. 21 through 42 all pertinent data on flight paths and flight burning characteristics may be deduced. Therefore, it is not necessary to show the actual flight paths. However, since they give a very clear impression of the final results, they will be included for some selected cases.

In Second Annual Report some examples of flight paths were shown for vertical and inclined convection columns. In the present Report flight paths will be shown for more realistic convection columns models and considering actual wind conditions.

Fig.47 shows some typical wind profiles above some major forest fires [5]. Figs. 48 and 49 show two examples of convection columns. They have been obtained by assuming that they result from the composition of a horizontal wind, as those of Fig.47, and a convective wind, as those resulting from theoretical considerations [6,7].

free fall times of the cylinders were measured at heights of 100 and 200 meters, first dropping the cylinders one by one and afterwards dropping 100 cylinders of the same time from a metalic box attached to the balloon * .

The following results were obtained:

a) The cylinders always fell tumbling.

b) The measured falling times of the cylinders were of the same order of magnitude than those calculated for the position of maximum drag. The errors were smaller than a 10%.

c) When the 100 cylinders were dropped there were an important horizontal dispersion but they fell in times differring less than a 10%.

According to these results it was concluded that the procedure of keeping during the tests the cylinders in their position of maximum drag did not introduce any important errors in the results, specially considering the order of approximation that it is required.

A similar study is now being performed for square plates and it is expected that in this case the measured free fall times will differ appreciably from the calculated values for the position of maximum drag.

---

* The actual weight of the cylinders was kept within $\pm$ 1% of the weight taken for the calculations.

II.5 Strain-gauges Balance

A new type of strain-gauges balance has been designed and constructed. This balance has a higher sensitivity and a better zero-stability than the balance previously utilized, which was not precise enough in the final zone of the curves of firebrand weight and aerodynamic drag as functions of time.

The same Kipp and Zonen Micrograph is being used as the recording instrument of the balance.

The balance is of the ring type, in which the strain gauges are placed on rings of high-duty steel, as shown in Fig.53. Two rings are used for each component (vertical-weight, horizontal-aerodynamic drag) and the other two branches of the Wheatstone bridge are formed by a box of small beams with strain-gauges attached as variable resistances.

A general sketch of the balance is shown in Fig.54, and the electric circuits in Fig.55. The connecting arm of the balance multiplies the measuring forces by a factor of about forty. The rings layout, the strain-gauges arrangement and the electrical circuits have been designed in a way that the effects of temperature, lateral stresses and forces are automatically compensated. Only forces which produce deformations of opposite sign are recorded by the Micrograph.

All rings are supported by means of movable supports which can be adjusted to impart initial stresses to compensate any possible threshold stress.

Additional reinforced rings can be fitted to increase the measuring range of the balance.

The first tests of the balance have shown that it has a linear response characteristic, with errors less than a 5% and that the influence of one component on the other one is practically negligeable.

II-6 Combustion of Wood with Forced Convection

A study is being carried out in order to know the general properties of the combustion of wood when forced convection exists.

By burning at constant wind speed wood particles of several sizes and shapes, empirical expressions are being determined of the laws of variation of the diameter and density of firebrands as functions of both time and wind speed. From these expressions it is possible to calculate the terminal velocity of fall of a burning particle, and them, its flight path under given wind conditions.

These studies may give very general conclusions, especially considering that results may be expressed in dimensionless form, from which scaling laws are readily derived.

Only one example will be given to show the method which is being applied, since these studies have been very recently initiated and only a few experimental data are available.

From the experimental data so far obtained it appears that the convective combustion at constant speed of small spheres and cylinders of wood may be approximated by expressions of the form (Fig.56):

$$\frac{\rho_w}{\rho_{w,o}} = \frac{1}{1 + \eta t^2} \qquad (48)$$

$$\frac{r^2}{r_o^2} = 1 - \frac{\beta + \delta_w}{r_o^2} t \; ; \quad (w = \text{constant}) \qquad (49)$$

In these expressions η , β and δ are parameters which depend on the kind of wood and on the moisture content.

It may be observed that, apparently, density does not depend appreciably on the wind speed and that the law of variation of the radius is similar to that of the combustion of liquid spheres.

Assuming that the rate of variation of the surface area of the firebrand, obtained by differentiating Eq.(49):

$$d\left(\frac{r}{r_o}\right)^2 = - \frac{\beta + \delta_w}{r_o^2} dt \qquad (50)$$

is the same that in a combustion taking place at the terminal valocity of fall; and then taking into (50) the value of w given by:

$$w = w_f = w_{f,o} \sqrt{\frac{\rho_w}{\rho_{w,o}}} \; \frac{r}{r_o} \qquad (51)$$

the following differential equation is obtained:

$$d\left(\frac{r}{r_o}\right)^2 = -\left[\beta + \delta\, w_{f,o}\,(1+\eta t^2)^{-\frac{1}{2}}\left(\frac{r}{r_o}\right)^{\frac{1}{2}}\right]\frac{dt}{r_o^2} \qquad (52)$$

which gives the variation of the firebrand radius as a function of time when the firebrand flies at its terminal velocity of fall.

In Fig.51 the experimental curve $w_f = f(t)$ and the theoretical curve given by (52) are compared, and fig.58 shows the flight paths obtained from both curves.

It may be observed that the approximation given by the theoretical curve is fairly good. However, the burning out time or final point of curve $w_f = f(t)$, obtained theoretically, in considerably longer than the experimental value. This is due to the fact that the particles of wood never burn-out down to a zero-diameter in the wind tunnel, but they always break off from the wire when they have burned down to a very small size. Therefore, theoretical results are, probably, more accurate in this case, but this discrepancy is not important, since it does not seem likely that a very small firebrand could ignite a forest fire.

PRINCIPAL CONCLUSIONS

The principal conclusions derived from the investigations so for performed (First, Second and Third Annual Reports) are as follows:

a) OPEN FIRES

1º.- In a pool-fire burning rates and temperature profiles in the fuel are calculated as functions of the heat received by the fuel surface.

2º.- When it is assumed that such heat is transferred exclusively through radiation, a fair approximation of the process is obtained, for n-heptane and dioxane fuels, when vessels of 25 cm in diameter are used. This approximation is excellent for a vessel of 50 cm in diameter.

3º.- Vessel or total fuel depth influences considerably the process when it is smaller than a certain minimum value.

4º.- Liquid depth influences considerably the time required to achieve quasi-stationary conditions, and that time may be extremely long.

5º.- From 3 and 4 it follows that vessel depth has to be chosen between certain limits. These limits depend considerably on the heat $\dot{Q}_s$ received by the fuel, that is to say, on the characteristics and size of the flame, and therefore, on the type of fuel,

6º.- Temperature profiles are very sharp in the vicinity of the fuel surface. Therefore, a thermocouple placed at the fuel surface would measure an average value of the temperature, somewhat smaller than its superficial value, which should be very close to the boiling temperature at ambient pressure.

7º.- Temperature profiles are specially sharp for transient combustion.

8º.- By changing the overflow from the pool it is possible to control, in a continuous way, the flame size and the burning rate.

9º.- By mixing dioxane with water it is possible to change continuosly the flame properties, specially the heat of reaction and the latent heat of evaporation.

10º.- A model of the fire has been developed which permits a calculation of the distribution of the heat transferred to the fuel surface between radiant and convective heat.

11º.-That model also permits the study of the over-all balance of energy in a fire.

b) TRANSPORT OF FIREBRANDS

1º.- The firebrands reach in a few seconds velocities very close to their terminal velocity of fall characterized by conditions $w_x = 0$ and $w_y = w_f$.

2º.- The flight paths and flight lifetimes of firebrands may be calculated, in all practical cases, by assuming

that the firebrands always fly at their terminal velocities of fall.

3º.- The aforementioned simplification permits an easy calculation of the flight paths and flight lifetimes, by means of the experimental data obtained by burning firebrands in air flow of velocity continually equal to the firebrand's terminal velocity of fall.

4º.- When the burning-out time is very small or the wind speed very low, condition 1 might not hold and the approximation of 2 might not be satisfactory, but these cases are of no practical interest.

5º.- There exists a critical height Y_m at which if the firebrand leaves the convection column it reaches a maximum horizontal distance X_m while still burning.

6º.- X_m is the maximum range from the flame front for which fire spread may be produced by firebrands of given initial size and for given wind conditions.

7º.- For adverse conditions, X_m may reach values of the order of several kilometers, even for small firebrands and for moderate wind conditions.

8º.- The zone of potential danger of fire propagation depends, to a considerable extent, on the size of the firebrands, the critical or more dangerous size depends, especially, on the value of the convective velocity.

9º.- The kind of wood has an appreciable influence on the process, depending its influence on the convective velocity u_y and on the initial size of the firebrands. Aspen firebrands, for example, are the most dangerous ones among the five kinds investigated, for low values of u_y and when the firebrands are large. On the other hand, if the firebrands are small oak is the most dangerous wood, especially for high values of u_y .

10º.- The shape of the firebrands is an important factor in the process. Only spherical and cylindrical firebrands have been studied so far, and between them, cylindrical firebrands are a little more dangerous.

11º.- The influence of the moisture content has not yet thoroughly studied. It lengthtens the ignition process but it seems that it does not change considerably the flight paths of the firebrands.

12º.- The free motion of cylindrical firebrands does not influence, to a significant extent, their combustion times and flight properties.

13º.- Empirical laws are being derived which give the burning rates of wood particles, measured as the recession velocity of the surface.

14º.- From those laws it is possible to calculate the burning rates of firebrands when they fly at their terminal velocities of fall.

15º.- Finally, the flight paths and flight lifetimes of firebrands may be calculated for any type of convection column or wind conditions.

Madrid, July 1964

= = = = = = = = = = =

NOTATION

O P E N F I R E S

a . . . Dimensionless parameter defined by $a^2 = \rho c / \lambda$

A_f . . Cross-section area of the flame

A_{ft} . . Total area of the flame

c . . Specific heats at constant pressure.

c_f . . Specific heat of the flame gases

c_l . . Specific heat of the liquid fuel

c_v . . Specific heat of the vapor fuel

D . . Diameter of the burner

K_d . . Dilation coefficient

L . . Flame height

L_h . . Mean beam length

$\dot{m}$ . . Fuel flow within the vessel

$\dot{m}_b$ . . Fuel flow burned

$\dot{M}_a$ . . Air flow entrained by the fire

n . . Number

$\dot{q}_{cl}$ . . Heat transferred through conduction throughout the liquid per unit area and per unit time.

$\dot{q}_{cf}$ . . Heat transferred through conduction to the liquid surface per unit area and per unit time.

$\dot{Q}_{cf}$ . . Total heat transferred through conduction

q_l . . Latent heat of evaporation

q_r . . Heat of the reaction

$\dot{Q}_{re}$ . . Heat radiated to the surroundings per unit time

$\dot{q}_{rf}$ . . Heat radiated to the fuel per unit area and per unit time

$\dot{Q}_{rf}$ . . Total heat radiated to the fuel per unit time

$\dot{Q}_s$ . . Heat received by the fuel per unit area and per unit time.

r . . . Radius

T . . . Temperature

T_f . . Flame temperature

T_s . . Surface temperature

T_v . . Vapor temperature

V . . . Velocity

X_s . . Vessel (fuel) depth

Y . . . Lateral coordinate

Z . . . Vertical coordinate

Z_v . . Vertical coordinate in the vapor zone.

α . . . Emission coefficient

β . . . Dimensionless parameter defined by (19)

δ . . Dimensionless parameter defined by (3)

δ_v . . . Dimensionless parameter defined by (13)

ϵ_f . . Flame emissivity

ξ . . . Dimensionless parameter defined by (9)

χ_s . . Dimensionless parameter defined by (4)

χ_1 . . Dimensionless parameter defined by (5)

λ . . . Thermal conductivity

φ_v . . . Dimensionless parameter defined by (21)

φ_{cl} . . Dimensionless parameter defined by (40)

φ_r . . Dimensionless parameter defined by (31)

ν . . . Dimensionless parameter defined by (1)

ρ . . . Fuel density

σ . . . Stefan-Boltzmann constant

θ . . . Dimensionless temperature defined by (2)

Subscripts

s . . . Indicates at the fuel surface.

v . . . Indicates at the fuel vapor zone.

f . . . " " " flame zone

l . . . " " " liquid zone

TRANSPORT OF FIREBRANDS

A . . . Cross-section area of a firebrand

C_D . . . Aerodynamic drag coefficient

g . . . Acceleration of gravity

m . . . Firebrand mass.

o . . . Initial value (subscript)

r . . . Firebrands radius

t . . . Time

t_f . . . Final time or total flight time

t_v . . . Flight time within a vertical convection column.

w_x, w_y . Horizontal and vertical components of the relative velocity of the wind with respect to the firebrand.

u_x, u_y . Horizontal and vertical components of the absolute velocity of the wind.

X . . . Horizontal distance.

X_m . . . Maximum range or maximum horizontal distance reached by a firebrand while still burning

Y . . . Vertical distance or height.

Y_m . . . Critical height

ρ . . . Air density

ρ_w . . . Wood density

η, β, σ - Parameters.

DIMENSIONLESS BURNING RATE AS A FUNCTION OF χ_s, $\Xi\chi_l$ AND θ_o

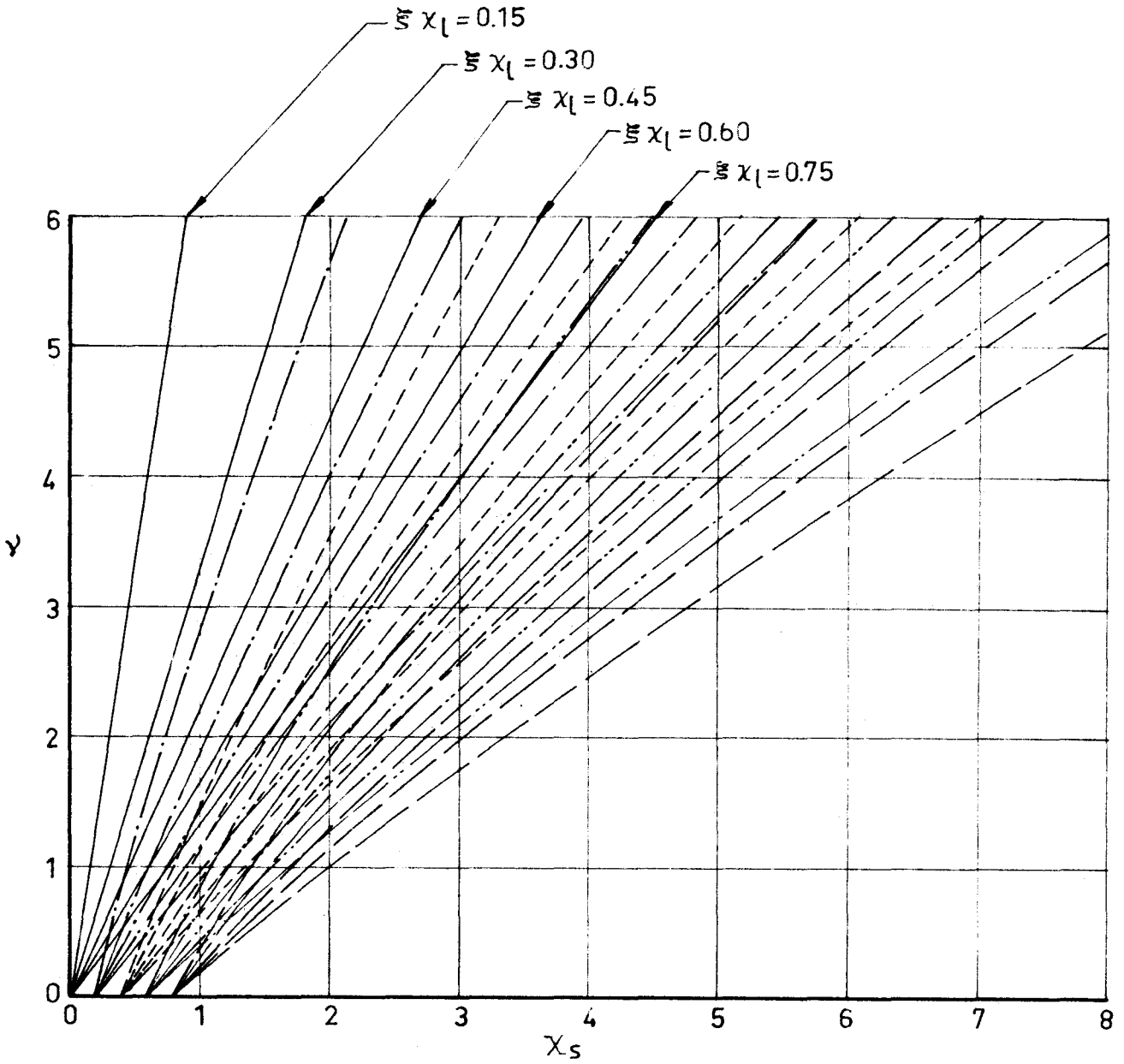

$\theta_o = 1.0$ ——————————

$\theta_o = .8$ —·—·—·—·—

$\theta_o = .6$ – – – – – – –

$\theta_o = .4$ —··—··—··—

$\theta_o = .2$ — — — — —

(Values of χ_s are the same as those indicated for $\theta_o = 1.0$ and in the same order)

(For $\nu > 5$ curves $\nu = f(\chi_s)$ are practically straight lines)

FIG. 1

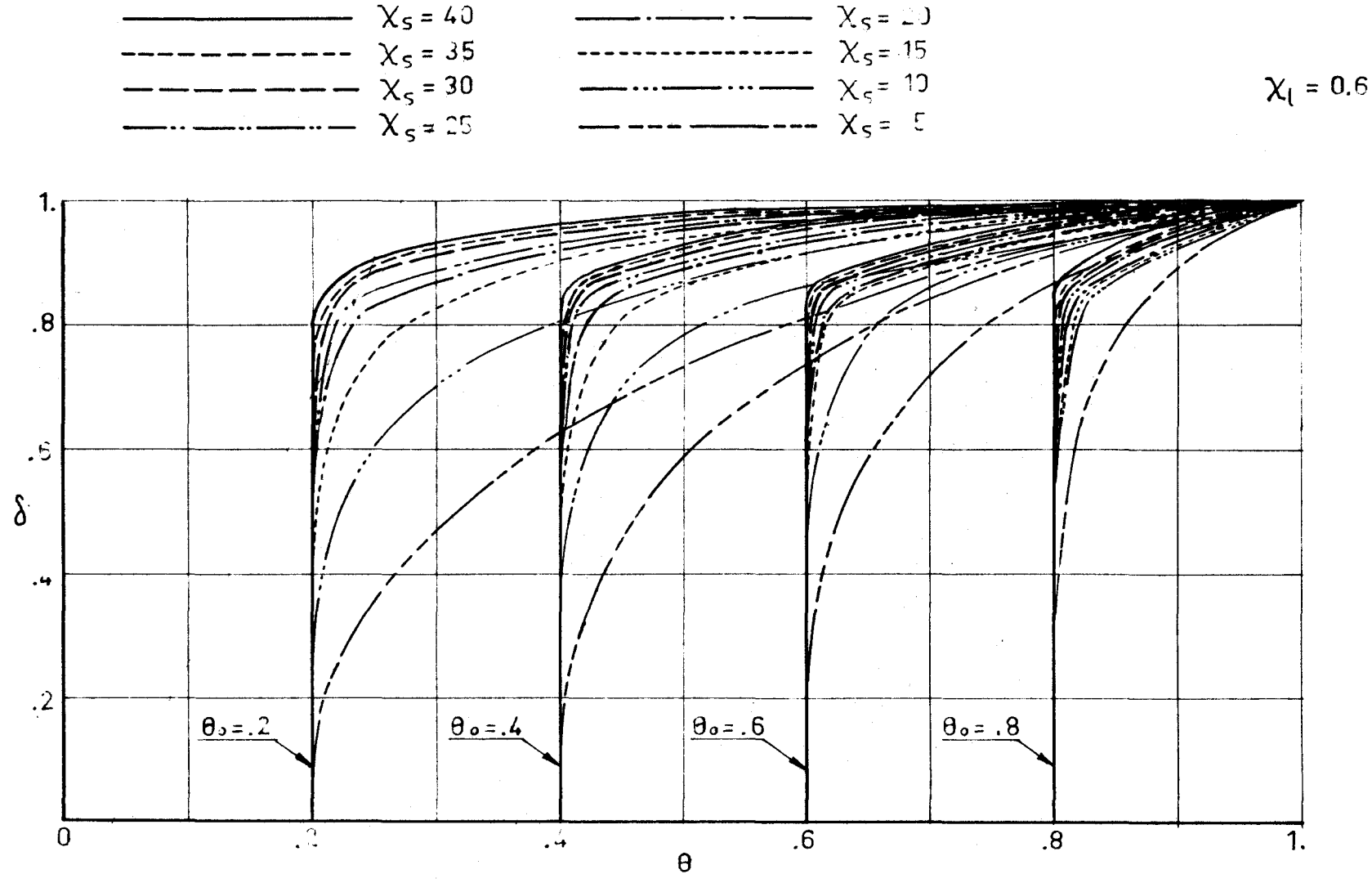

DIMENSIONLESS TEMPERATURE PROFILES FOR SEVERAL VALUES OF χ_s AND θ_o

FIG. 3

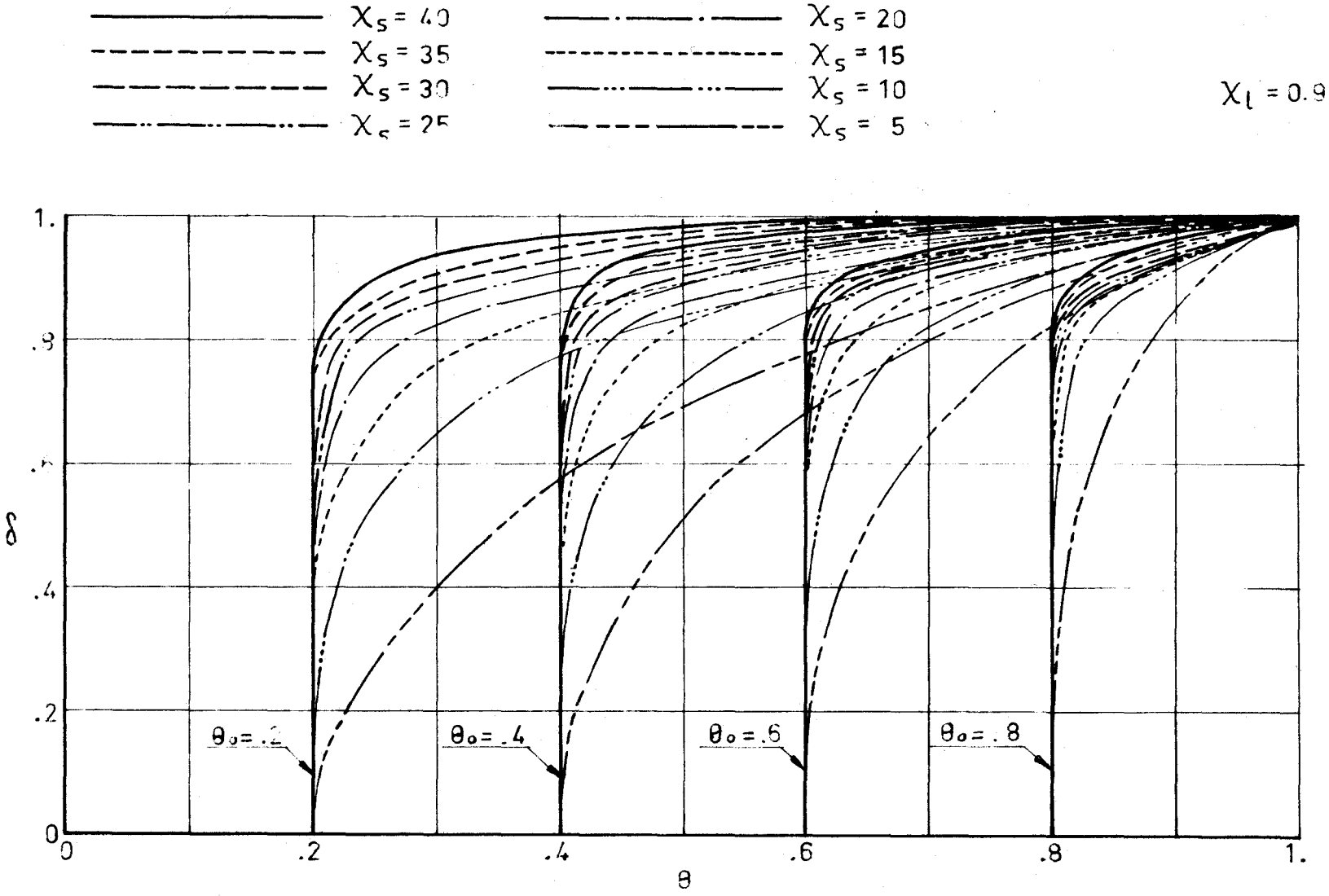

DIMENSIONLESS TEMPERATURE PROFILES FOR SEVERAL VALUES OF χ_s AND θ_o

FIG. 4

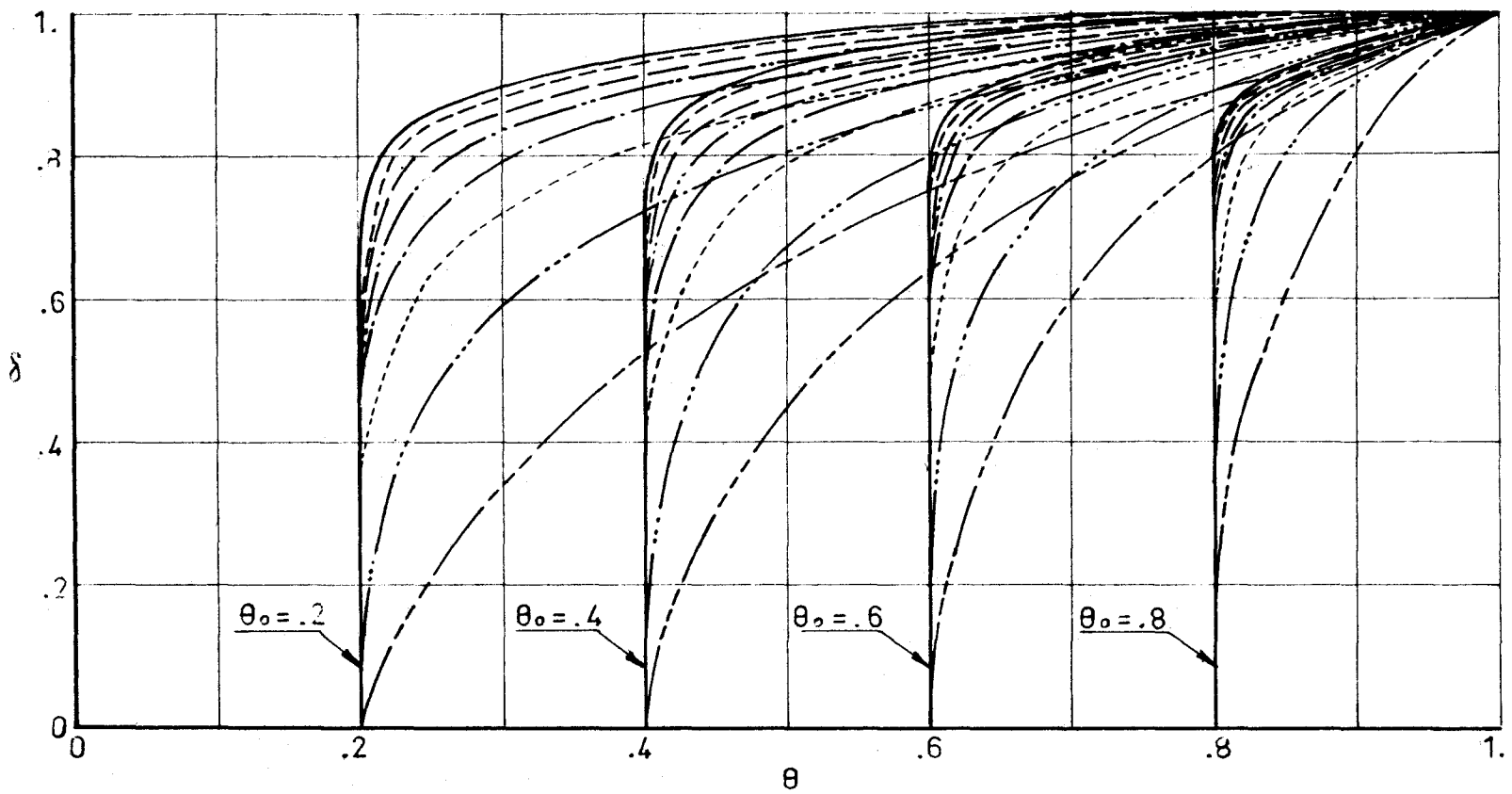

DIMENSIONLESS TEMPERATURE PROFILES FOR SEVERAL VALUES OF χ_s AND θ_o

FIG. 5

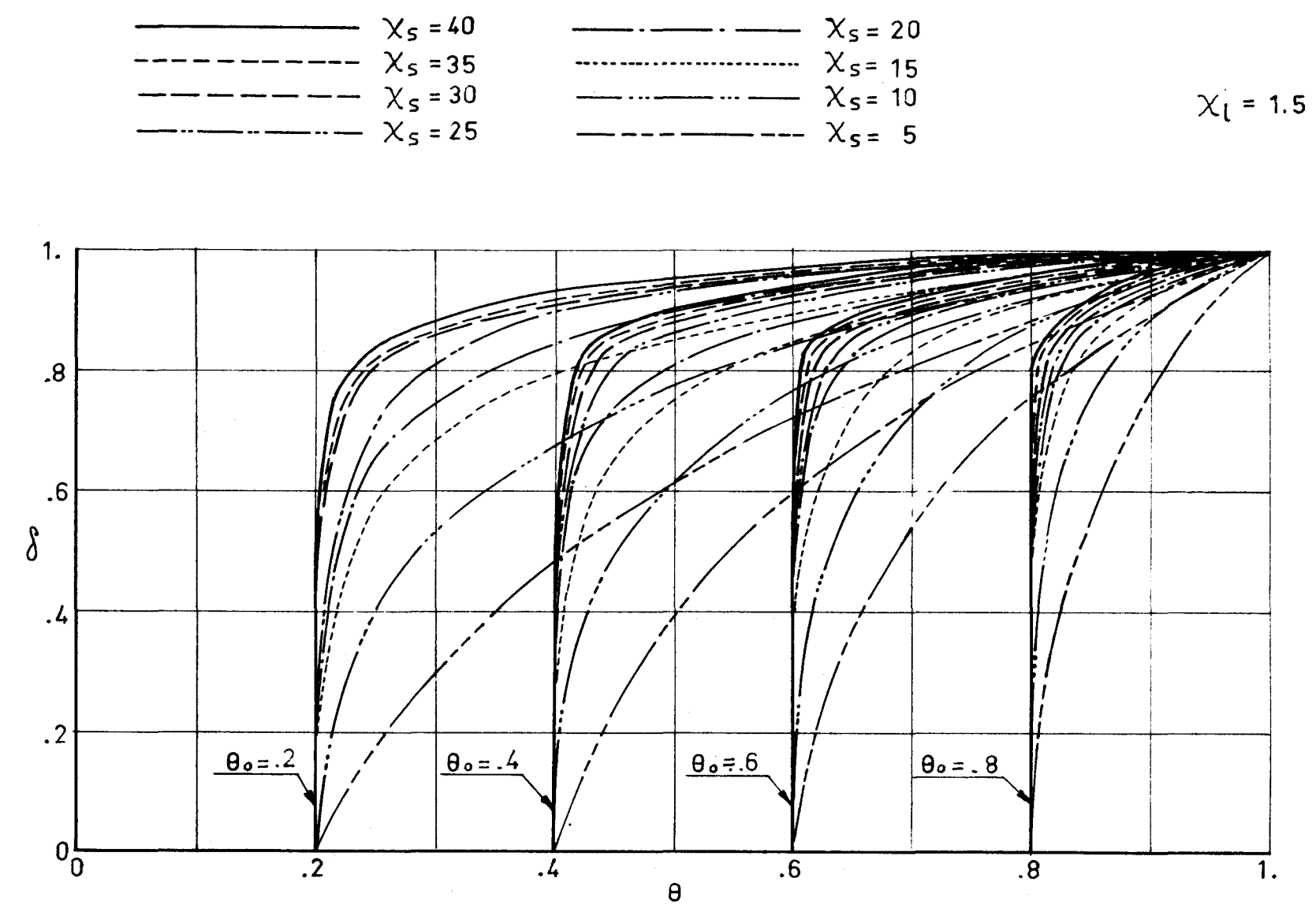

DIMENSIONLESS TEMPERATURE PROFILES FOR SEVERAL VALUES OF χ_s AND θ_o

FIG. 6

FIG. 7

× ——— $\xi = \frac{\dot{m}_b}{\dot{m}}$ = 0.91

△ – – – – – = 0.71

○ —·—·—·— = 0.25

N – HEPTANE

D_V = 50 cm

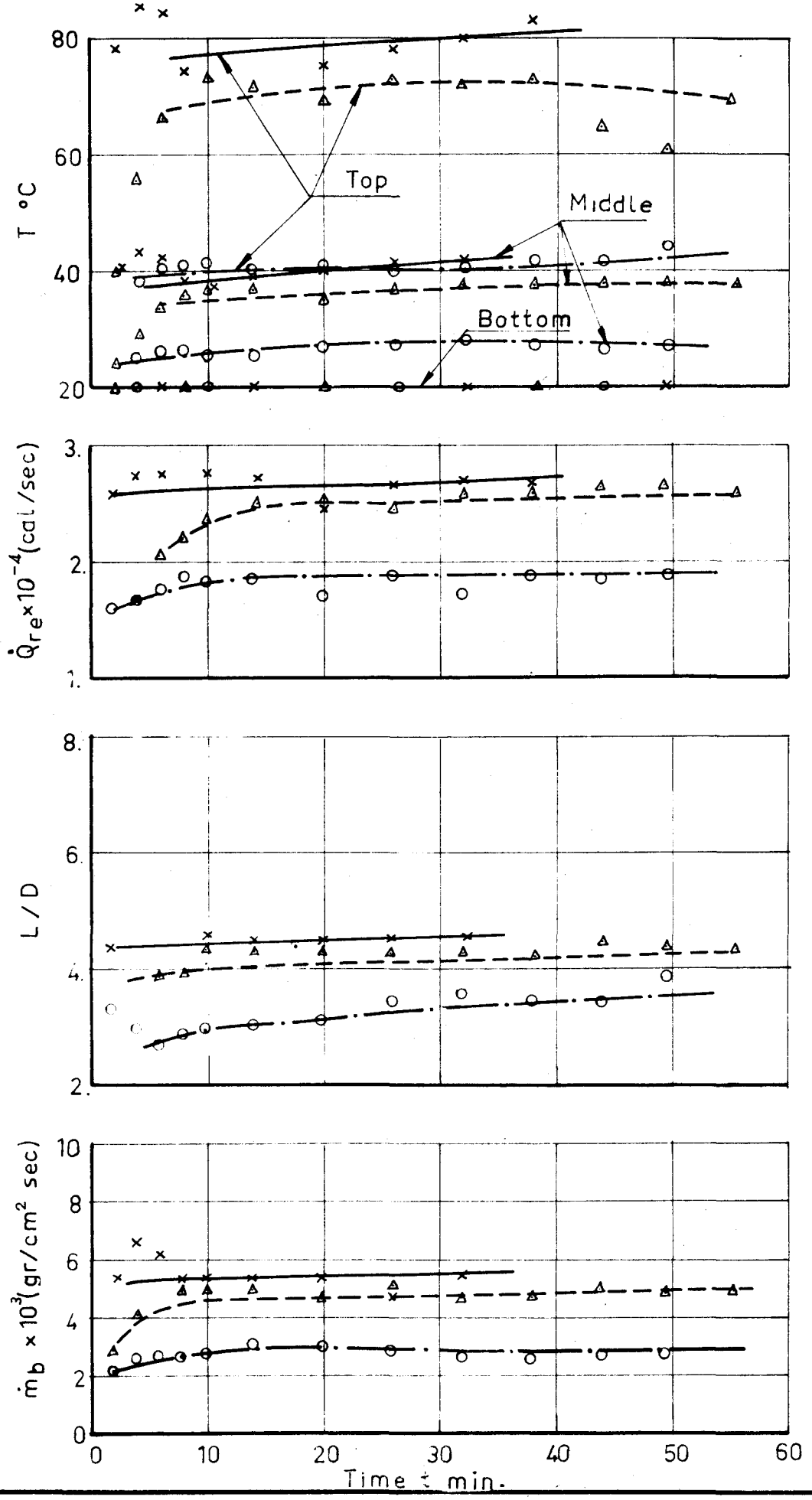

FIG. 8

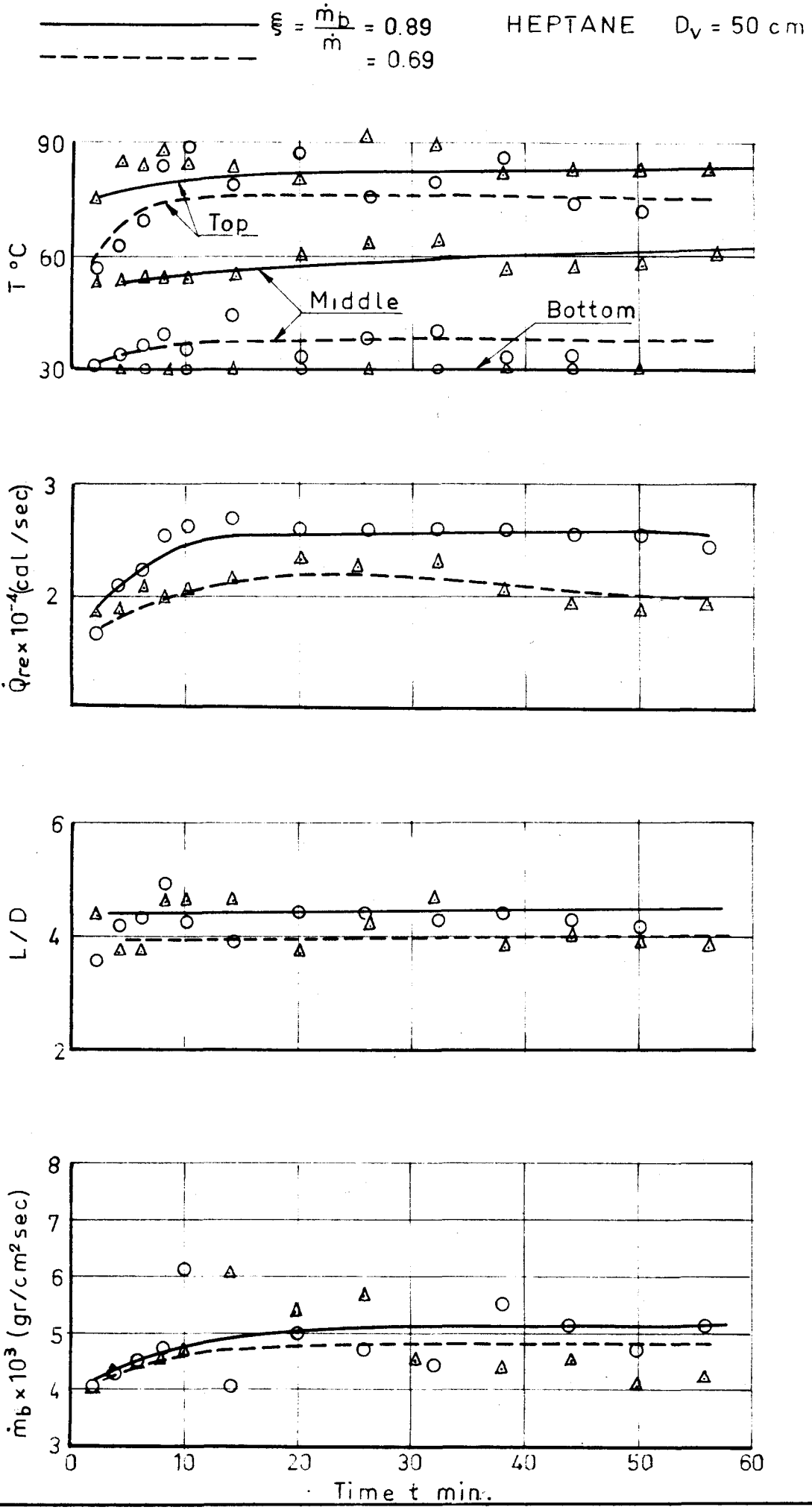
ξ = ṁb/ṁ = 0.89
= 0.69
HEPTANE Dv = 50 cm
T °C
90
60
30
Top
Middle
Bottom
Q̇re × 10⁻⁴(cal/sec)
3
2
L/D
6
4
2
ṁb × 10³ (gr/cm²sec)
8
7
6
5
4
3
0
10
20
30
40
50
60
Time t min.

FIG. 9

N - HEPTANE

D_V = 50 cm

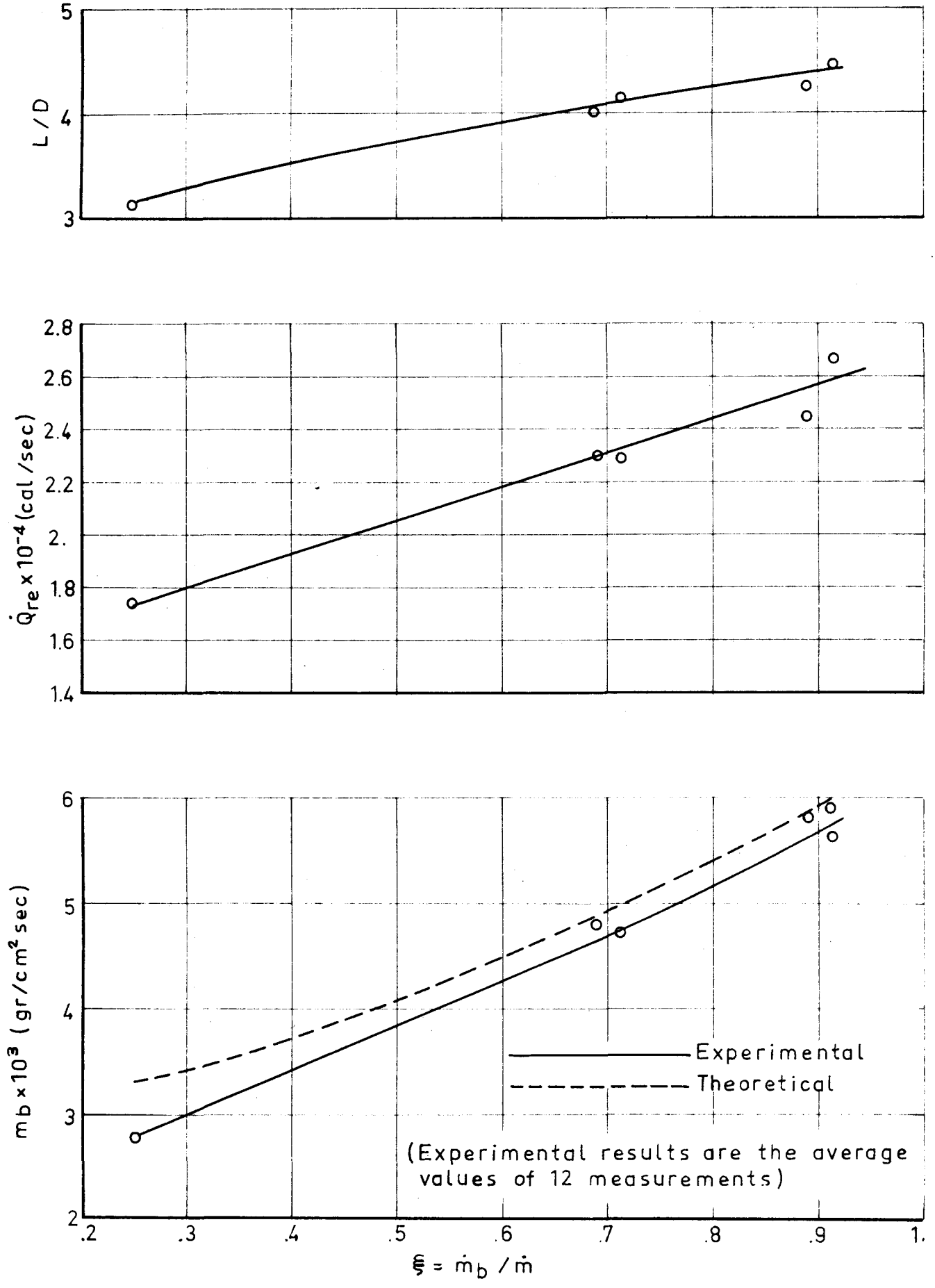

FIG. 10

100 % ξ = 0.22

75 % ξ = 0.34

DIOXANE D_V = 50 cm

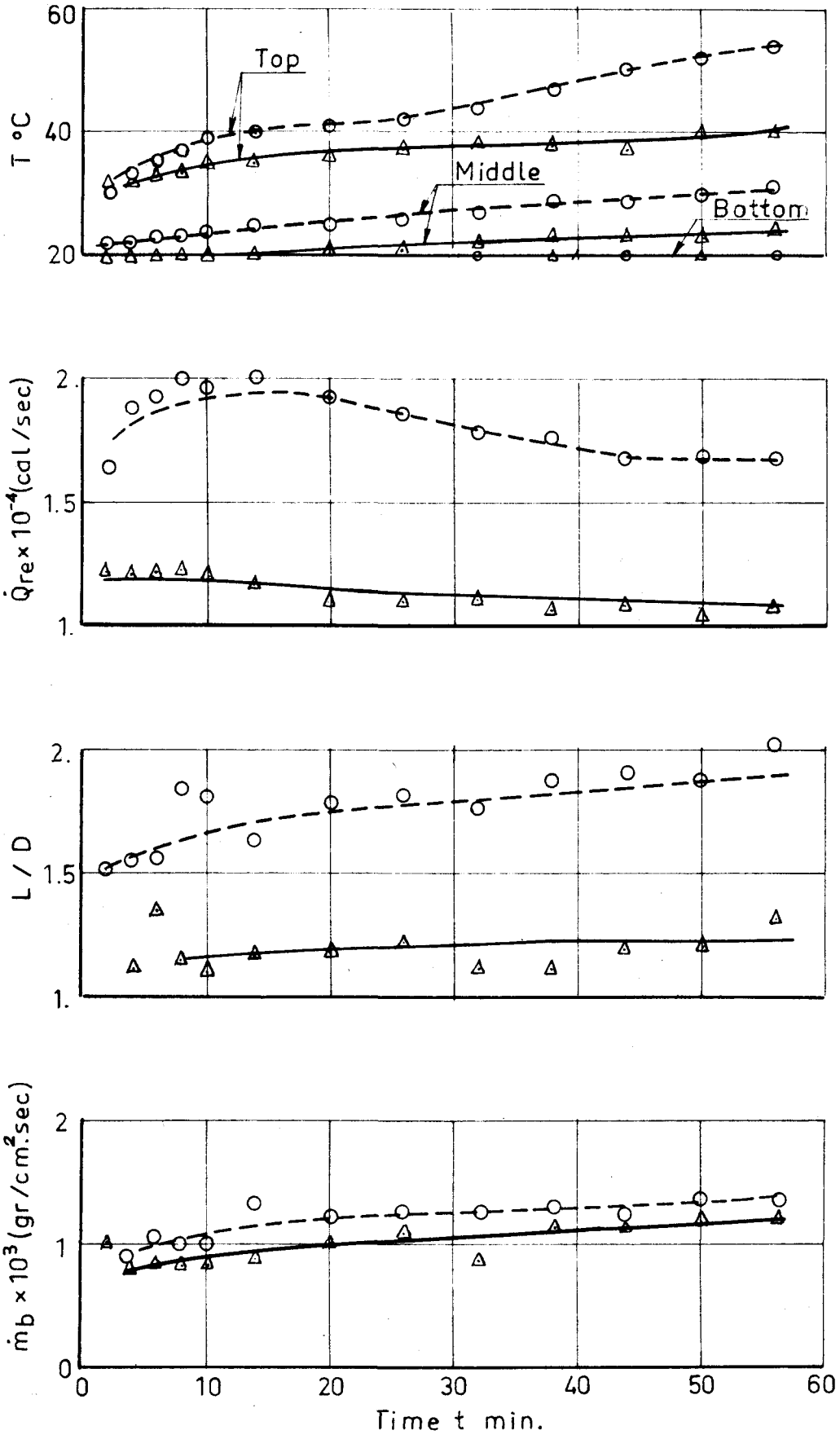

FIG. 11

DIOXANE

D_V = 50 cm

——— Experimental result

- - - - - - - Theoretical result

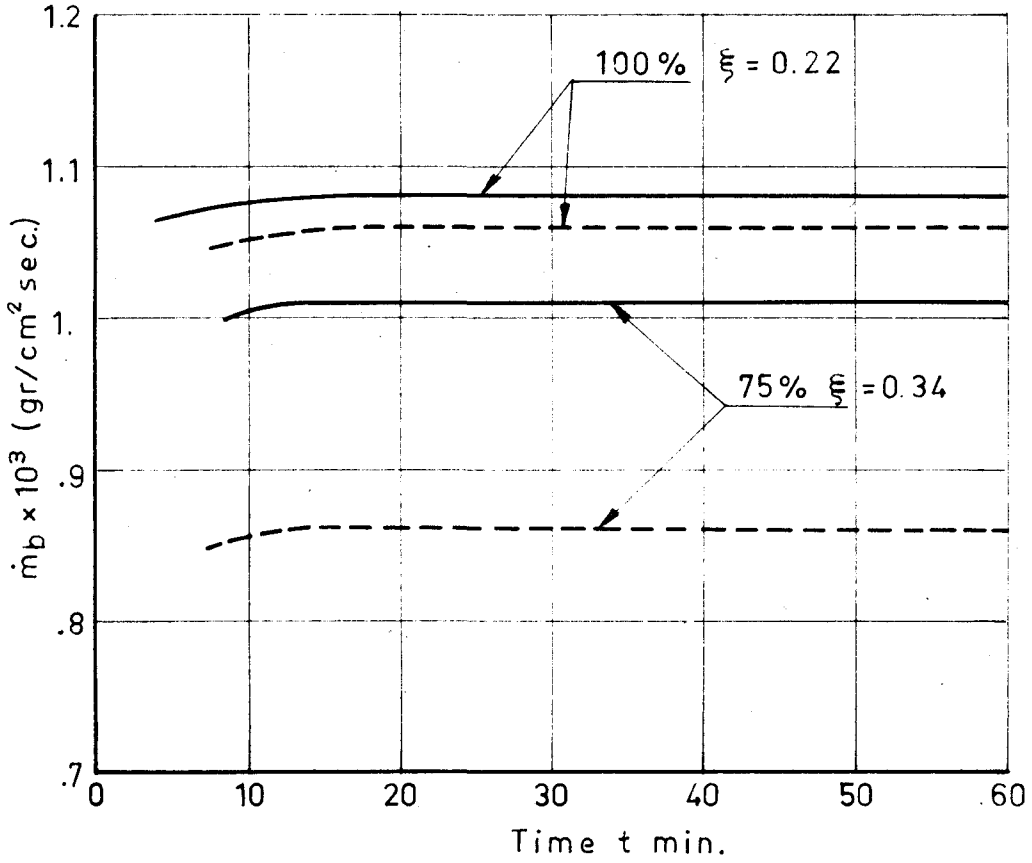

COMPARISON OF RESULTS

FIG. 12

OPEN FIRE MODEL

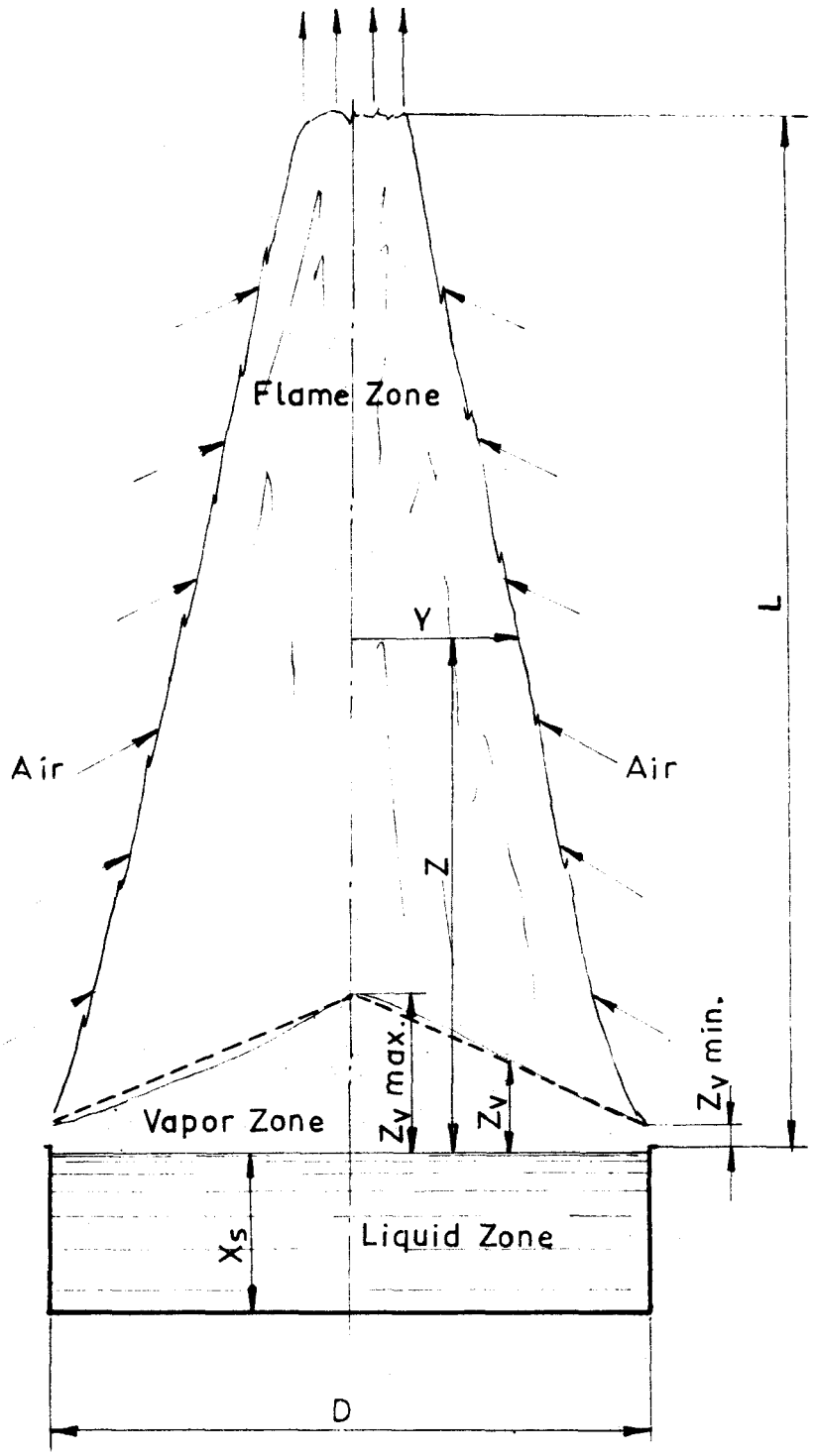

FIG. 13

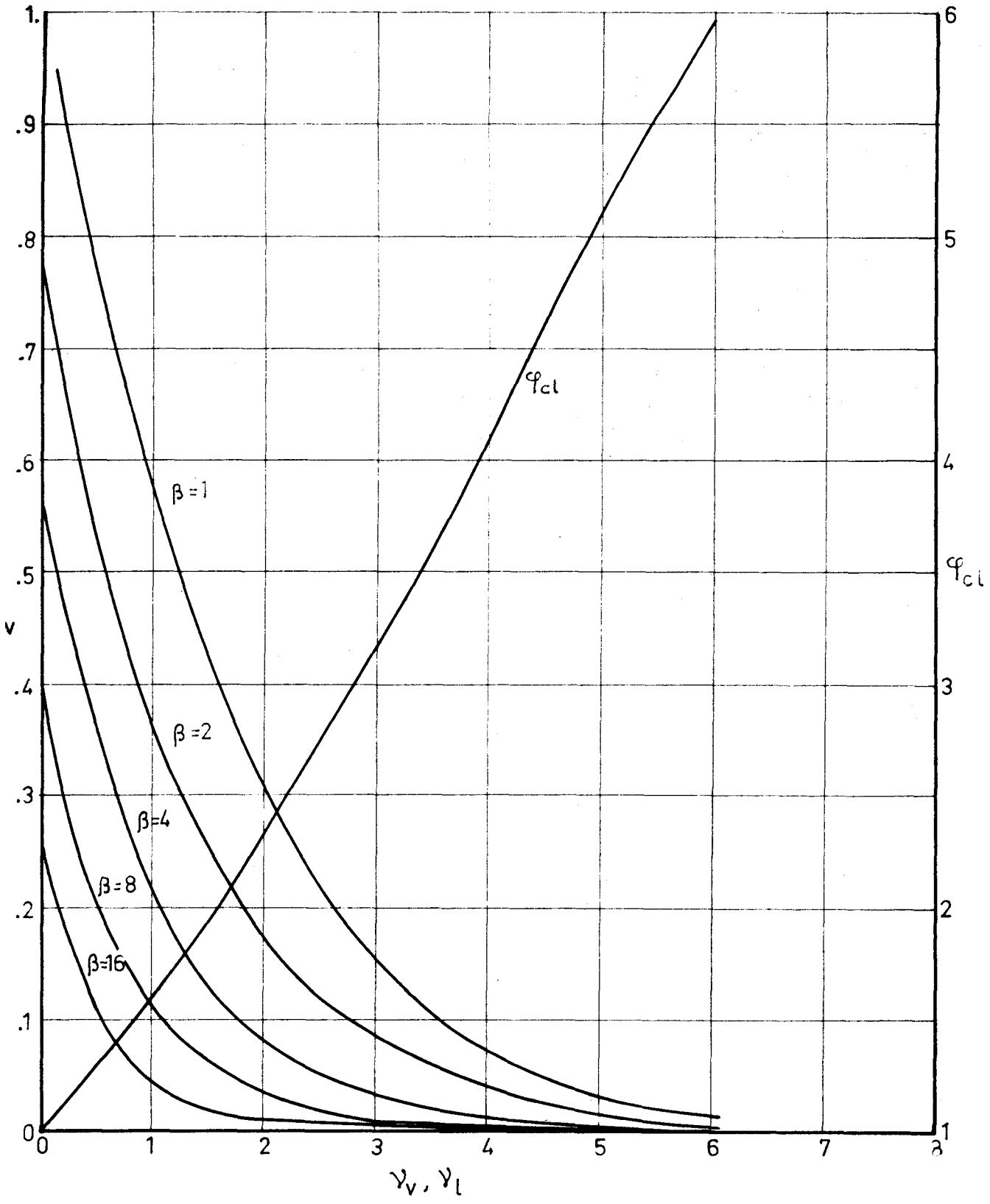
1.
.9
.8
.7
.6
.5
.4
.3
.2
.1
0
v
0
1
2
3
4
5
6
7
8
γ_v , γ_l
φ_{cl}
β = 1
β = 2
β=4
β = 8
β=16
6
5
4
3
2
1
φ_{cl}

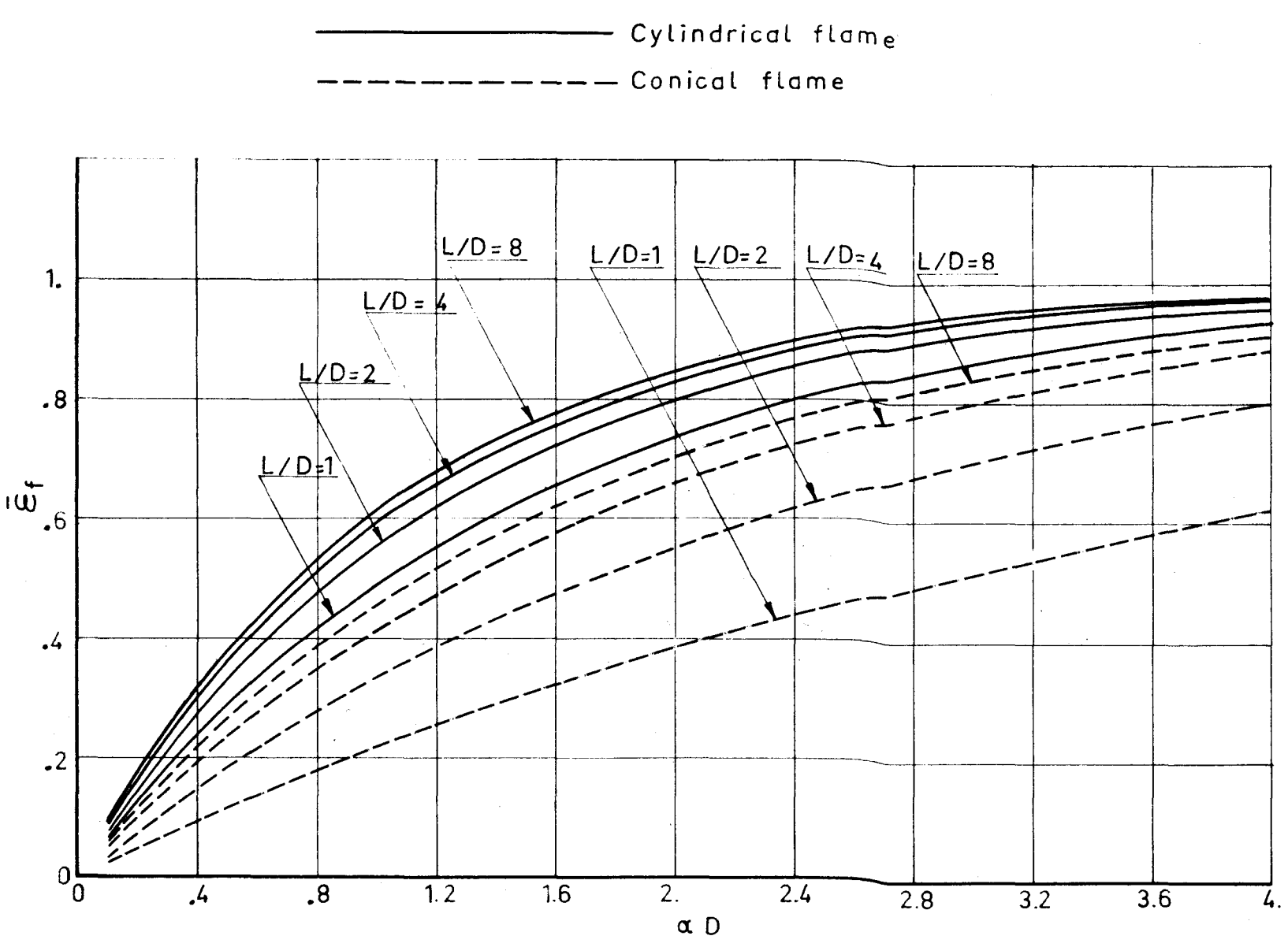
Cylindrical flame
Conical flame
L/D = 8
L/D = 4
L/D=2
L/D=1
L/D=1
L/D=2
L/D=4
L/D=8
$\bar{\varepsilon}_f$
1.
.8
.6
.4
.2
0
0
.4
.8
1.2
1.6
2.
2.4
2.8
3.2
3.6
4.
α D

FIG. 14

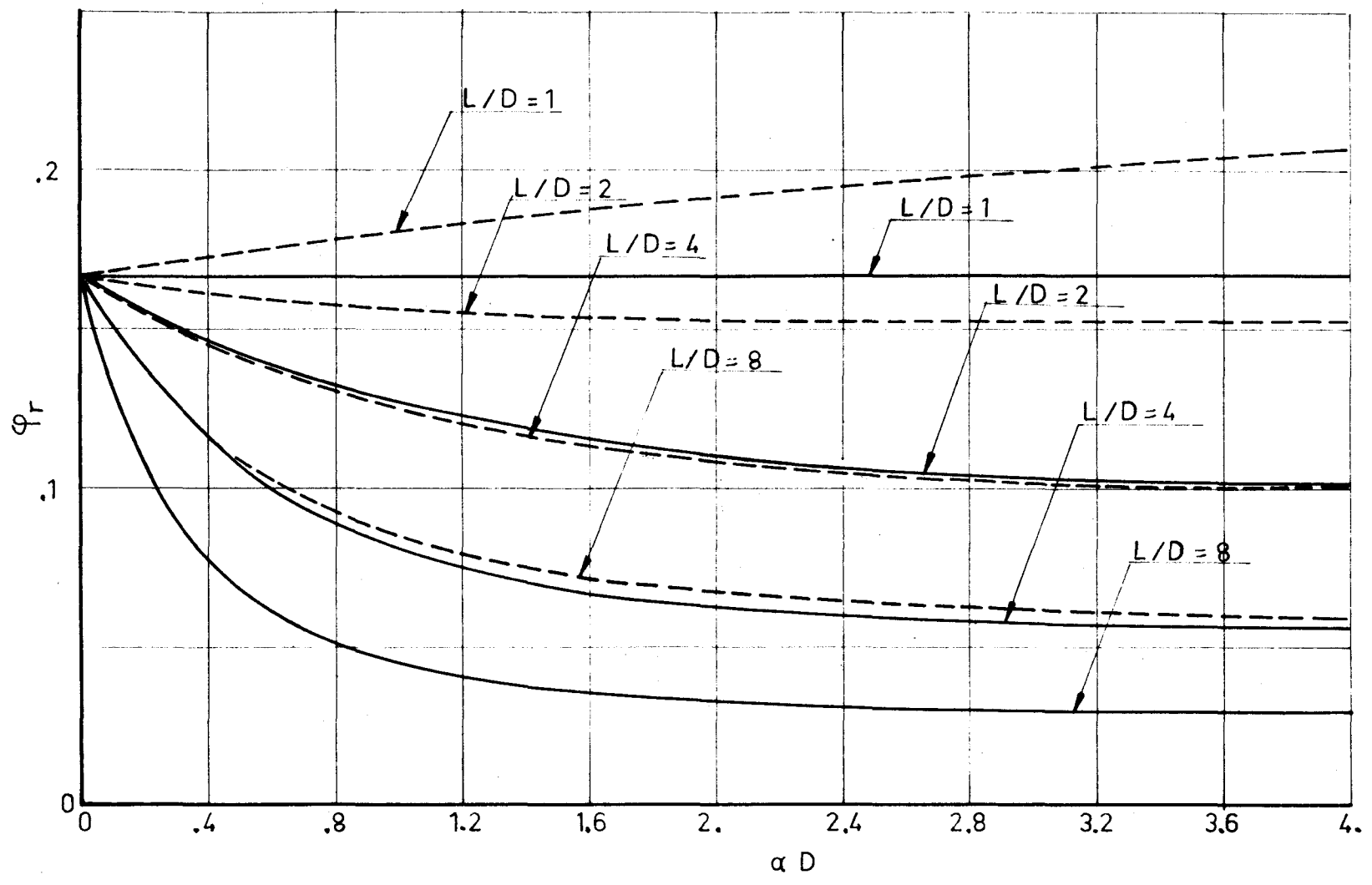
Cylindrical flame
Conical flame
L/D = 1
L/D = 2
L/D = 4
L/D = 8
L/D = 1
L/D = 2
L/D = 4
L/D = 8
φ_r
.2
.1
0
0
.4
.8
1.2
1.6
2.
2.4
2.8
3.2
3.6
4.
α D

FIG. 15

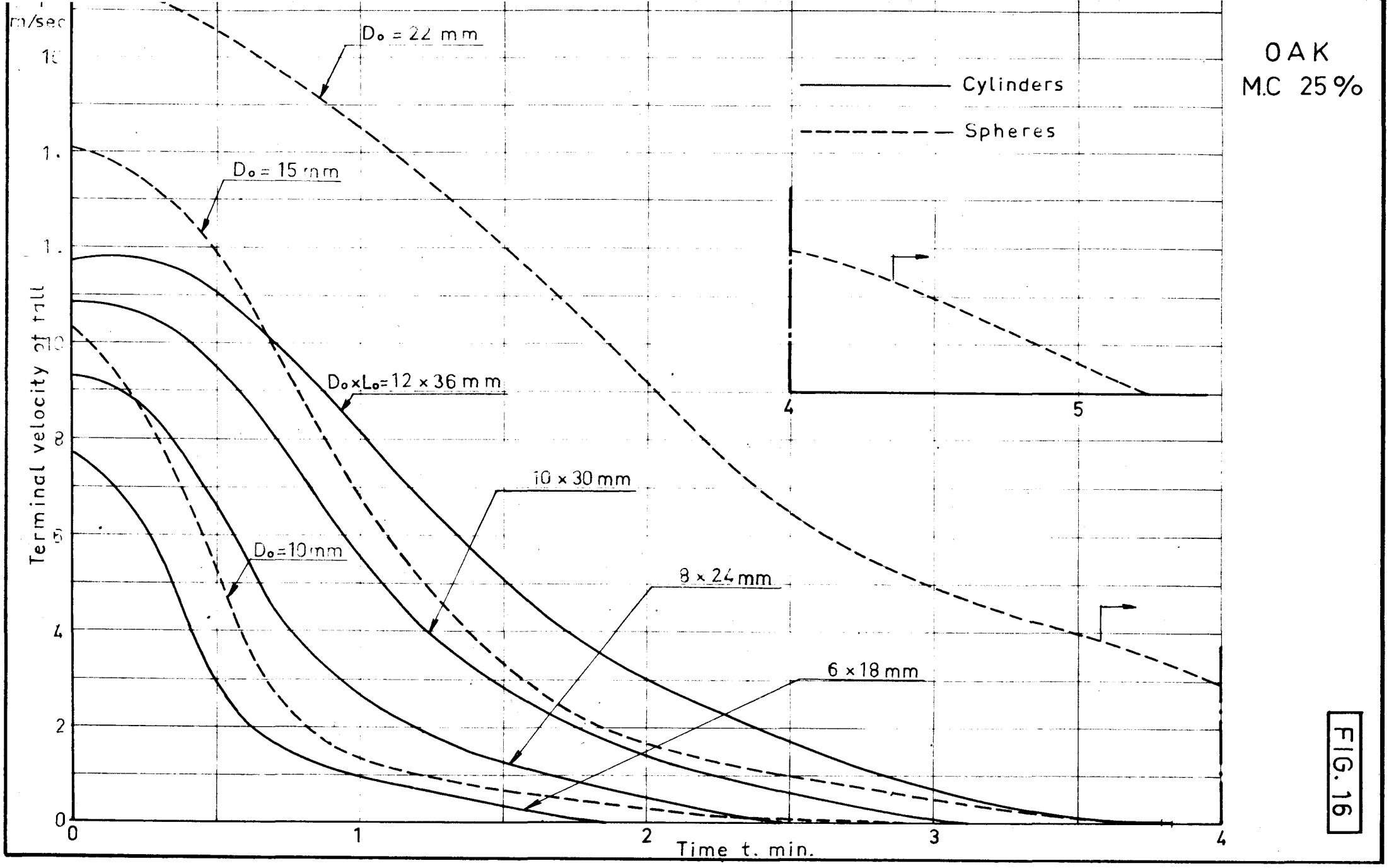
OAK
M.C 25%
Cylinders
Spheres
D_o = 22 mm
D_o = 15 mm
$D_o \times L_o$ = 12 × 36 mm
10 × 30 mm
8 × 24 mm
6 × 18 mm
D_o = 10 mm
Terminal velocity of fall
m/sec
Time t. min.
0
1
2
3
4
5
4
2

FIG. 16

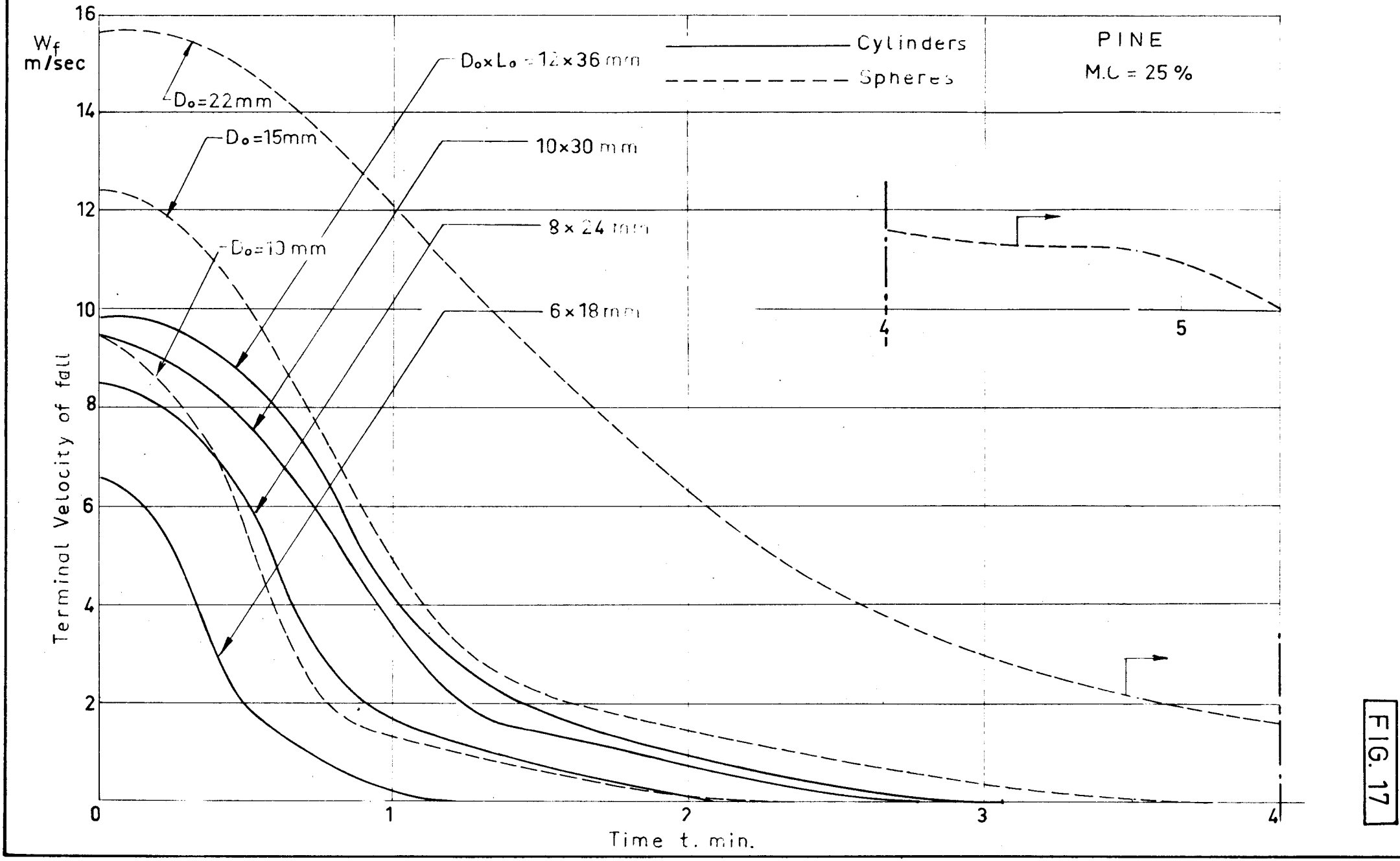
W_f m/sec
Terminal Velocity of fall
Time t. min.
Cylinders
Spheres
PINE
M.C = 25 %
D_o=22mm
D_o=15mm
D_o=10 mm
$D_o \times L_o$ = 12×36 mm
10×30 mm
8×24 mm
6×18 mm
0
1
2
3
4
5
2
4
6
8
10
12
14
16

FIG. 17

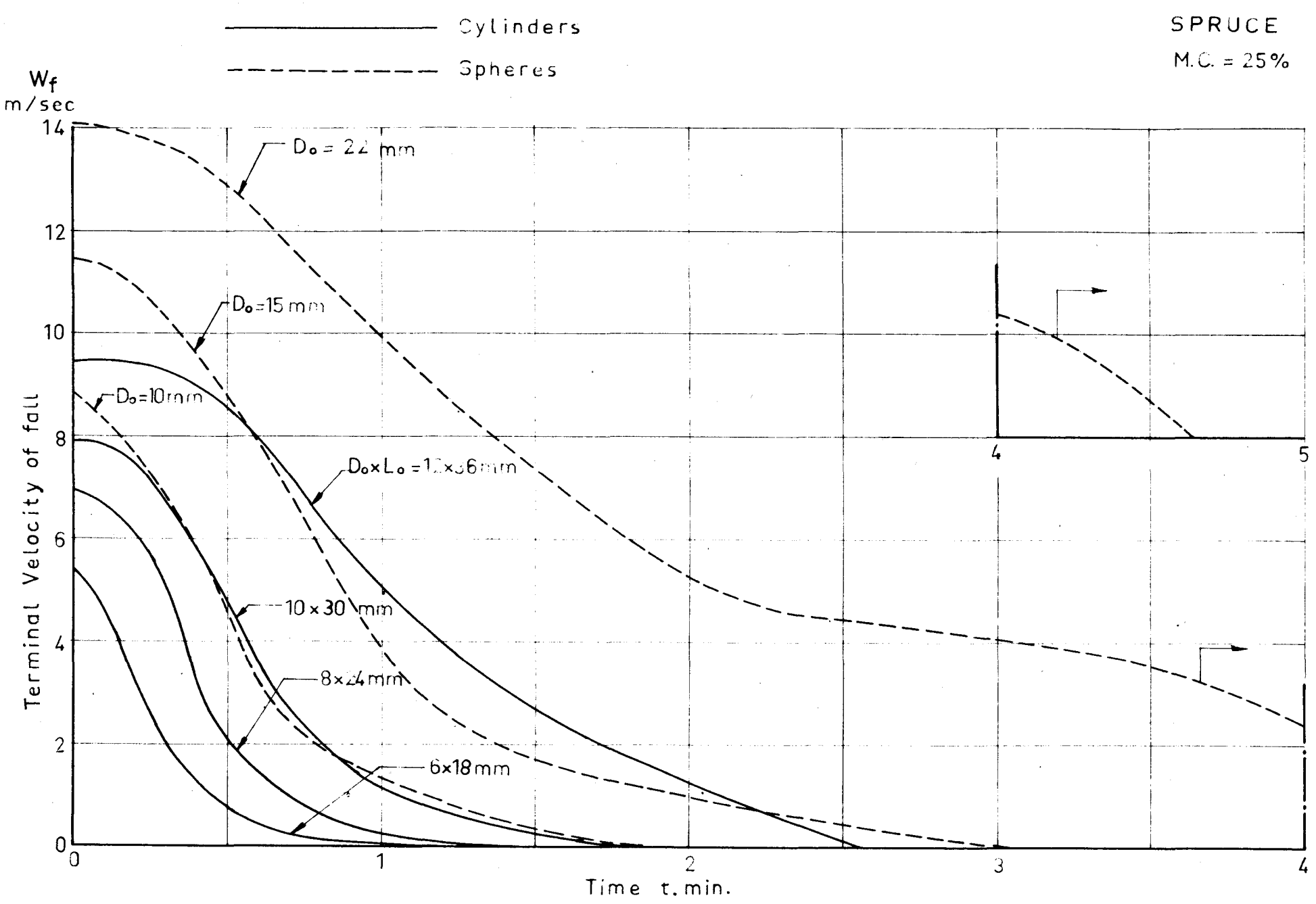
Cylinders
Spheres
SPRUCE
M.C. = 25%
W_f
m/sec
D_o = 22 mm
D_o=15 mm
D_o=10mm
$D_o \times L_o$ = 10×36mm
10 × 30 mm
8×24mm
6×18mm
Terminal Velocity of fall
Time t. min.
0
1
2
3
4
5
6
8
10
12
14

FIG. 18

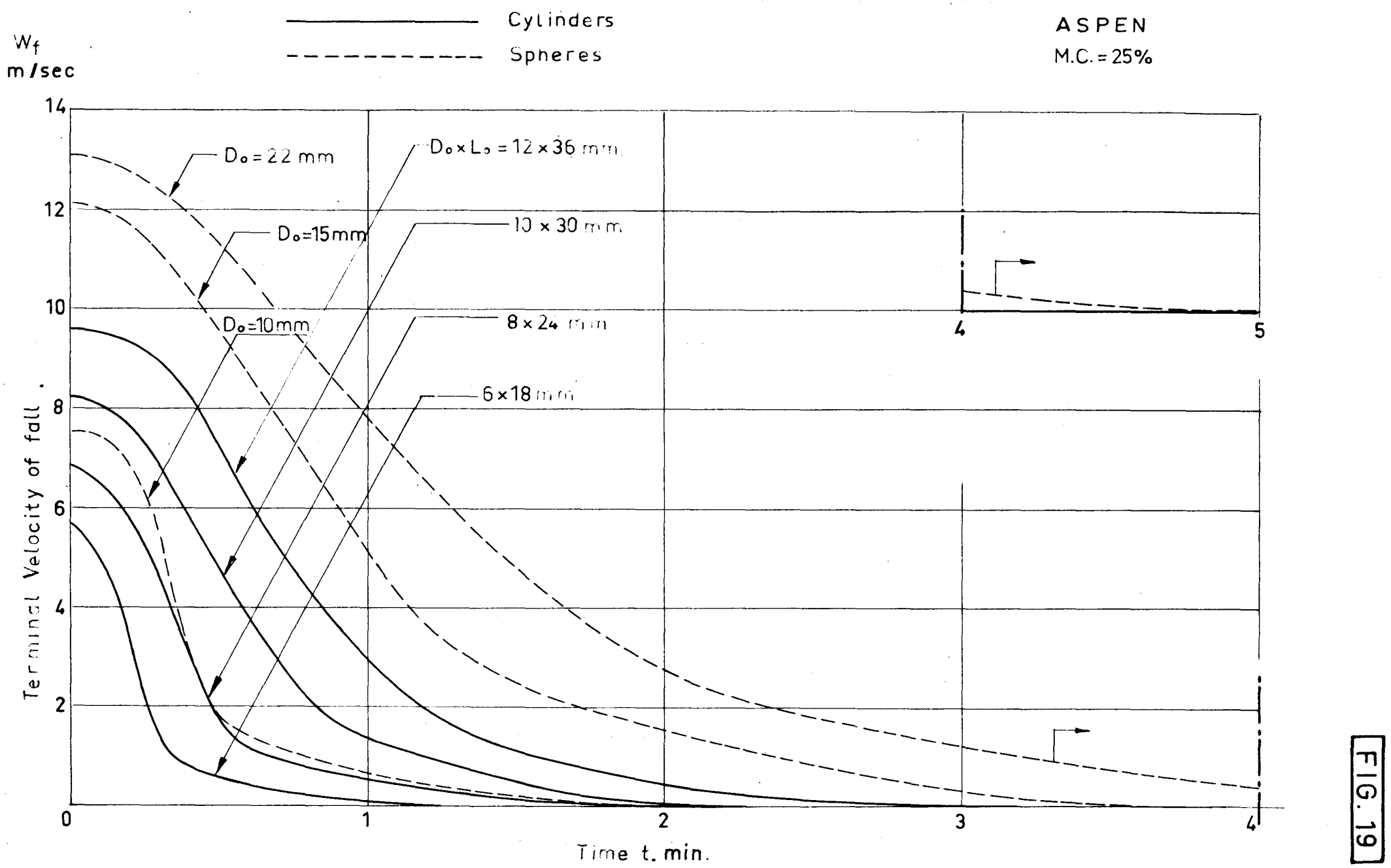
Cylinders
Spheres
ASPEN
M.C. = 25%
W_f
m/sec
D_o = 22 mm
D_o × L_o = 12 × 36 mm
D_o = 15 mm
10 × 30 mm
D_o = 10 mm
8 × 24 mm
6 × 18 mm
Terminal Velocity of fall .
Time t. min.
0
1
2
3
4
5
6
8
10
12
14

FIG. 19

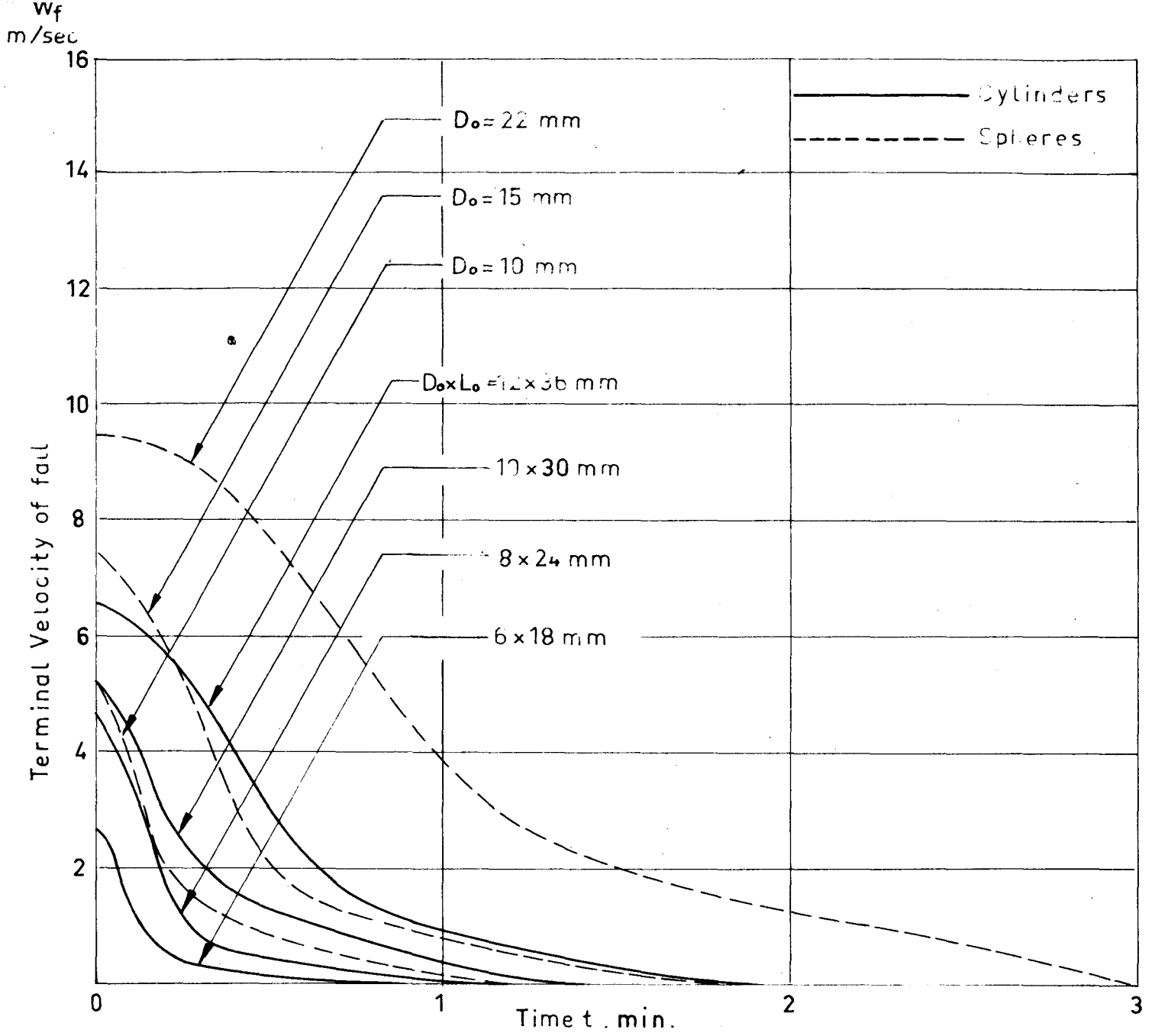

BALSA

M.C. = 25%

FIG. 20

FIG. 21

PINE
SPHERES
M.C.= 25 %

——— D_o = 22 mm
– – – – – D_o = 15 mm
—·—·— D_o = 10 mm

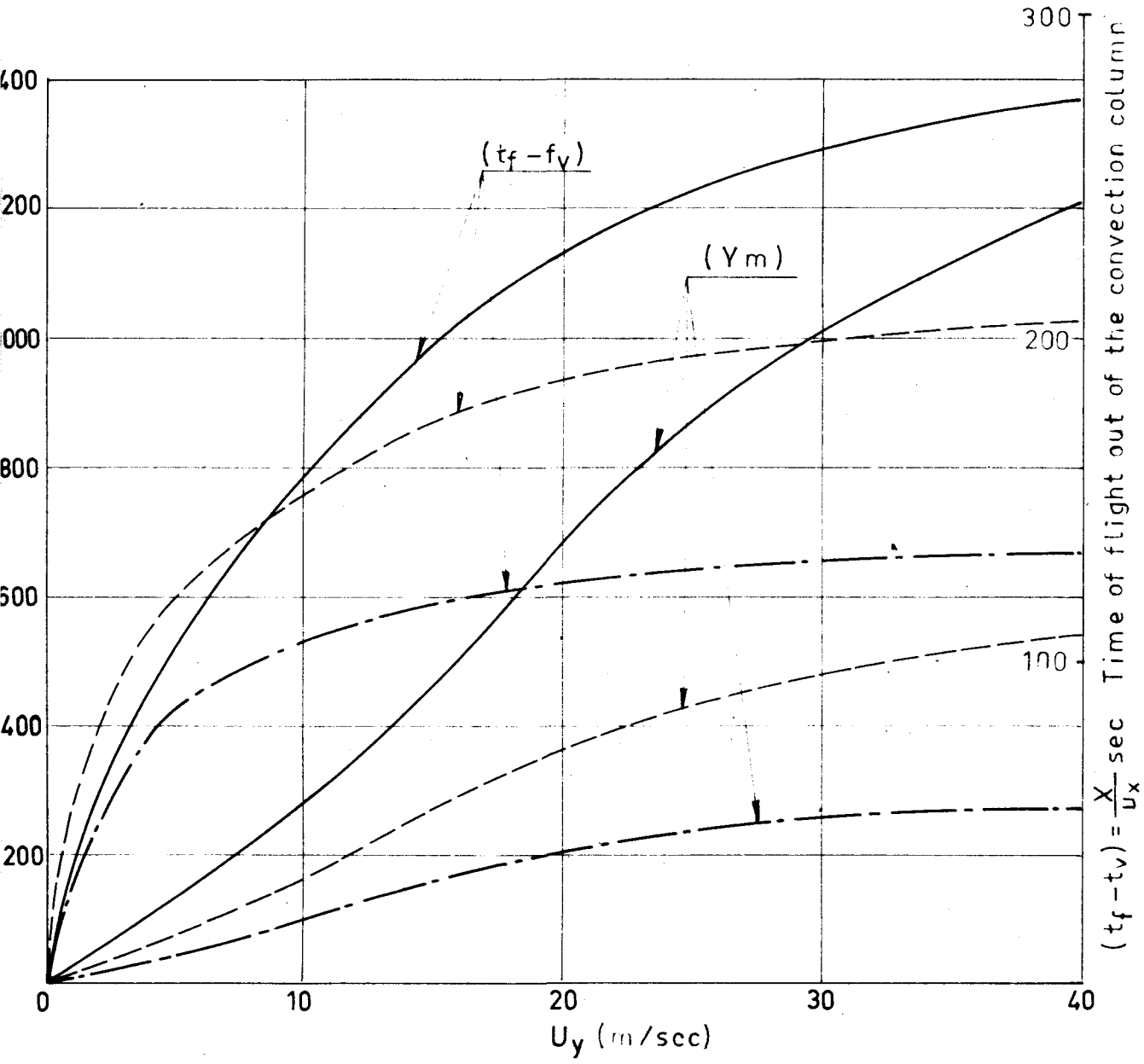

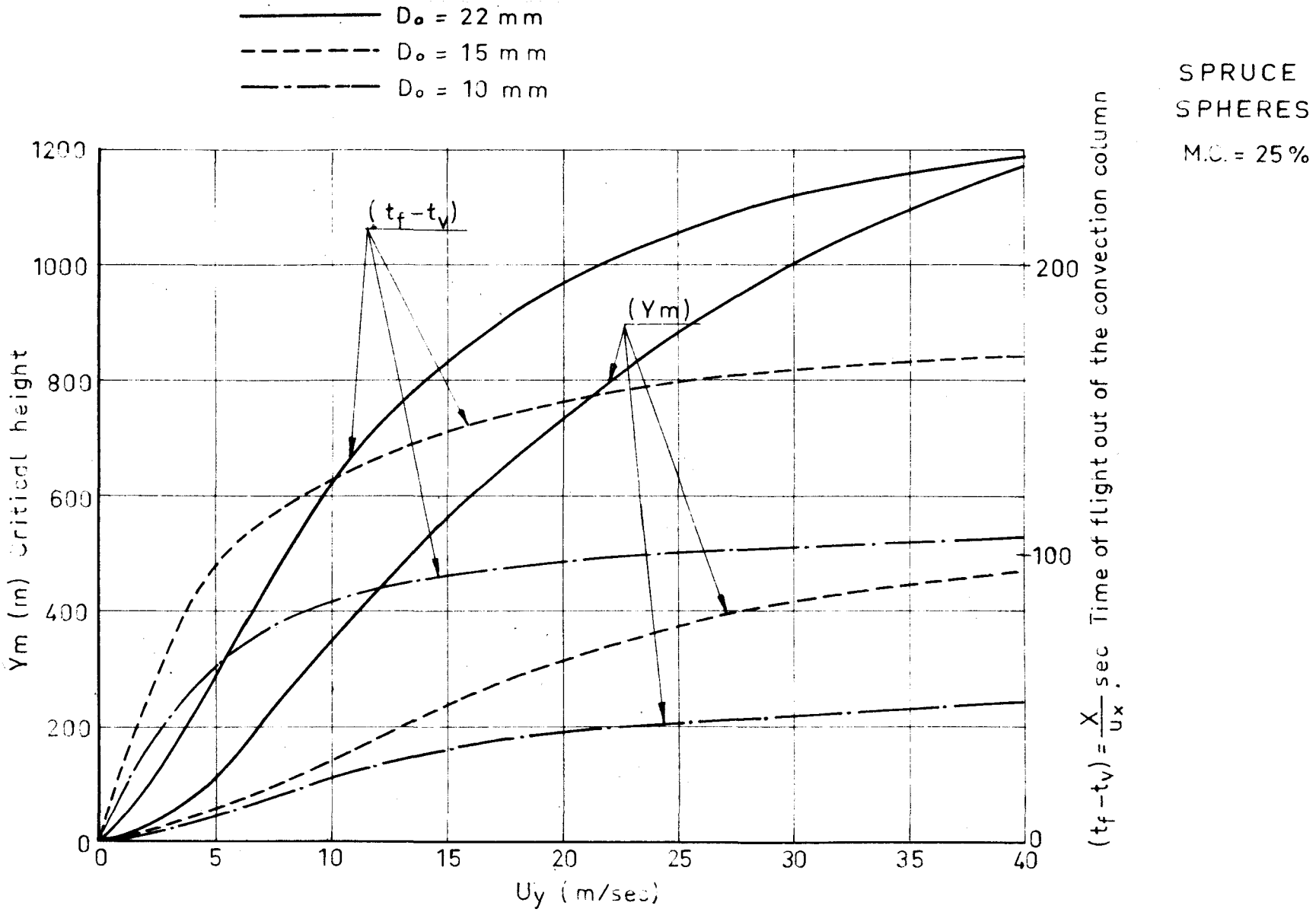
D₀ = 22 mm
D₀ = 15 mm
D₀ = 10 mm
SPRUCE
SPHERES
M.C. = 25 %
(tf − tv)
(Ym)
Ym (m) critical height
Uy (m/sec)
(tf − tv) = X/ux sec Time of flight out of the convection column
0
200
400
600
800
1000
1200
5
10
15
20
25
30
35
40
100

FIG. 22

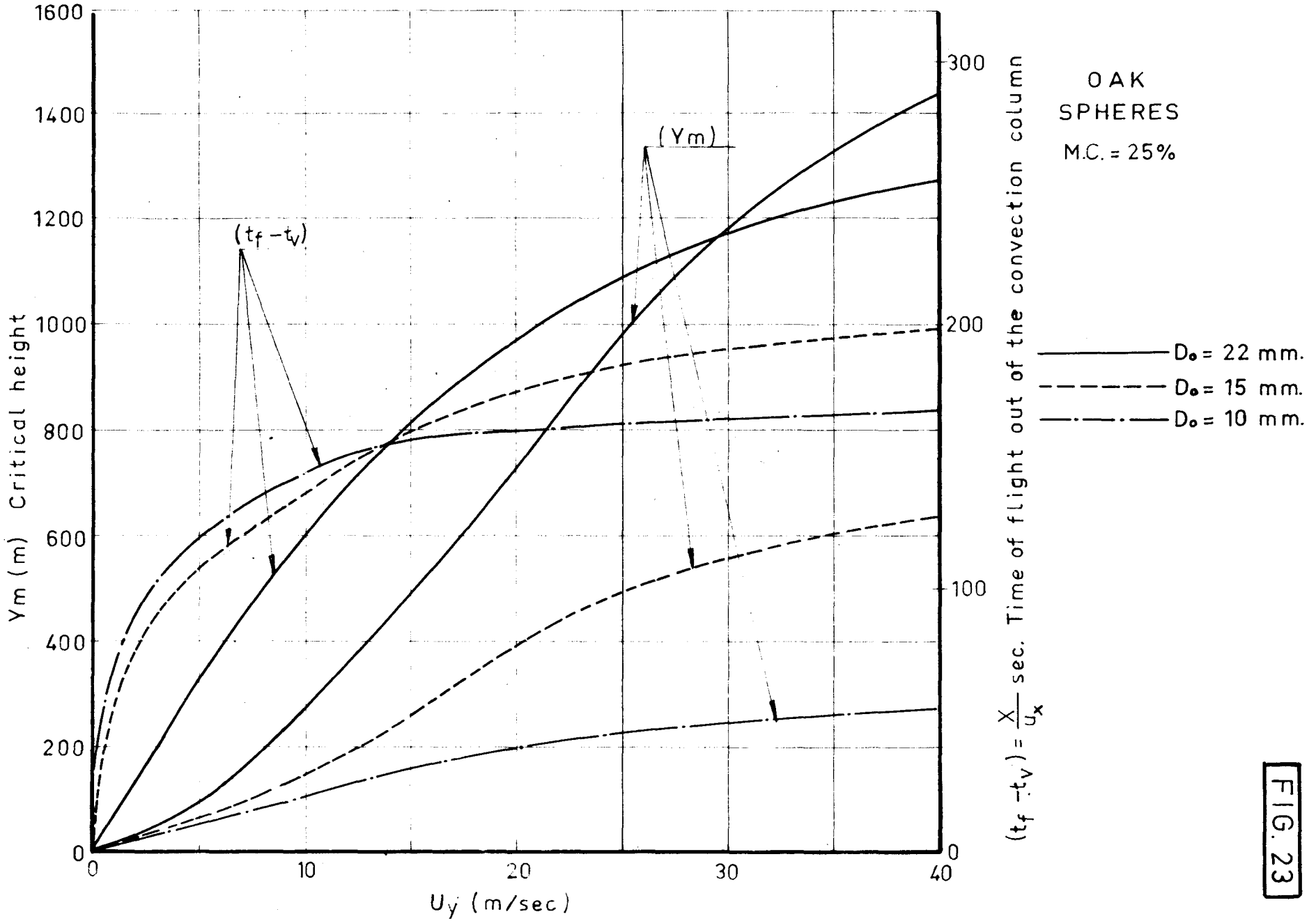
1600
1400
1200
1000
800
600
400
200
0
Ym (m) Critical height
0
10
20
30
40
Uy (m/sec)
300
200
100
0
(tf - tv) = X/ux sec. Time of flight out of the convection column
(Ym)
(tf - tv)
OAK
SPHERES
M.C. = 25%
Do = 22 mm.
Do = 15 mm.
Do = 10 mm.

FIG. 23

FIG. 24

ASPEN
SPHERES
M.C. = 25%

——— D_o = 22 mm
– – – – – D_o = 15 mm
—·—·— D_o = 10 mm

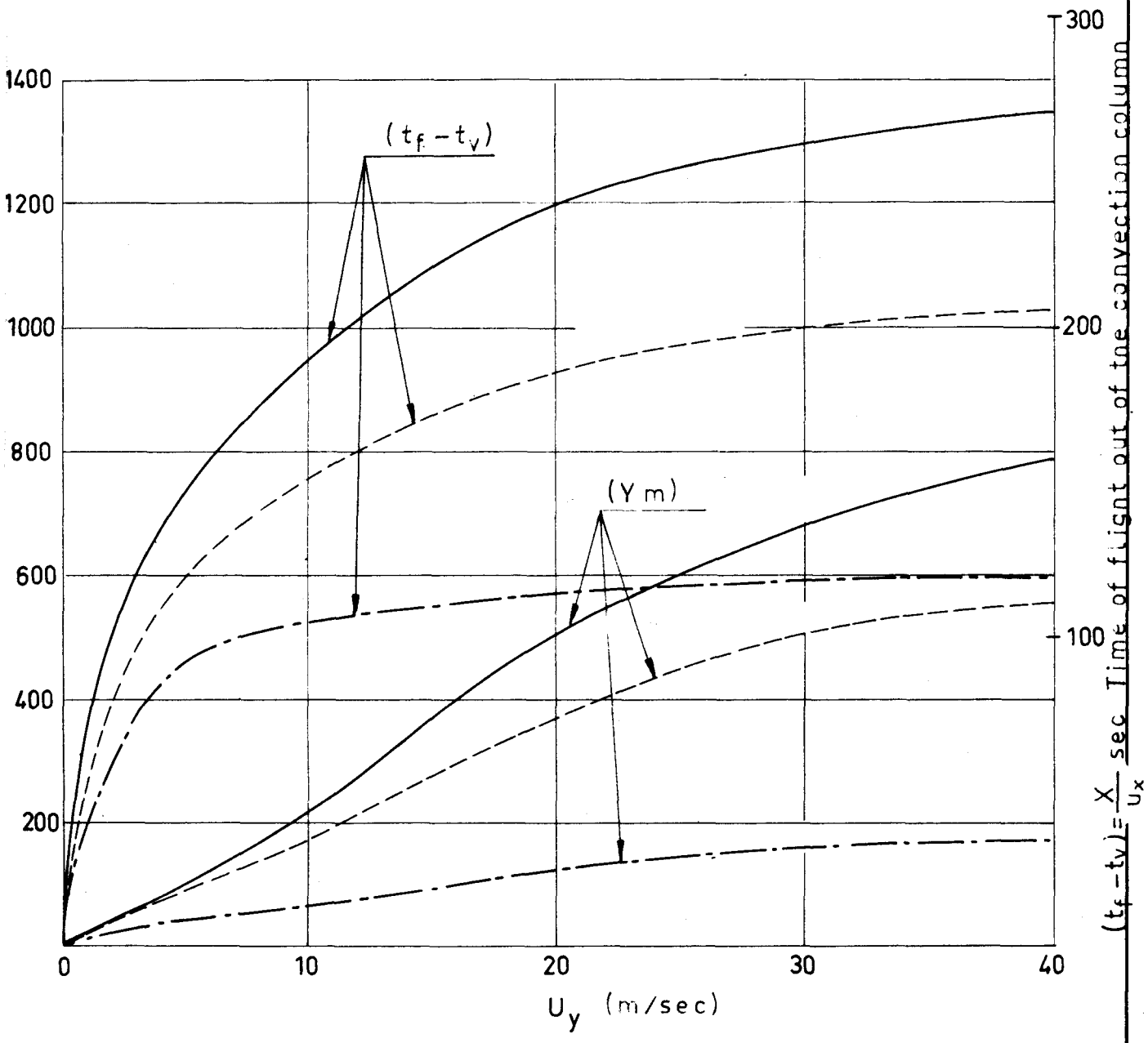

FIG. 25

BALSA
SPHERES
M.C.= 25%

——— D_o = 22 mm
– – – – D_o = 15 mm
—·—·— D_o = 10 mm

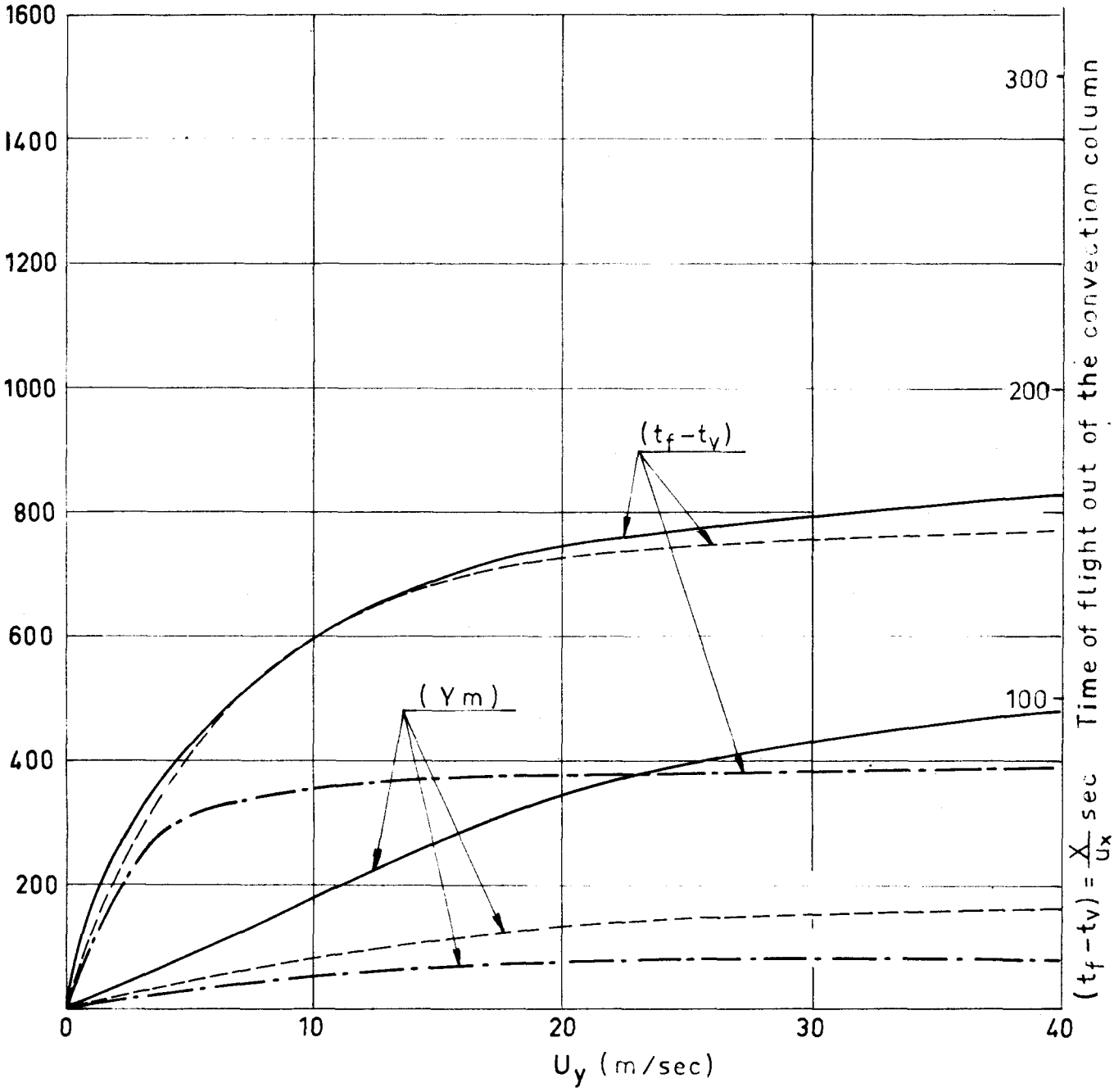

FIG. 26

PINE
CYLINDERS
M.C. = 25 %

$D_o \times L_o = 12 \times 36$
$= 10 \times 30$
$= 6 \times 18$
$= 8 \times 24$

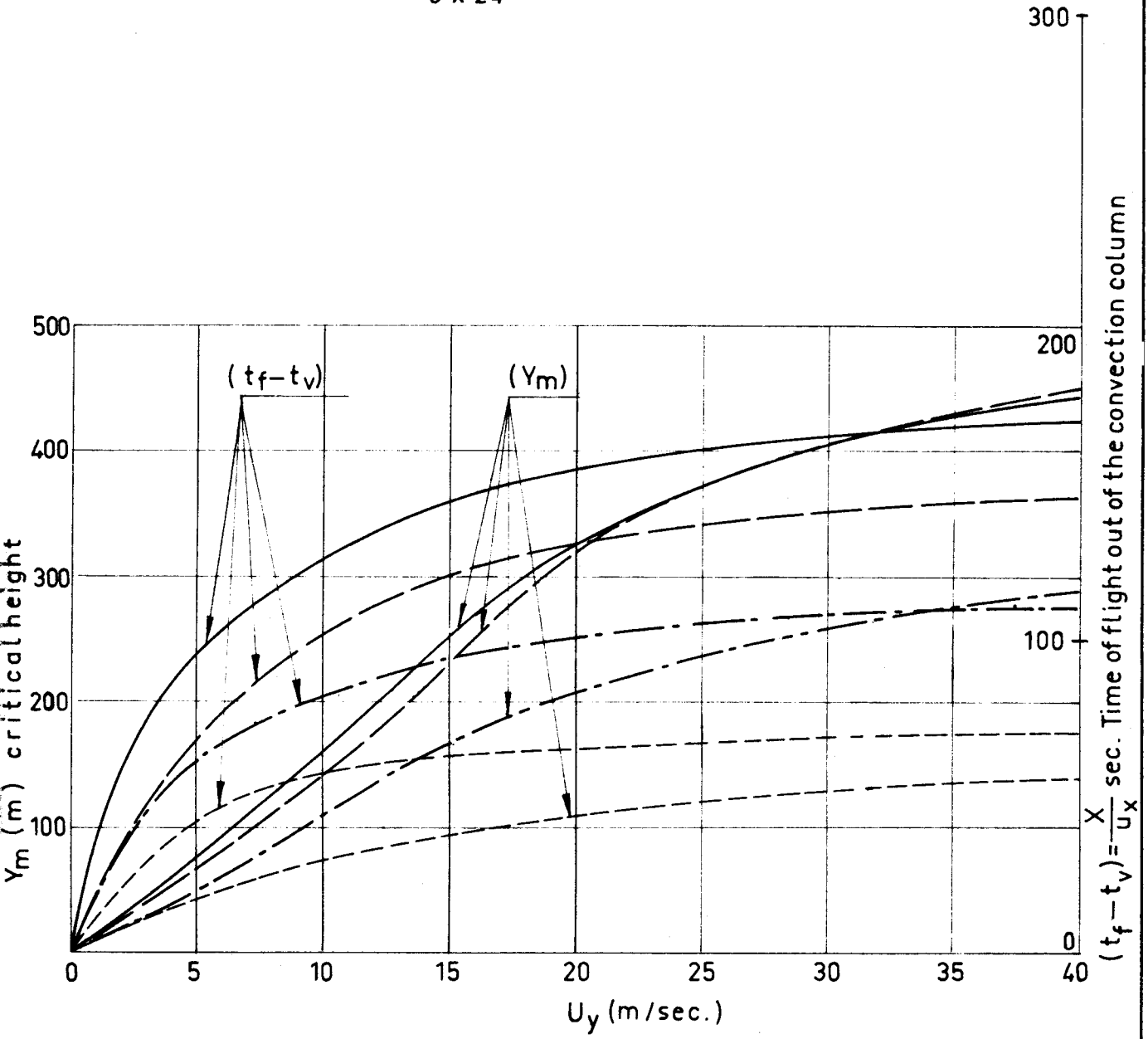

FIG: 27

SPRUCE
CYLINDERS
M.C. = 25%

$D_o \times L_o = 12 \times 36$ mm
$= 10 \times 30$ mm
$= 6 \times 18$ mm
$= 8 \times 24$ mm

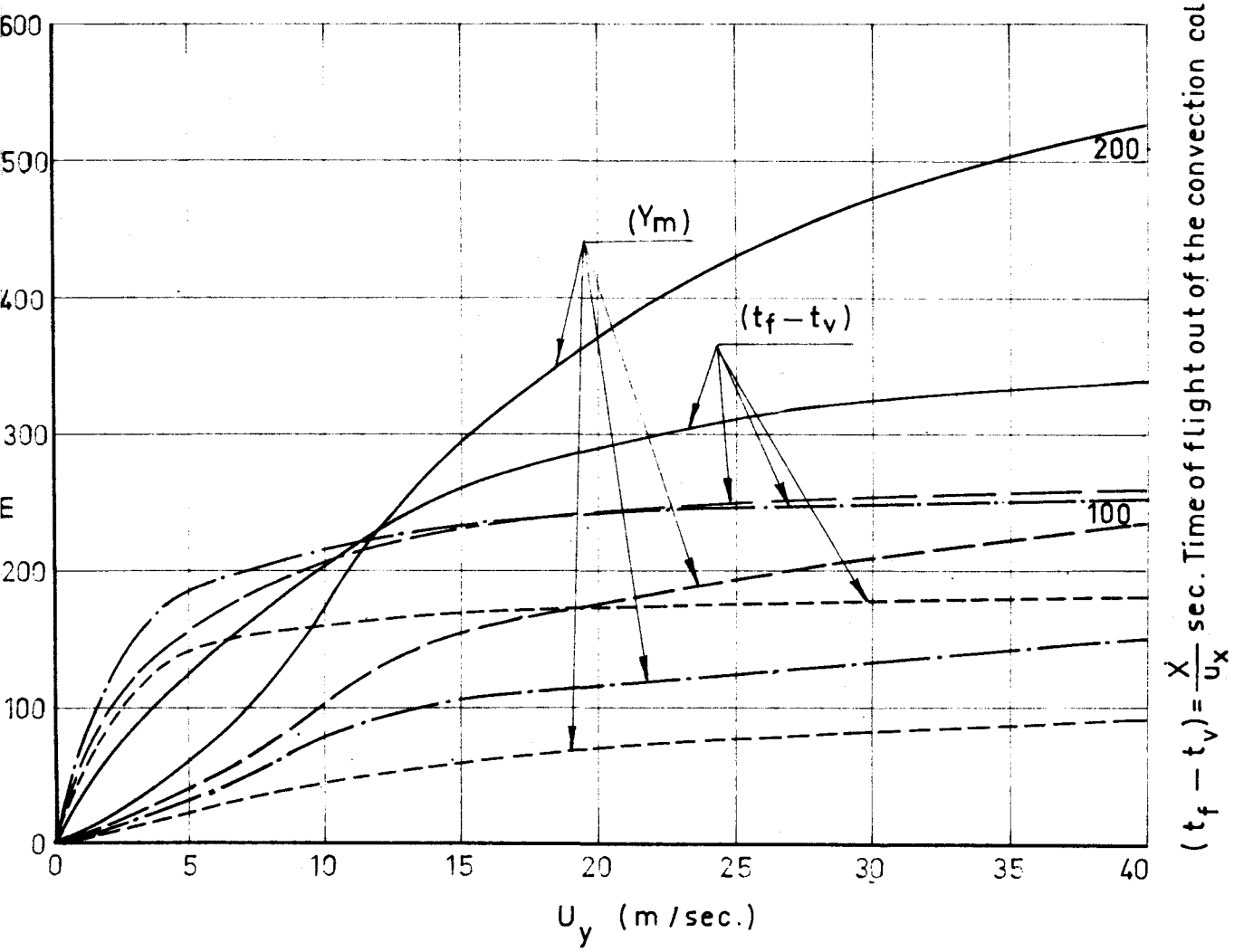

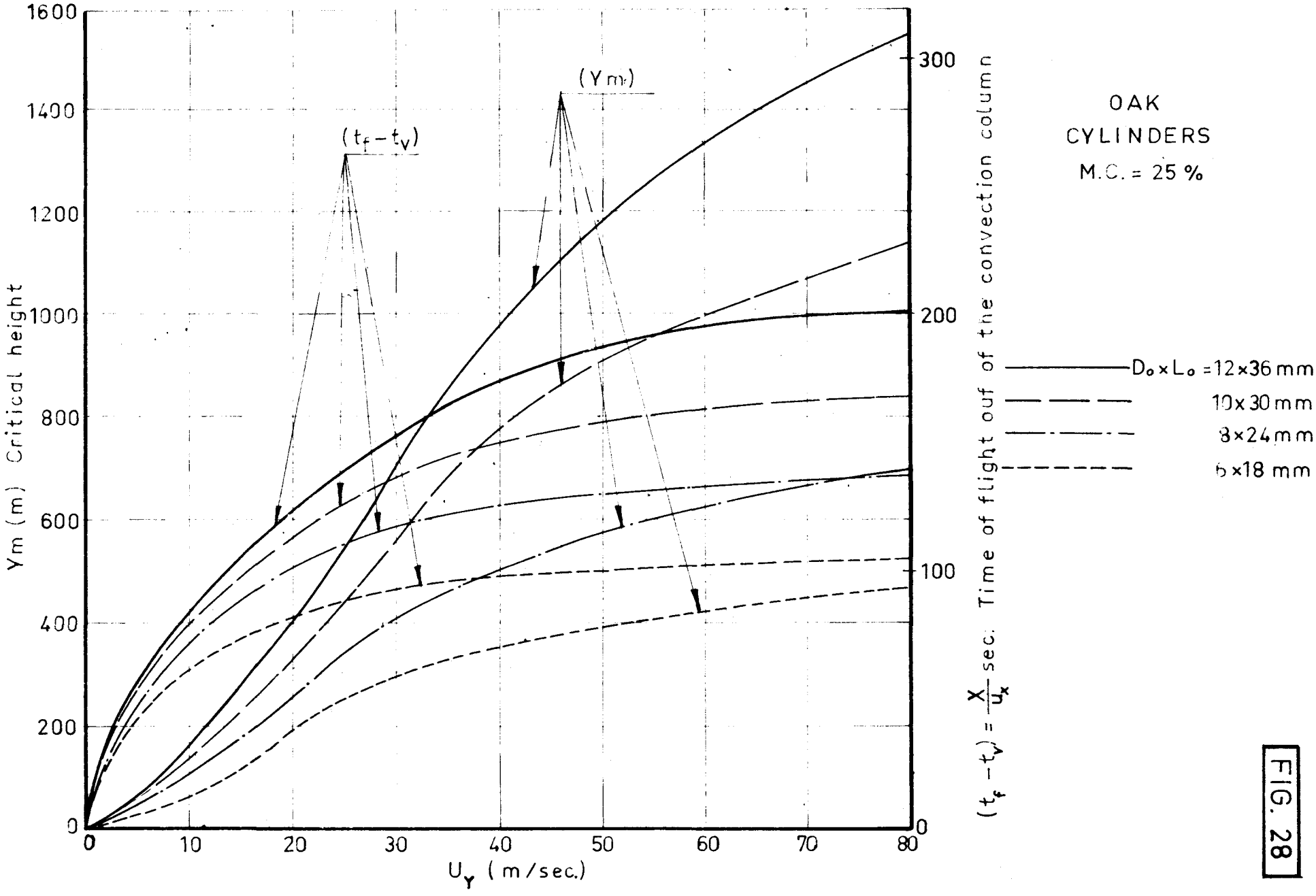
1600
1400
1200
1000
800
600
400
200
0
Ym (m) Critical height
0
10
20
30
40
50
60
70
80
U_Y (m/sec.)
$(t_f - t_v)$
(Y_m)
300
200
100
0
$(t_f - t_v) = \frac{X}{u_x}$ sec. Time of flight out of the convection column
OAK
CYLINDERS
M.C. = 25 %
$D_o \times L_o$ = 12×36 mm
10×30 mm
8×24 mm
6×18 mm

FIG. 28

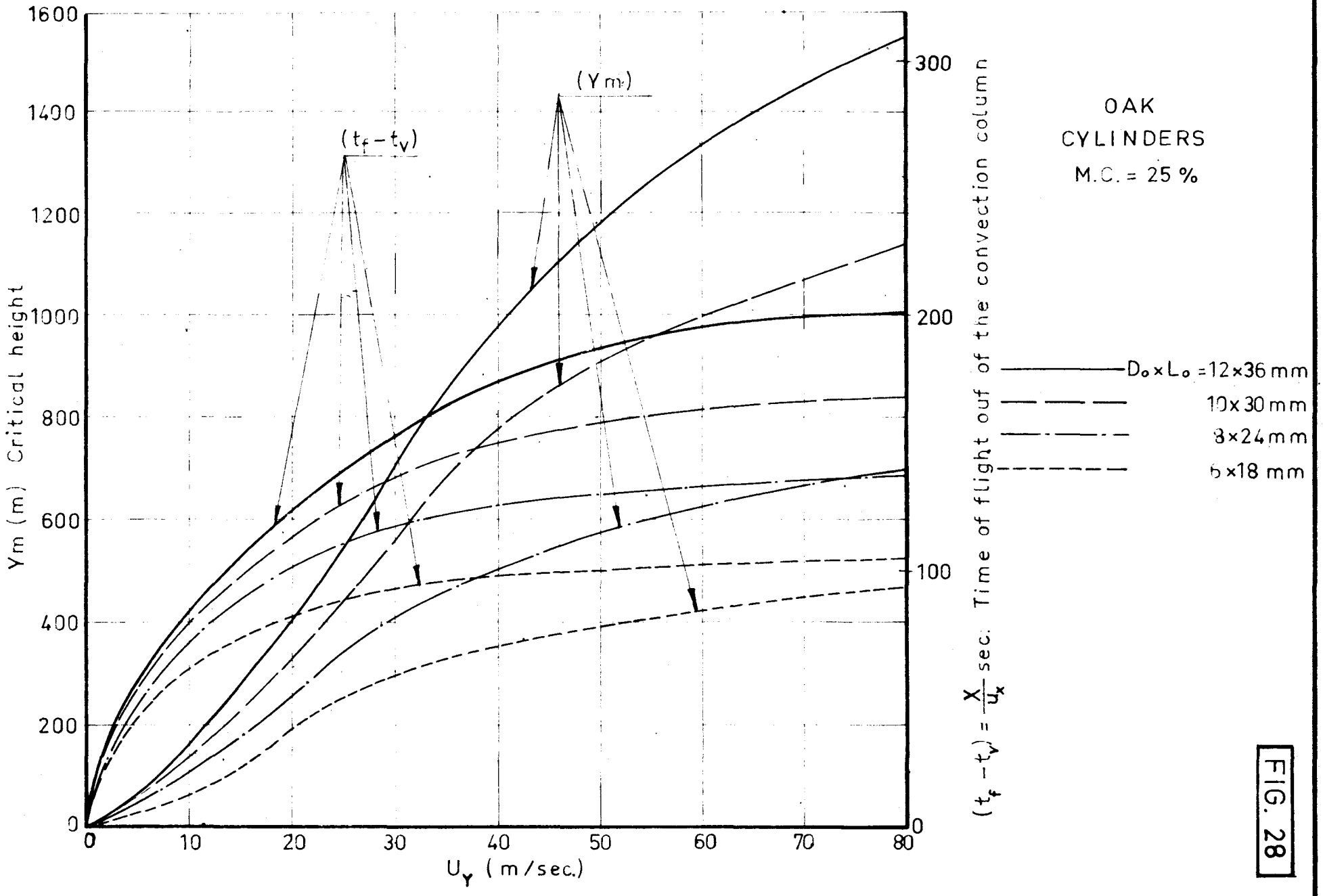
1600
1400
1200
1000
800
600
400
200
0
Ym (m) Critical height
0
10
20
30
40
50
60
70
80
U_Y (m/sec.)
$(t_f - t_v)$
(Ym)
300
200
100
0
$(t_f - t_v) = \frac{X}{u_x}$ sec. Time of flight out of the convection column
OAK
CYLINDERS
M.C. = 25 %
$D_o \times L_o$ = 12×36 mm
10×30 mm
8×24 mm
6×18 mm

FIG. 28

FIG. 29

ASPEN
CYLINDERS
M.C. = 25 %

$D_o \times L_o$ = 12 × 36 mm
10 × 30 mm
8 × 24 mm
6 × 18 mm

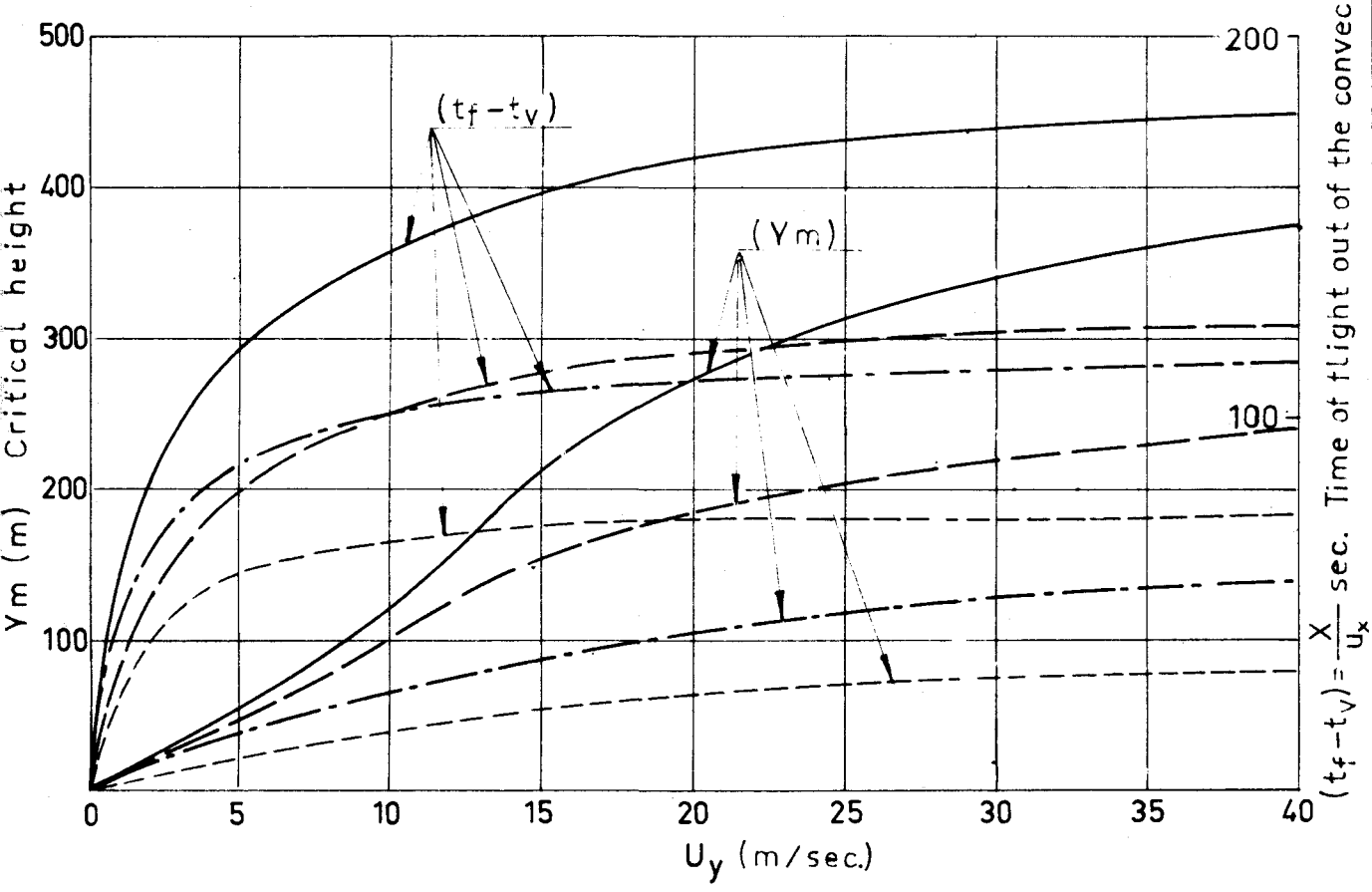

FIG. 30

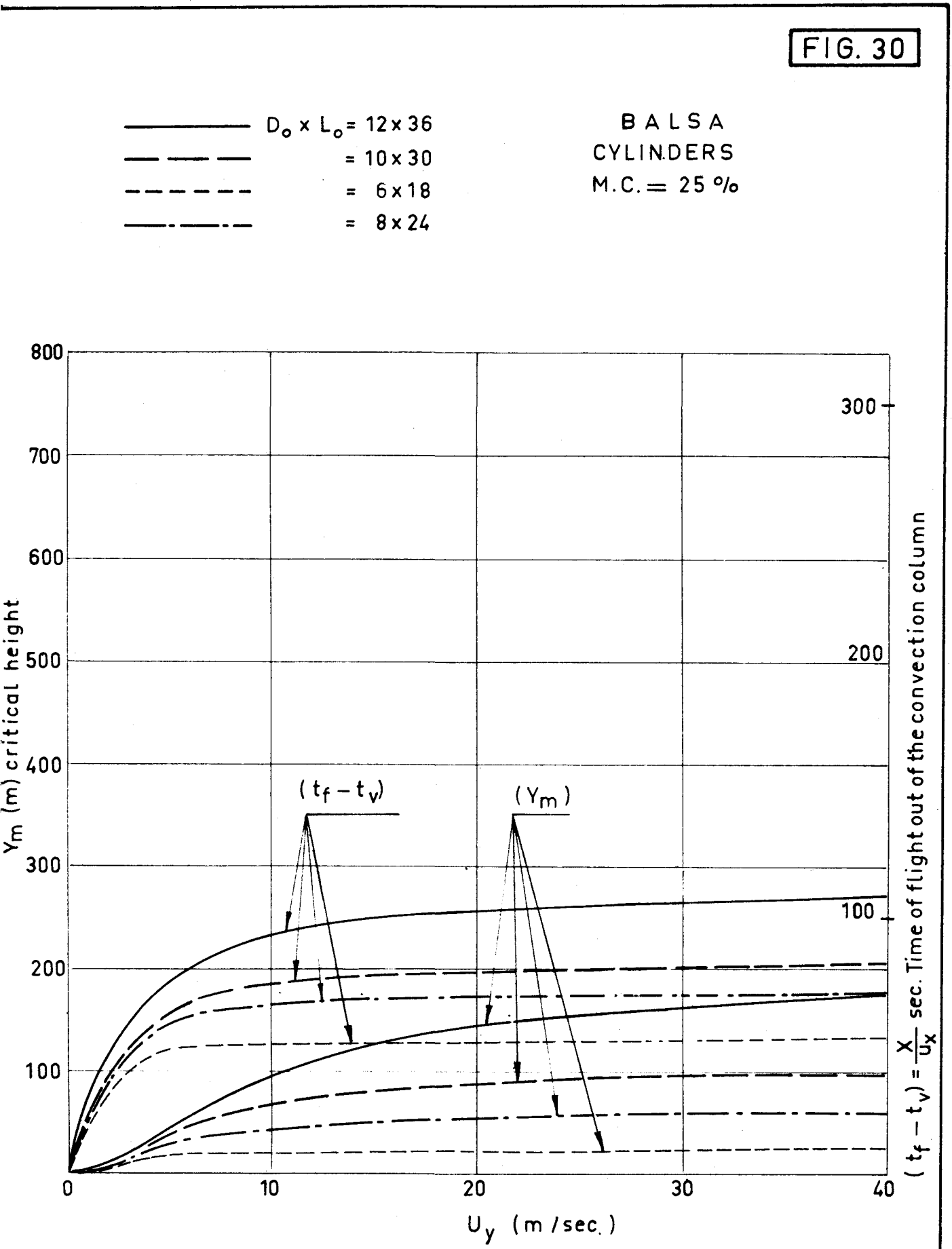
$D_o \times L_o = 12 \times 36$
$= 10 \times 30$
$= 6 \times 18$
$= 8 \times 24$
BALSA
CYLINDERS
M.C. = 25 %
800
700
600
500
400
300
200
100
0
10
20
30
40
Y_m (m) critical height
U_y (m / sec.)
$(t_f - t_v)$
(Y_m)
300
200
100
$(t_f - t_v) = \frac{X}{U_x}$ sec. Time of flight out of the convection column

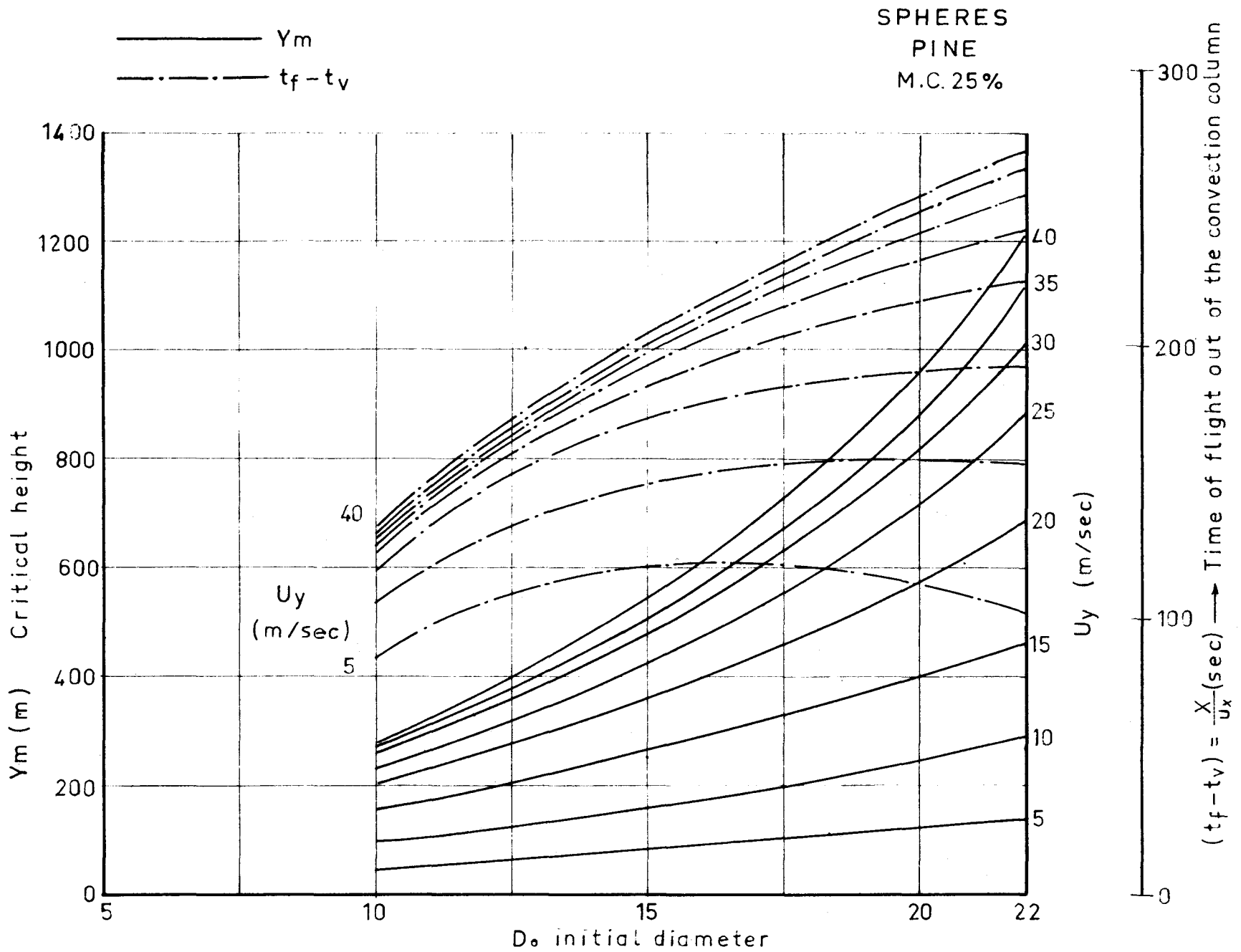
Ym
$t_f - t_v$
SPHERES
PINE
M.C. 25%
Ym (m) Critical height
1400
1200
1000
800
600
400
200
0
5
10
15
20
22
Do initial diameter
Uy (m/sec)
40
5
40
35
30
25
20
15
10
5
Uy (m/sec)
300
200
100
0
$(t_f - t_v) = \frac{X}{u_x}$(sec) ⟶ Time of flight out of the convection column

FIG. 31

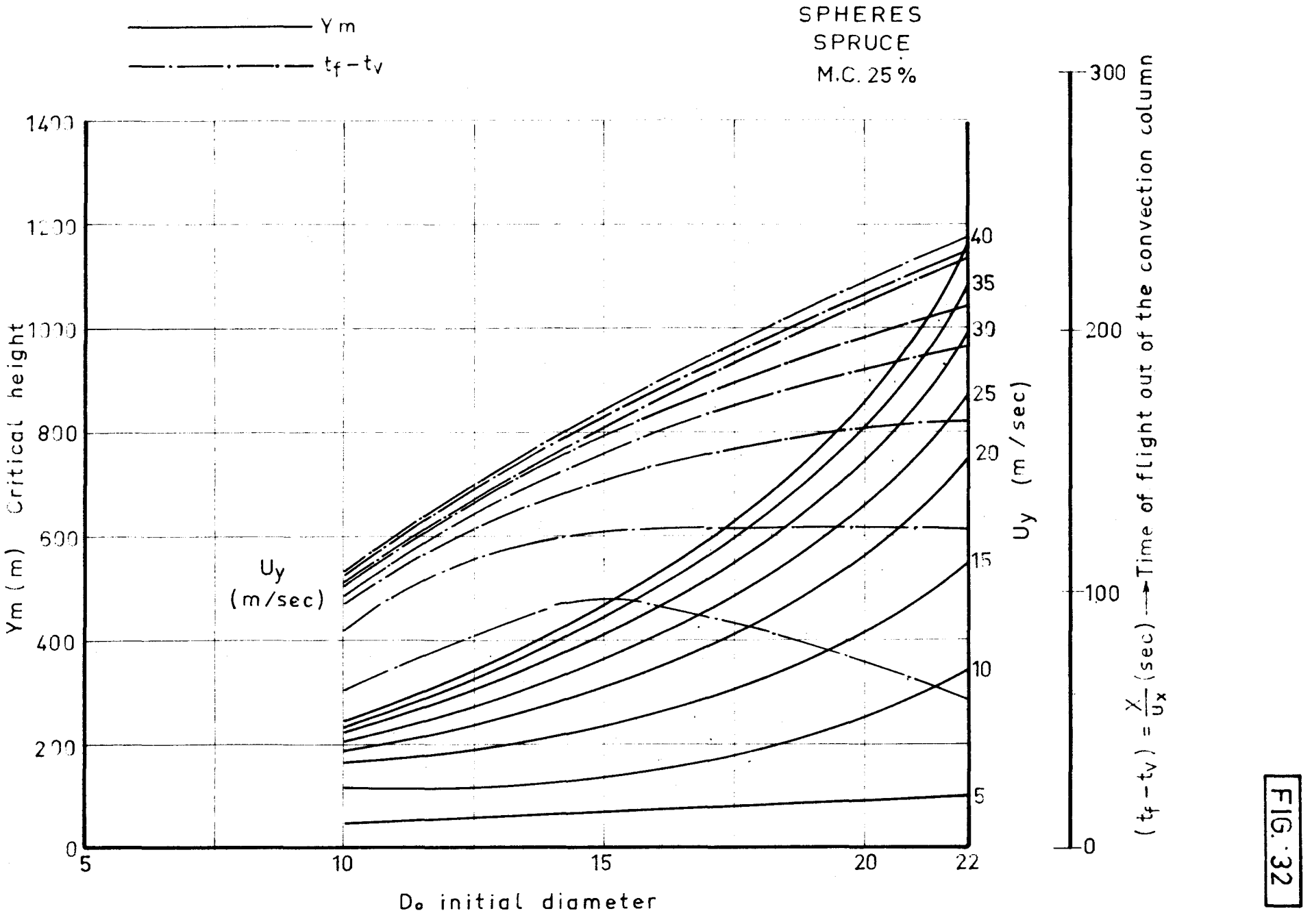
Ym
$t_f - t_v$
SPHERES
SPRUCE
M.C. 25 %
Ym (m) Critical height
1400
1200
1000
800
600
400
200
0
5
10
15
20
22
Do initial diameter
Uy (m/sec)
40
35
30
25
20
15
10
5
Uy (m / sec)
300
200
100
0
$(t_f - t_v) = \frac{X}{U_x}$ (sec) → Time of flight out of the convection column

FIG. 32

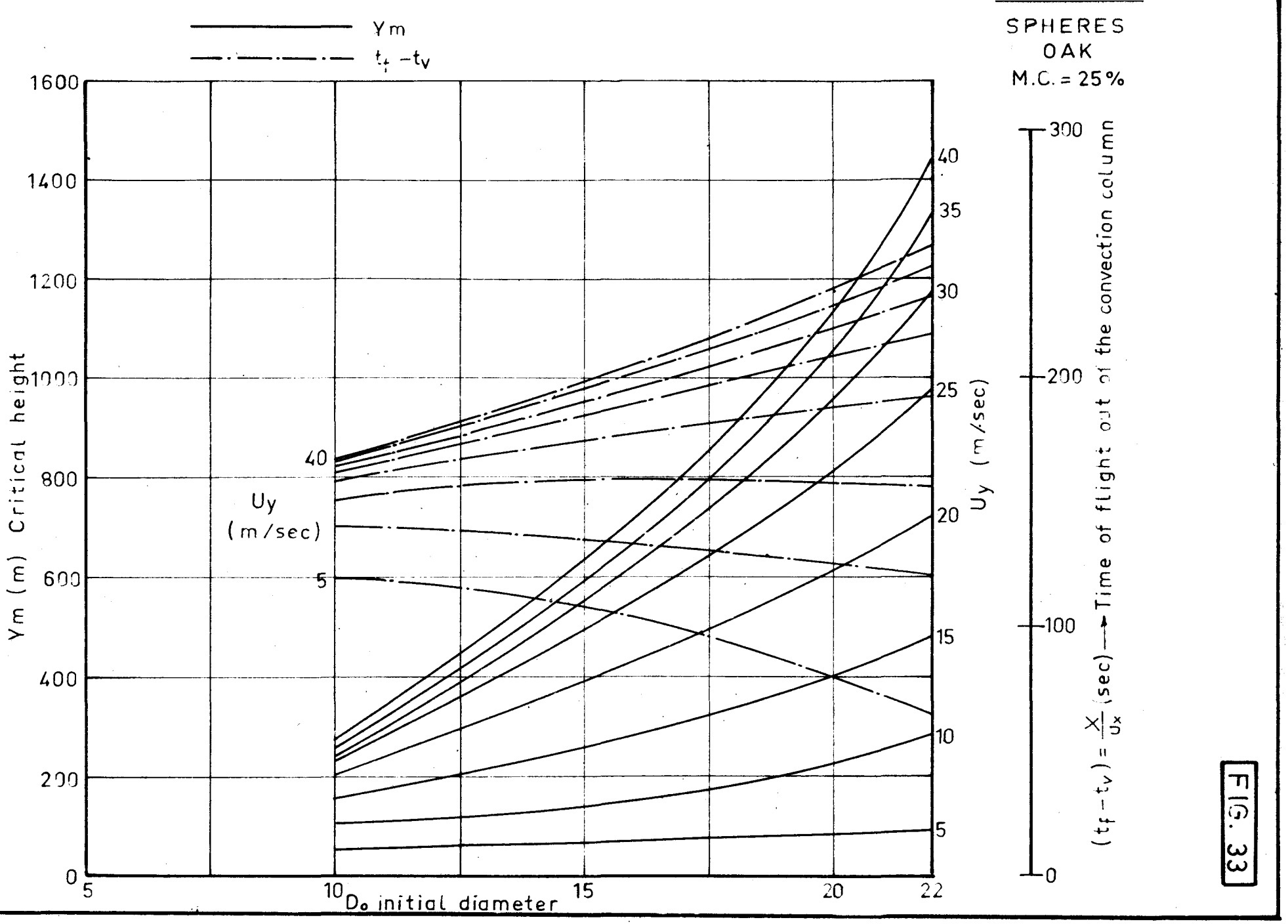
Ym
$t_f - t_v$
SPHERES
OAK
M.C. = 25%
Ym (m) Critical height
Uy (m/sec)
Uy
(m/sec)
40
5
D_o initial diameter
$(t_f - t_v) = \frac{X}{U_x}$ (sec) → Time of flight out of the convection column
FIG. 33

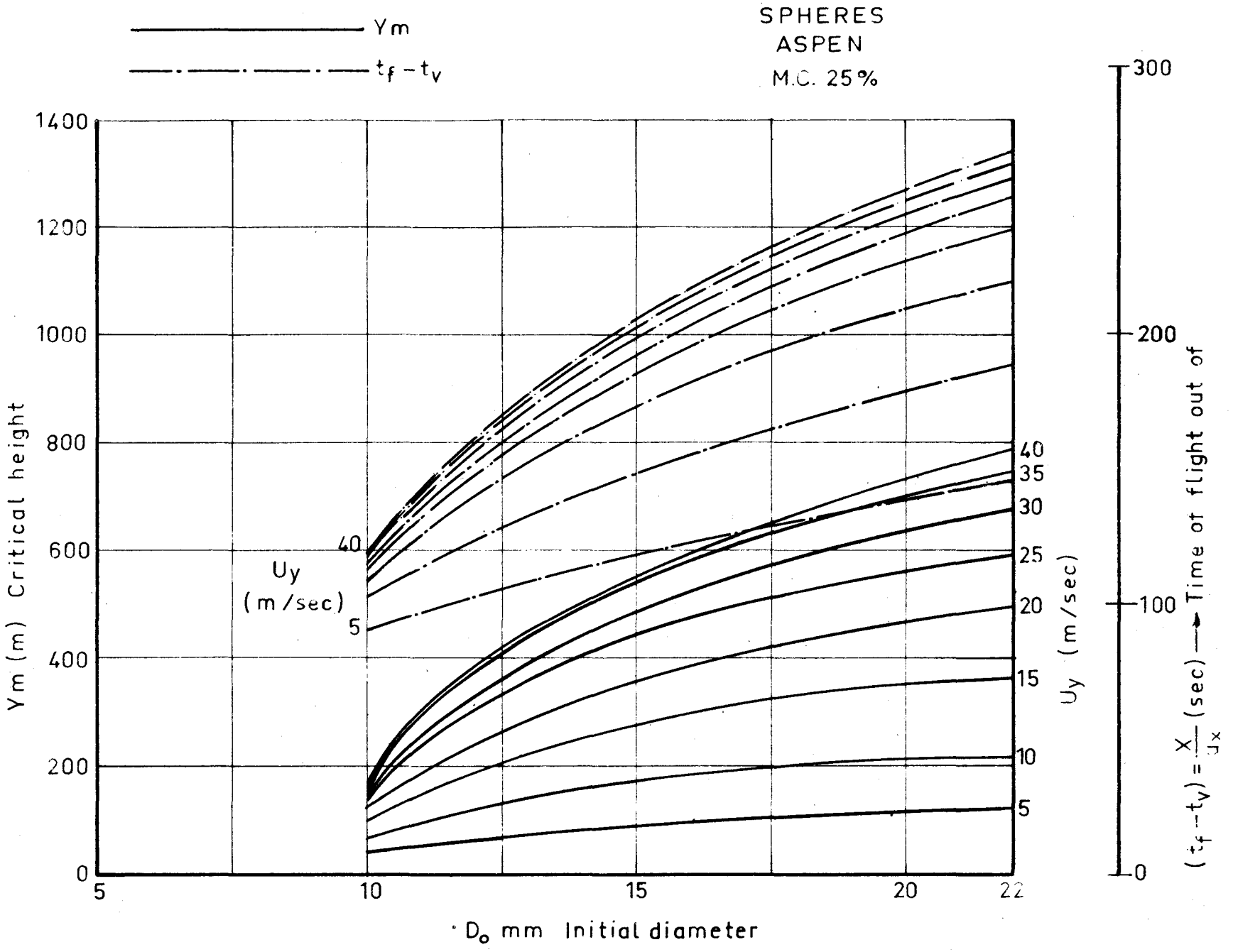
Ym
$t_f - t_v$
SPHERES
ASPEN
M.C. 25%
Ym (m) Critical height
1400
1200
1000
800
600
400
200
0
5
10
15
20
22
D_o mm Initial diameter
Uy
(m/sec)
40
5
40
35
30
25
20
15
10
5
Uy (m/sec)
300
200
100
0
$(t_f - t_v) = \frac{X}{U_x}$ (sec) → Time of flight out of

FIG. 34

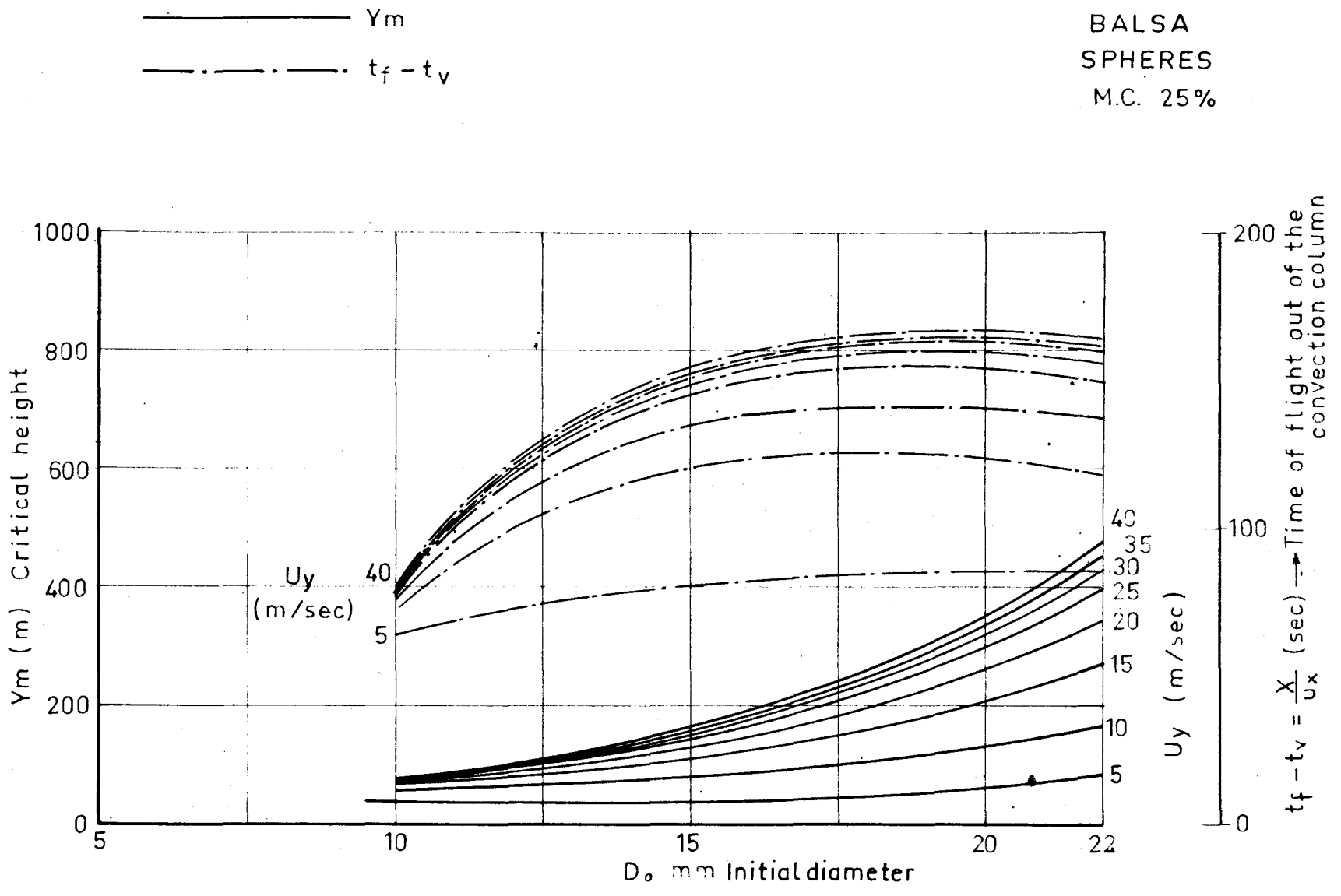
Ym
$t_f - t_v$
BALSA
SPHERES
M.C. 25%
Ym (m) Critical height
1000
800
600
400
200
0
5
10
15
20
22
D_o mm Initial diameter
Uy
(m/sec)
40
5
40
35
30
25
20
15
10
5
Uy (m/sec)
200
100
0
$t_f - t_v = \frac{X}{ux}$ (sec) → Time of flight out of the convection column

FIG. 35

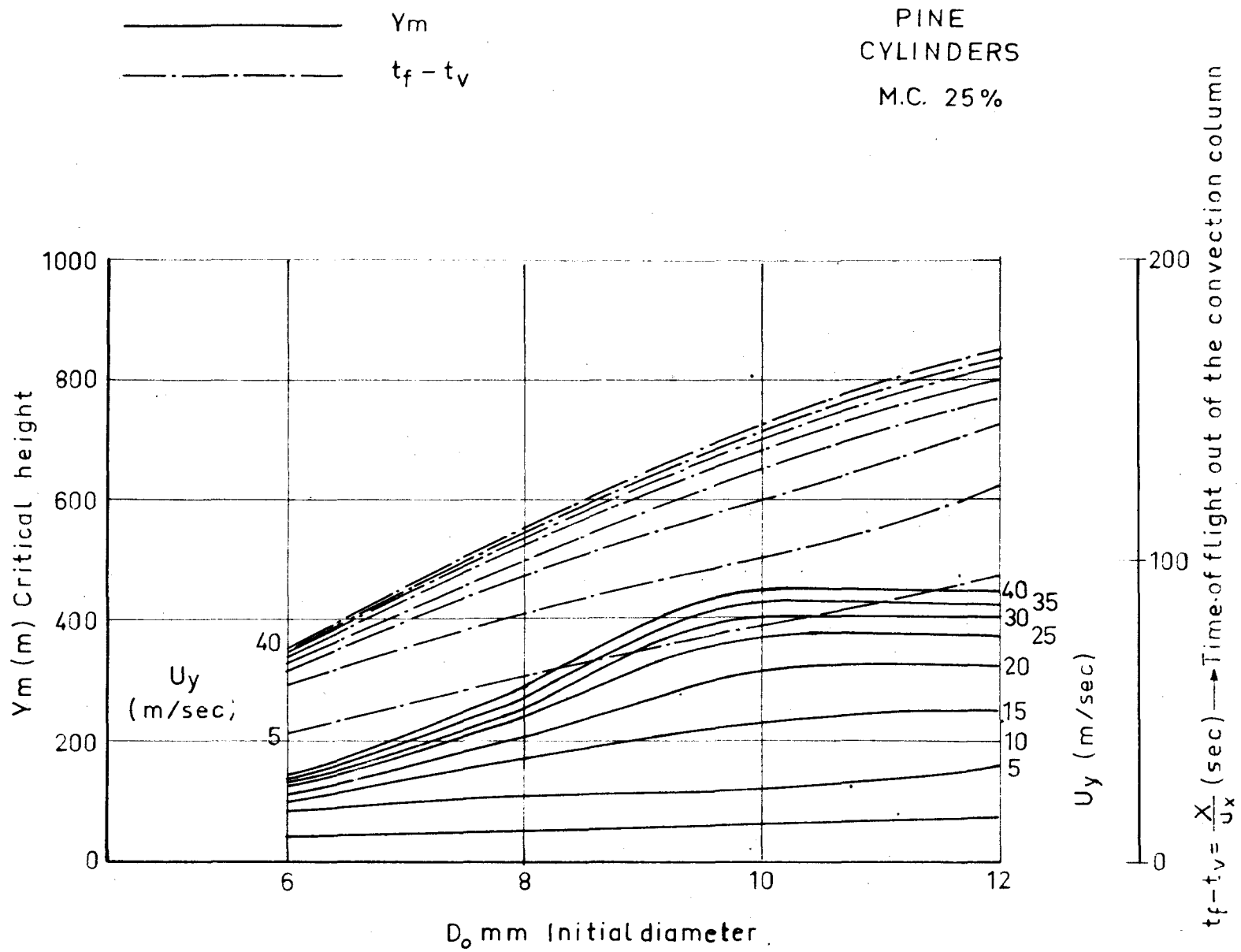
Ym
$t_f - t_v$
PINE
CYLINDERS
M.C. 25%
Ym (m) Critical height
1000
800
600
400
200
0
Uy
(m/sec)
40
5
6
8
10
12
D_o mm Initial diameter
40
35
30
25
20
15
10
5
Uy (m/sec)
200
100
0
$t_f - t_v = \frac{X}{U_x}$ (sec) → Time of flight out of the convection column

FIG. 36

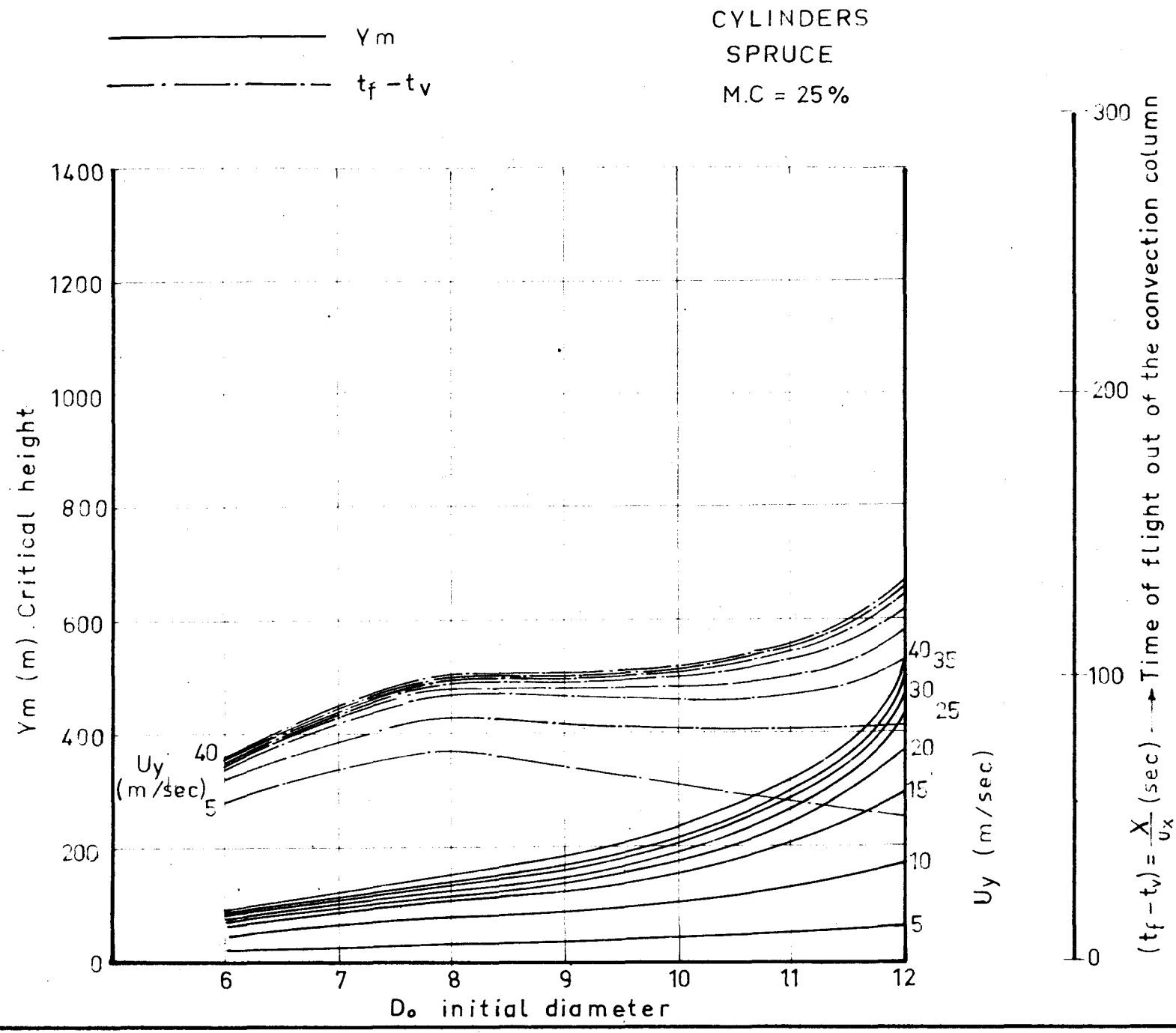
Ym
$t_f - t_v$
CYLINDERS
SPRUCE
M.C = 25%
Ym (m). Critical height
1400
1200
1000
800
600
400
200
0
Uy (m/sec)
40
5
40
35
30
25
20
15
10
5
6
7
8
9
10
11
12
D_o initial diameter
300
200
100
0
$(t_f - t_v) = \frac{X}{u_x}$ (sec) → Time of flight out of the convection column

FIG. 37

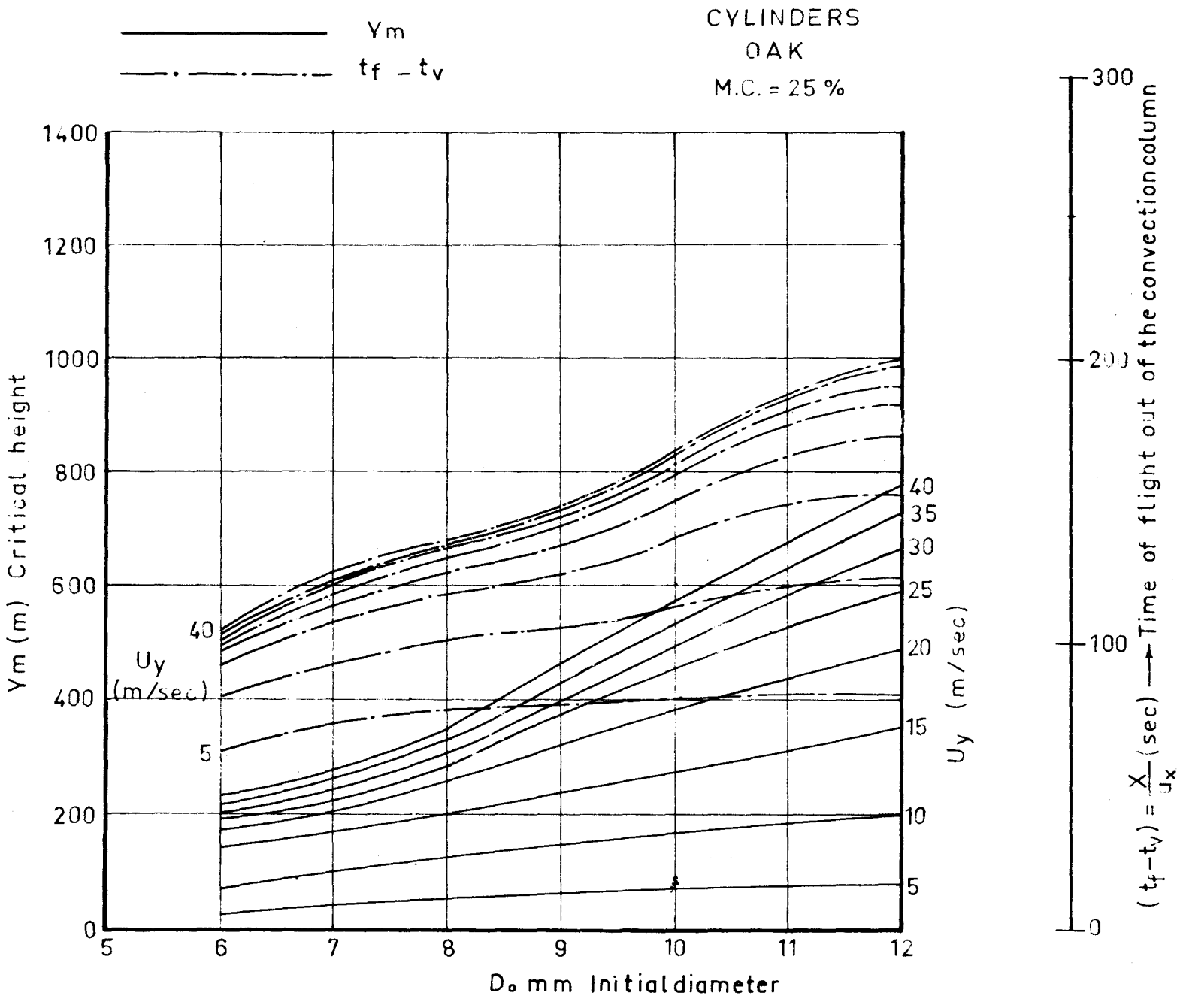
Ym
$t_f - t_v$
CYLINDERS
OAK
M.C. = 25 %
Ym (m) Critical height
1400
1200
1000
800
600
400
200
0
Uy (m/sec)
40
5
40
35
30
25
20
15
10
5
Uy (m/sec)
5
6
7
8
9
10
11
12
Do mm Initial diameter
300
200
100
0
$(t_f - t_v) = \frac{X}{U_x}$ (sec) → Time of flight out of the convection column

FIG. 38

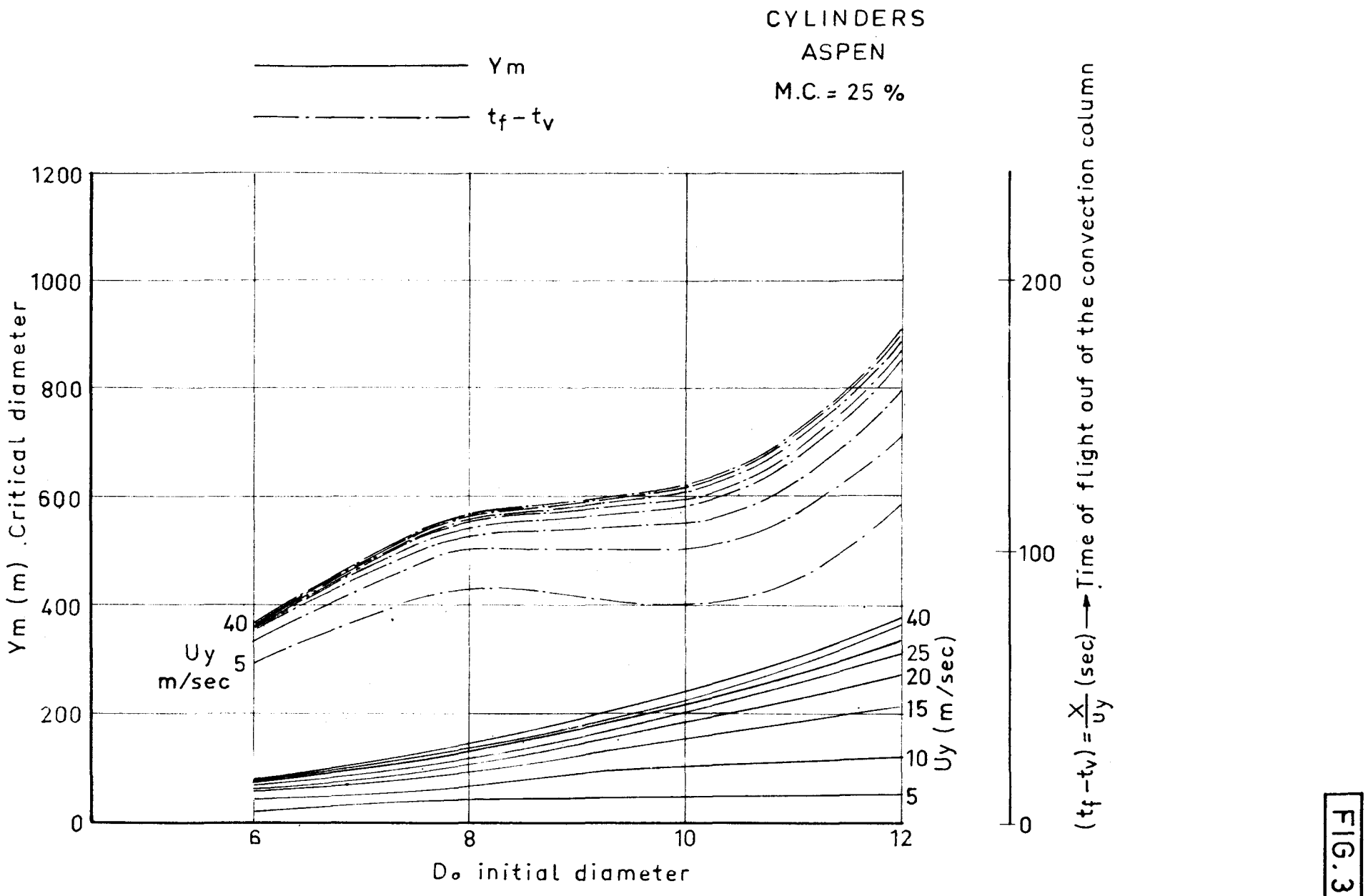
CYLINDERS
ASPEN
M.C. = 25 %
Ym
$t_f - t_v$
Ym (m) .Critical diameter
1200
1000
800
600
400
200
0
Uy m/sec
40
5
6
8
10
12
D_o initial diameter
40
25
20
15
10
5
Uy (m/sec)
200
100
0
$(t_f - t_v) = \frac{X}{Uy}$ (sec) → Time of flight out of the convection column

FIG. 39

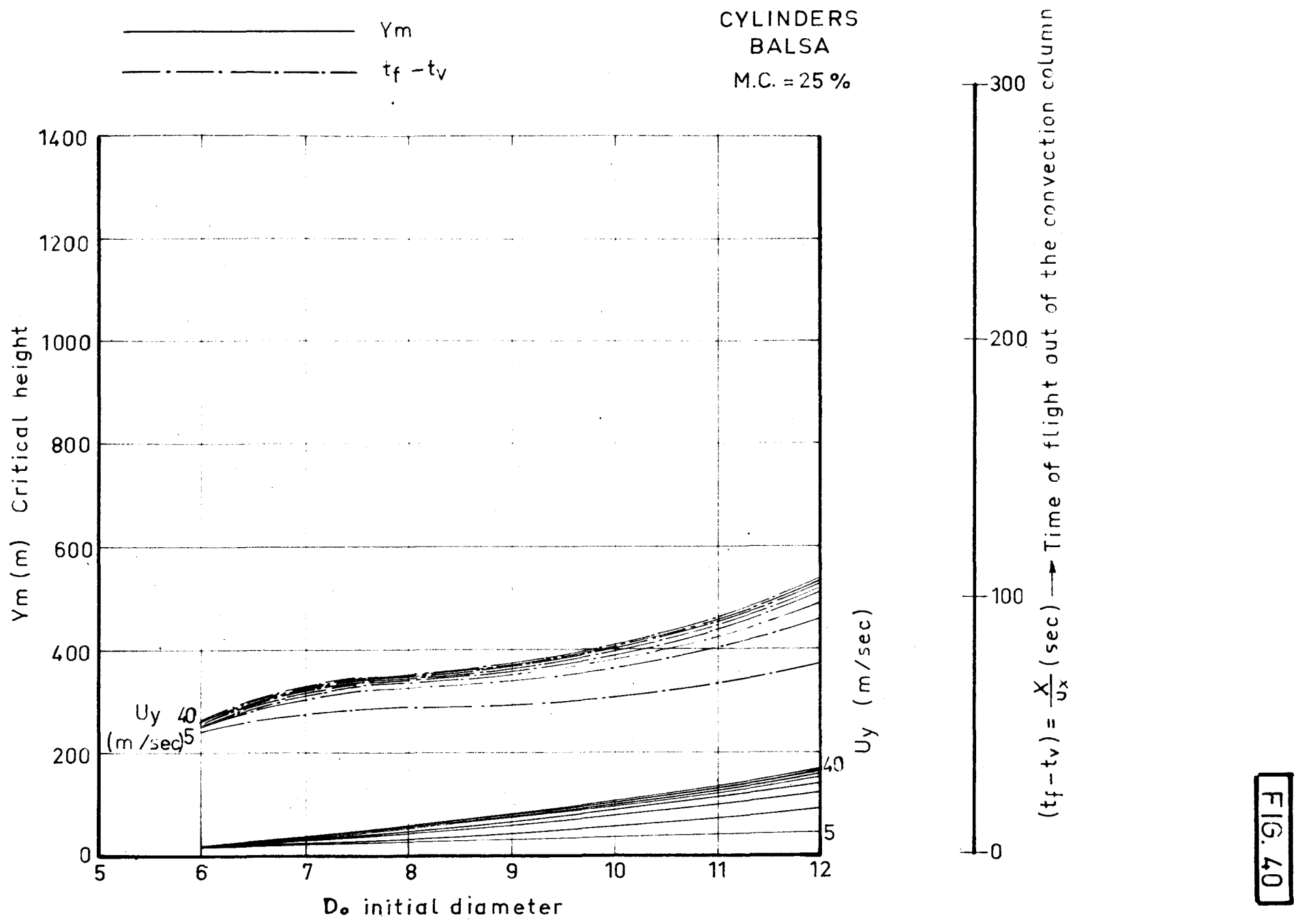
Ym
$t_f - t_v$
CYLINDERS
BALSA
M.C. = 25 %
Ym (m) Critical height
1400
1200
1000
800
600
400
200
0
Uy (m/sec)
40
5
5
6
7
8
9
10
11
12
D_o initial diameter
300
200
100
0
$(t_f - t_v) = \frac{X}{U_x}$ (sec) → Time of flight out of the convection column

FIG. 40

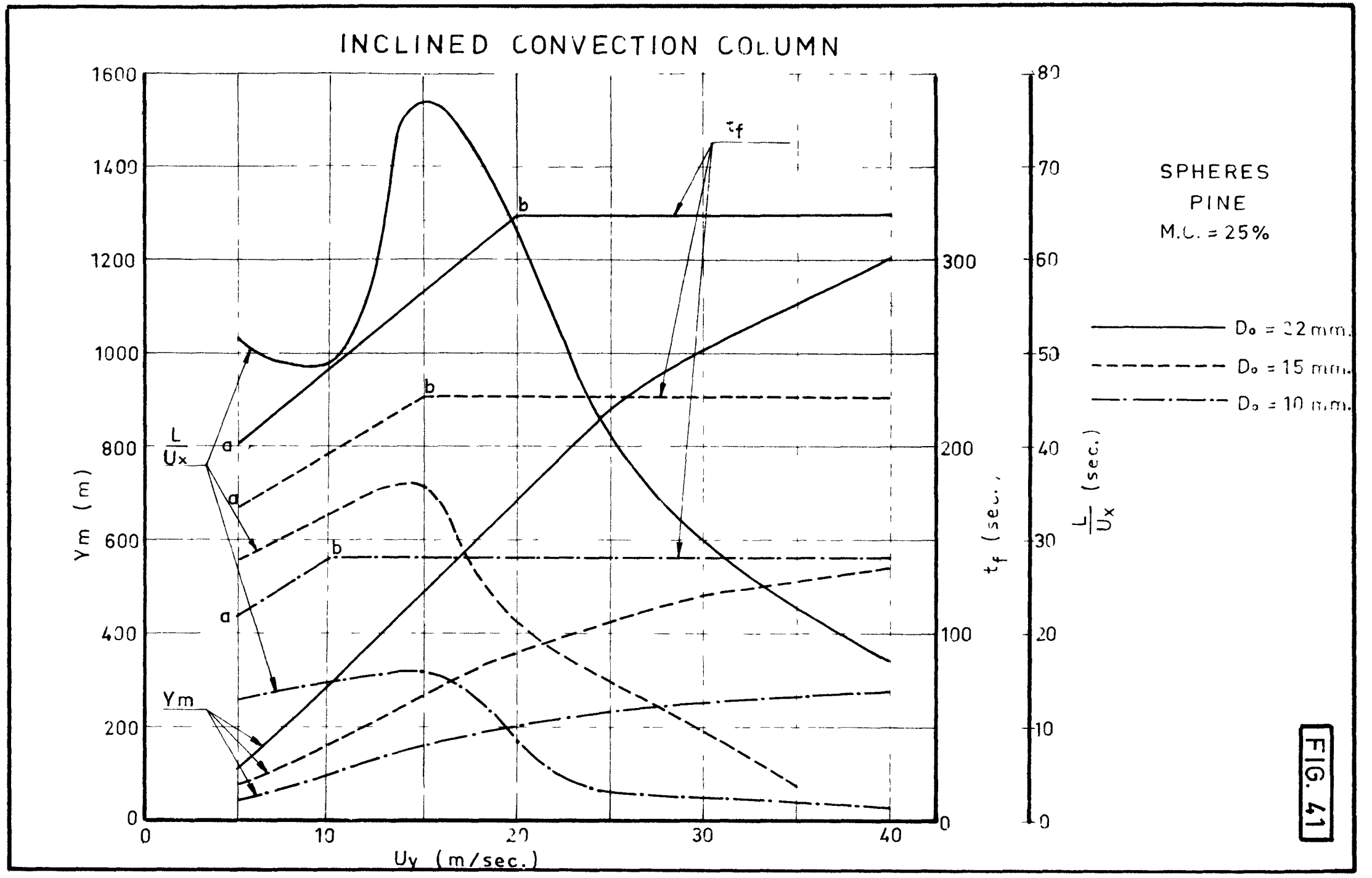
INCLINED CONVECTION COLUMN
1600
1400
1200
1000
800
600
400
200
0
Ym (m)
0
10
20
30
40
Uy (m/sec.)
300
200
100
0
t_f (sec.)
80
70
60
50
40
30
20
10
0
$\frac{L}{U_x}$ (sec.)
τ_f
b
a
$\frac{L}{U_x}$
Ym
SPHERES
PINE
M.C. = 25%
D_o = 22 mm.
D_o = 15 mm.
D_o = 10 mm.
FIG. 41

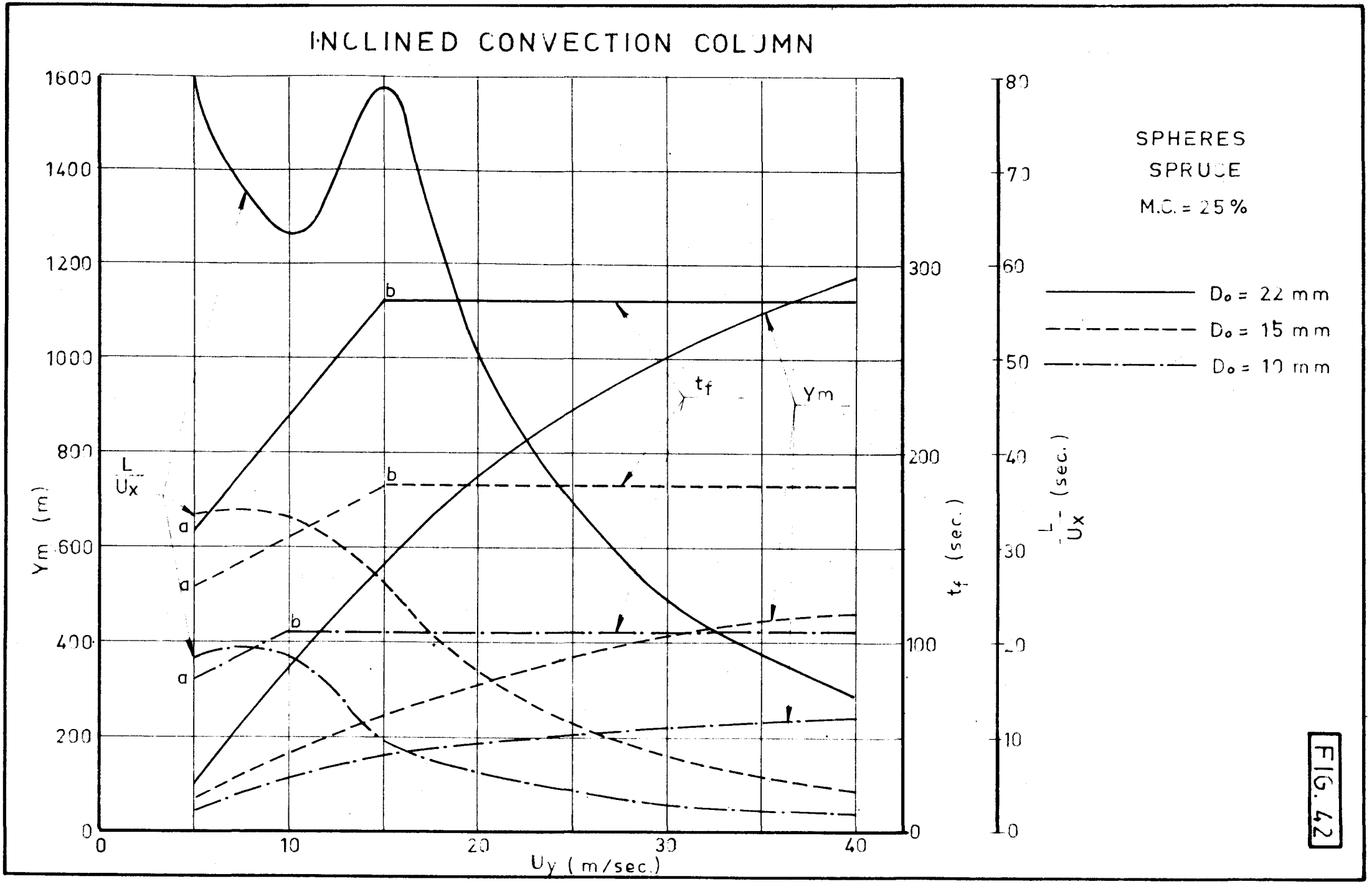
INCLINED CONVECTION COLUMN
SPHERES
SPRUCE
M.C. = 25 %
Do = 22 mm
Do = 15 mm
Do = 10 mm
Ym (m)
tf (sec.)
L/Ux (sec.)
Uy (m/sec.)
tf
Ym
L/Ux
a
b
0
200
400
600
800
1000
1200
1400
1600
100
300
10
20
30
40
50
60
70
80

FIG. 42

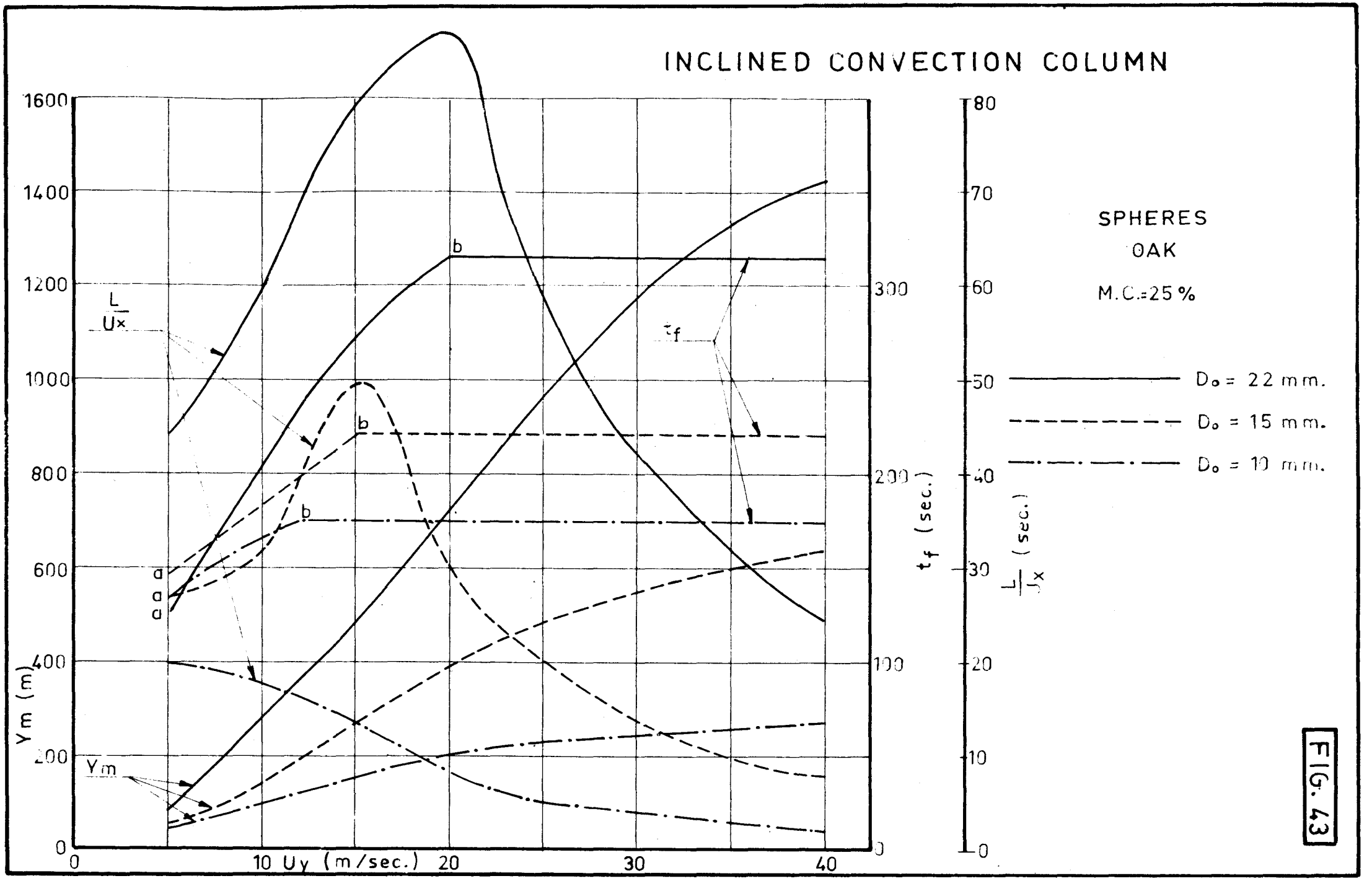
INCLINED CONVECTION COLUMN
SPHERES
OAK
M.C.=25 %
Do = 22 mm.
Do = 15 mm.
Do = 10 mm.
L/Ux
Ym
tf
a
b
Ym (m)
tf (sec.)
L/Jx (sec.)
10 Uy (m/sec.)
0
200
400
600
800
1000
1200
1400
1600
100
300
10
20
30
40
50
60
70
80

FIG. 43

INCLINED CONVECTION COLUMN

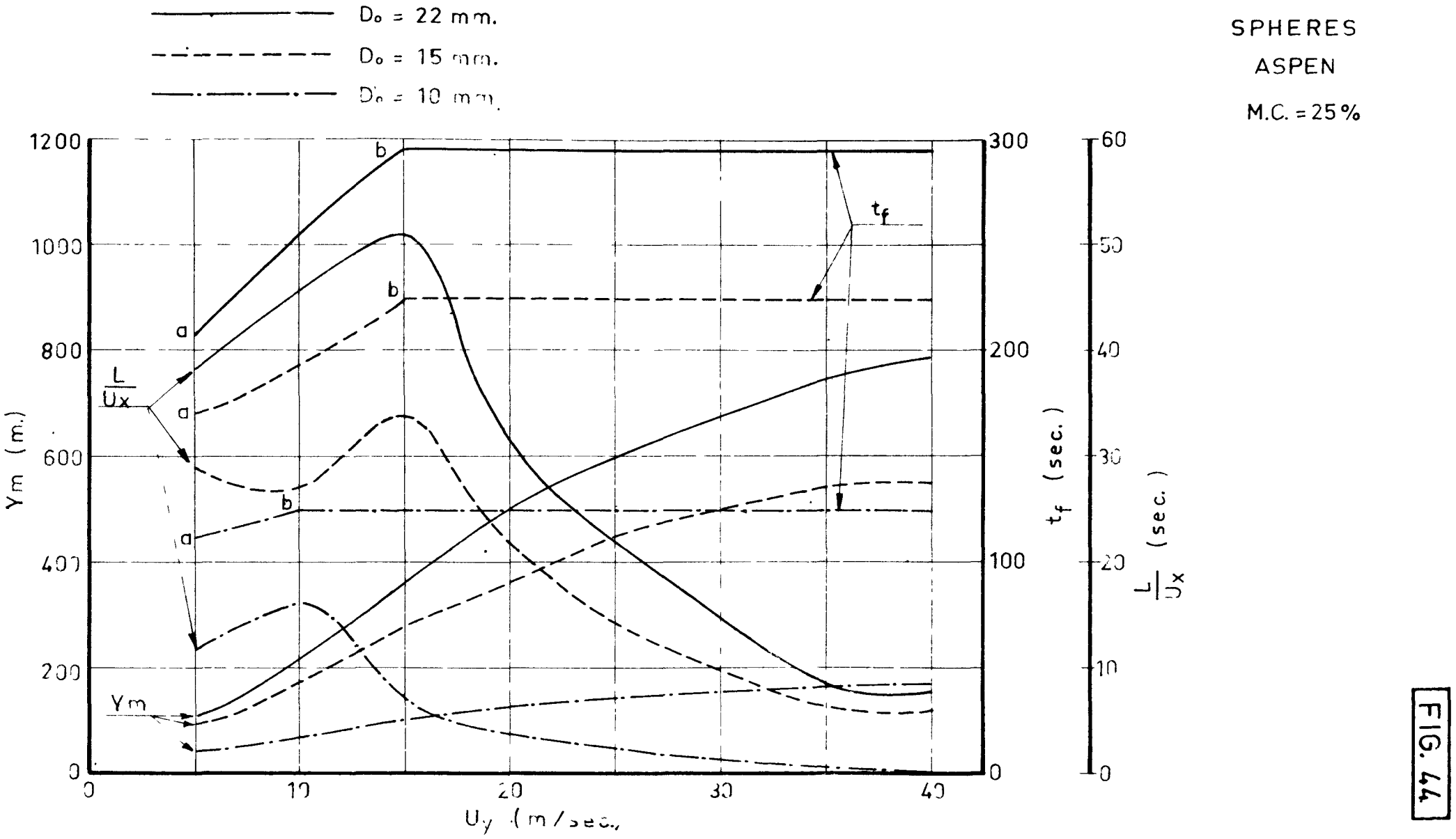

FIG. 44

INCLINED CONVECTION COLUMN

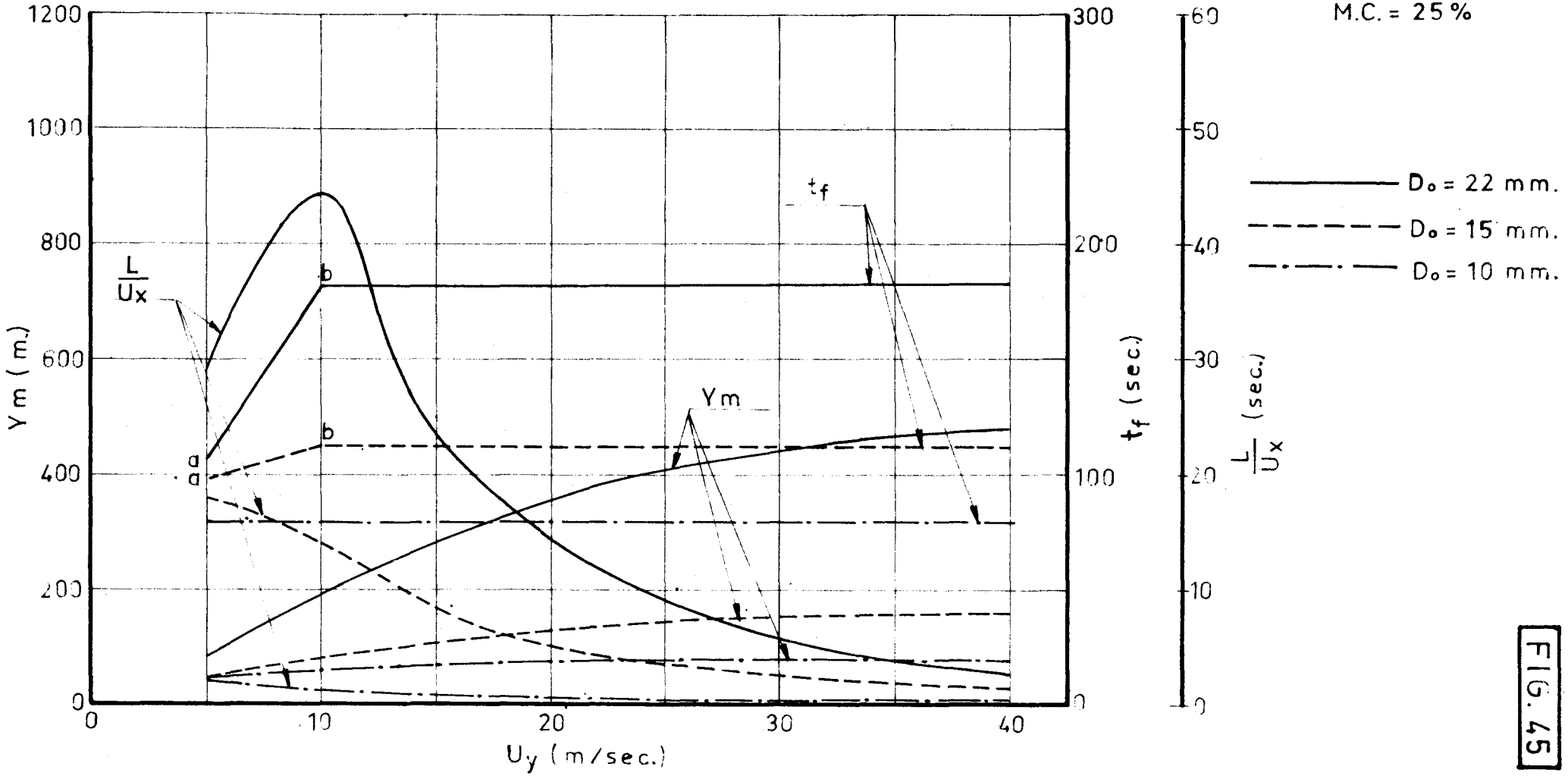

FIG. 45

INCLINED CONVECTION COLUMN

CYLINDERS
PINE
M.C. = 25 %

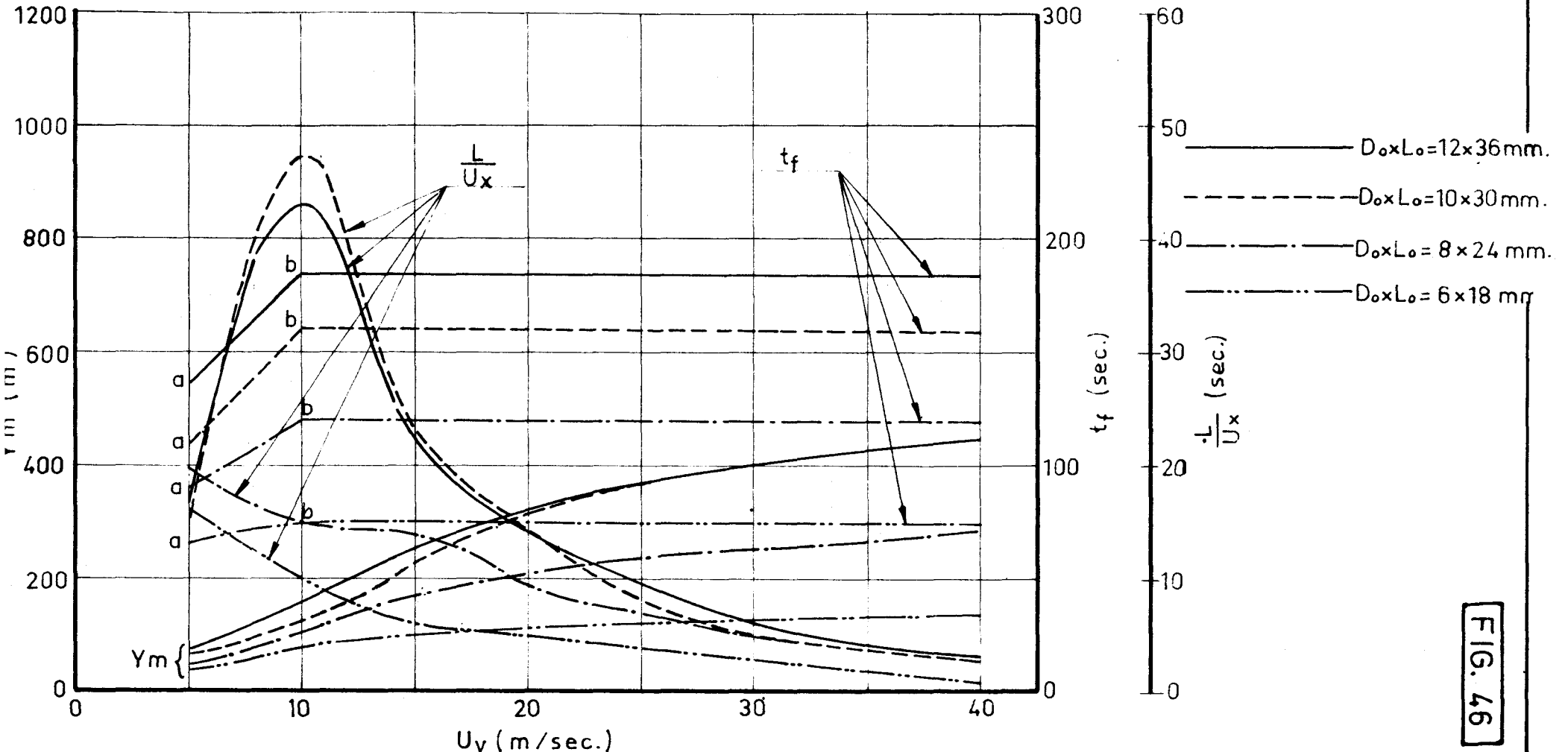

FIG. 46

FIG. 47

Wind profiles above some major forest fires. A: Wood River Valley fire, May 2, 1951; B: Chatsworth fire, July 14, 1954; C: Fort Lewis fire, October 23, 1953; D: Jamison fire, August 31, 1954. (Taken from Ref. 5)

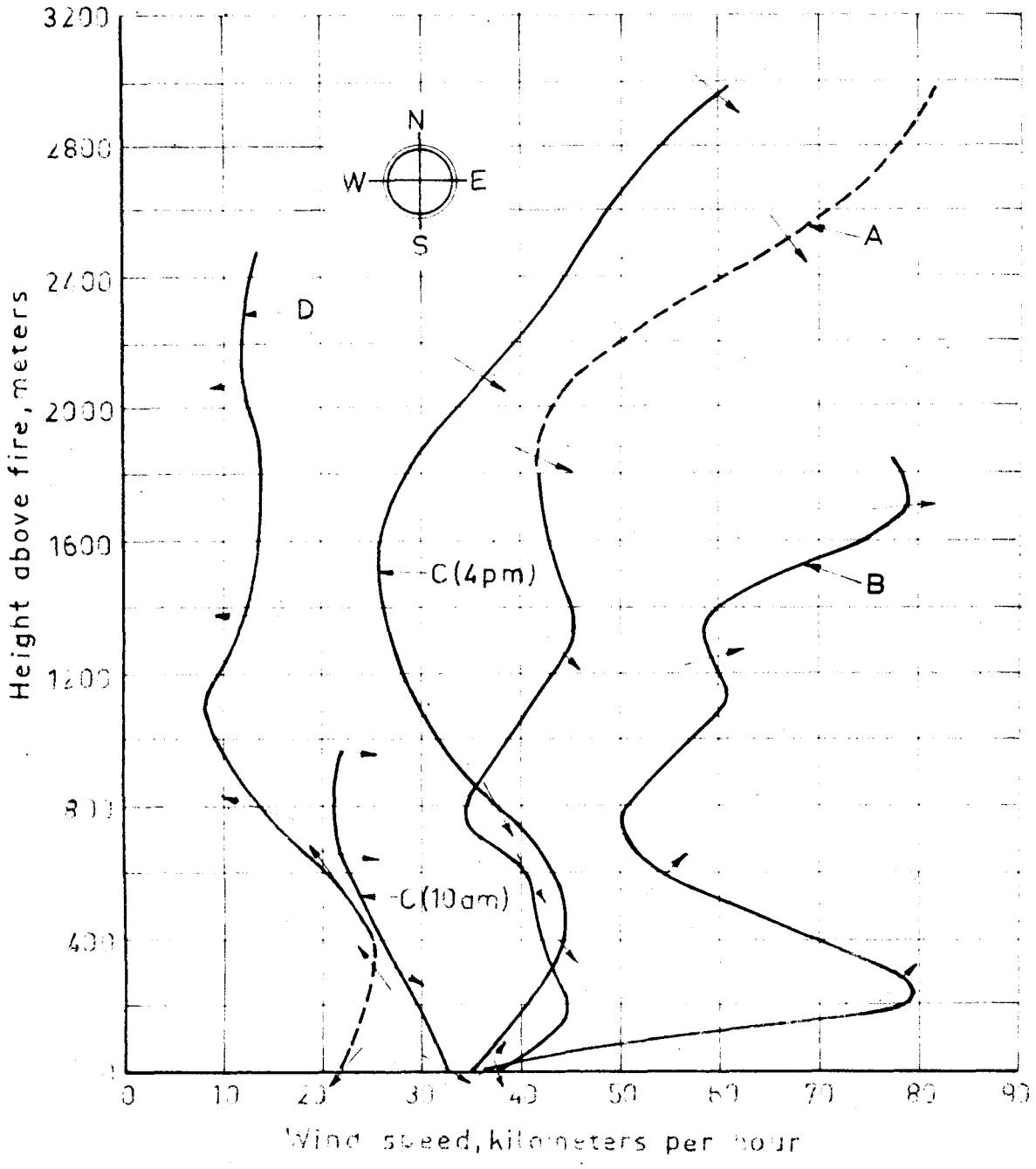

FIG. 48

VELOCITY PROFILES AND RESULTING CONVECTION ZONE

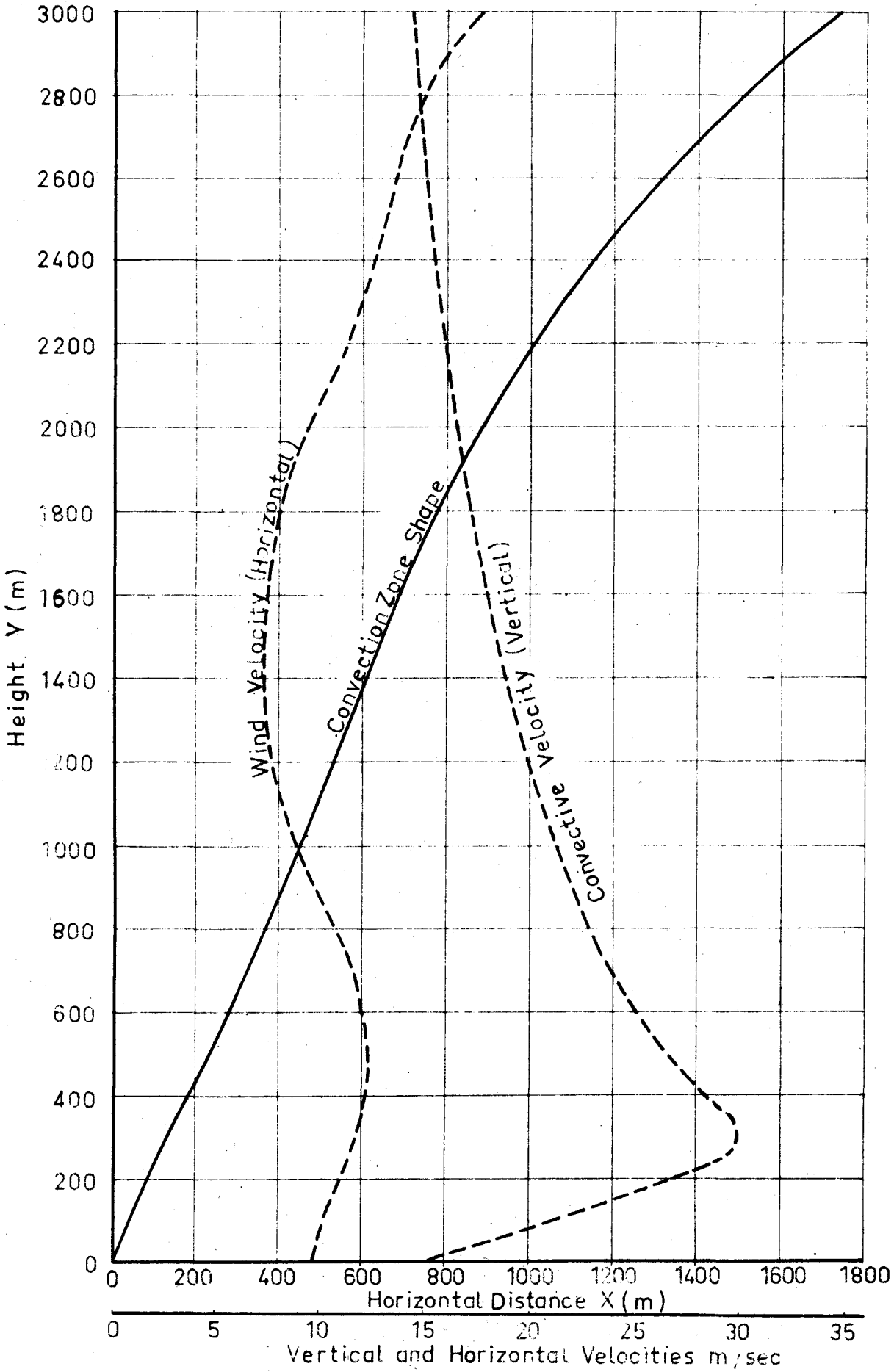

FIG. 49

VELOCITY PROFILES AND RESULTING CONVECTION ZONE

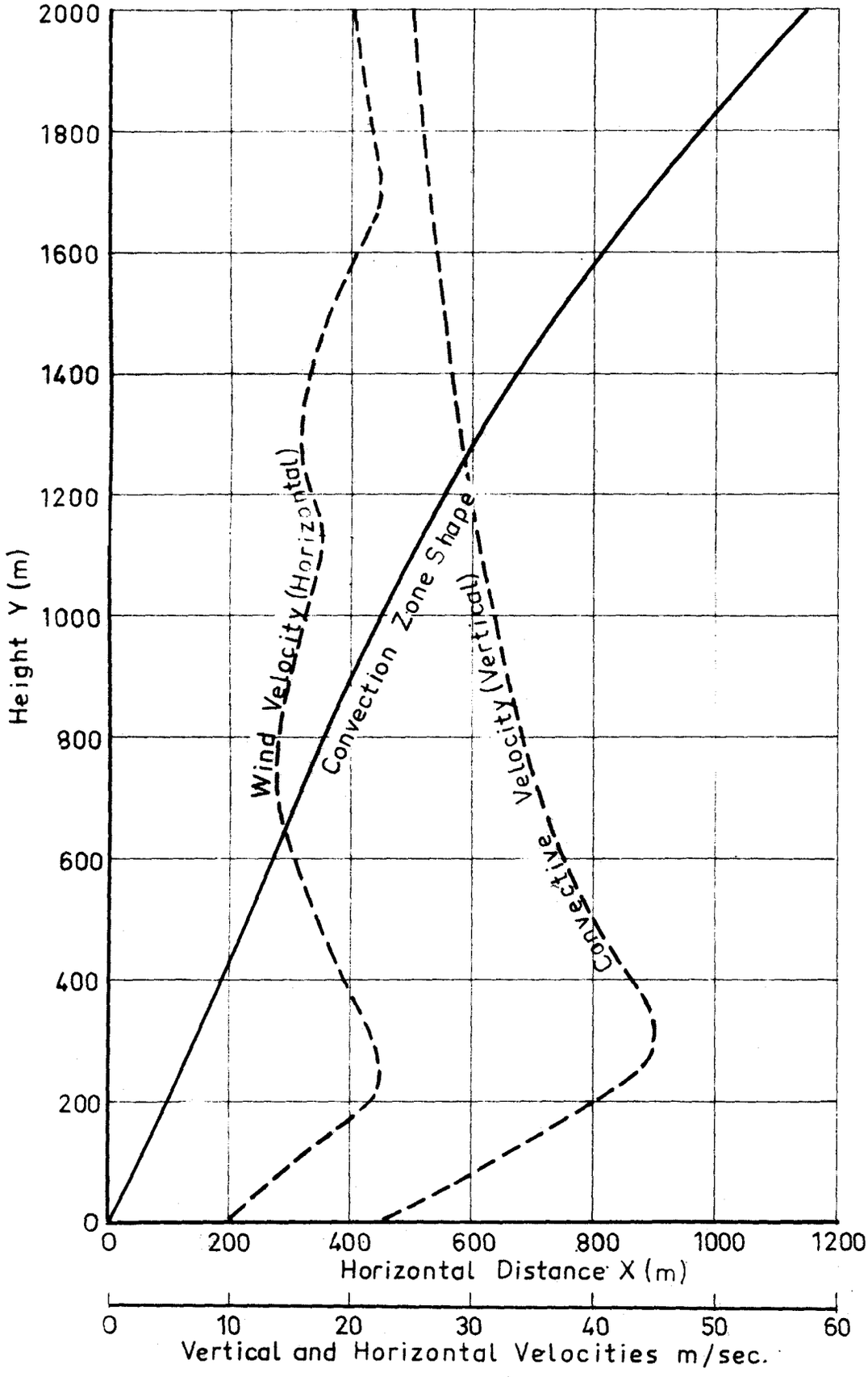

FIG. 50

FLIGHT PATHS OF BURNING SPHERES

PINUS· PINASTER
SPHERES D_o = 22 mm

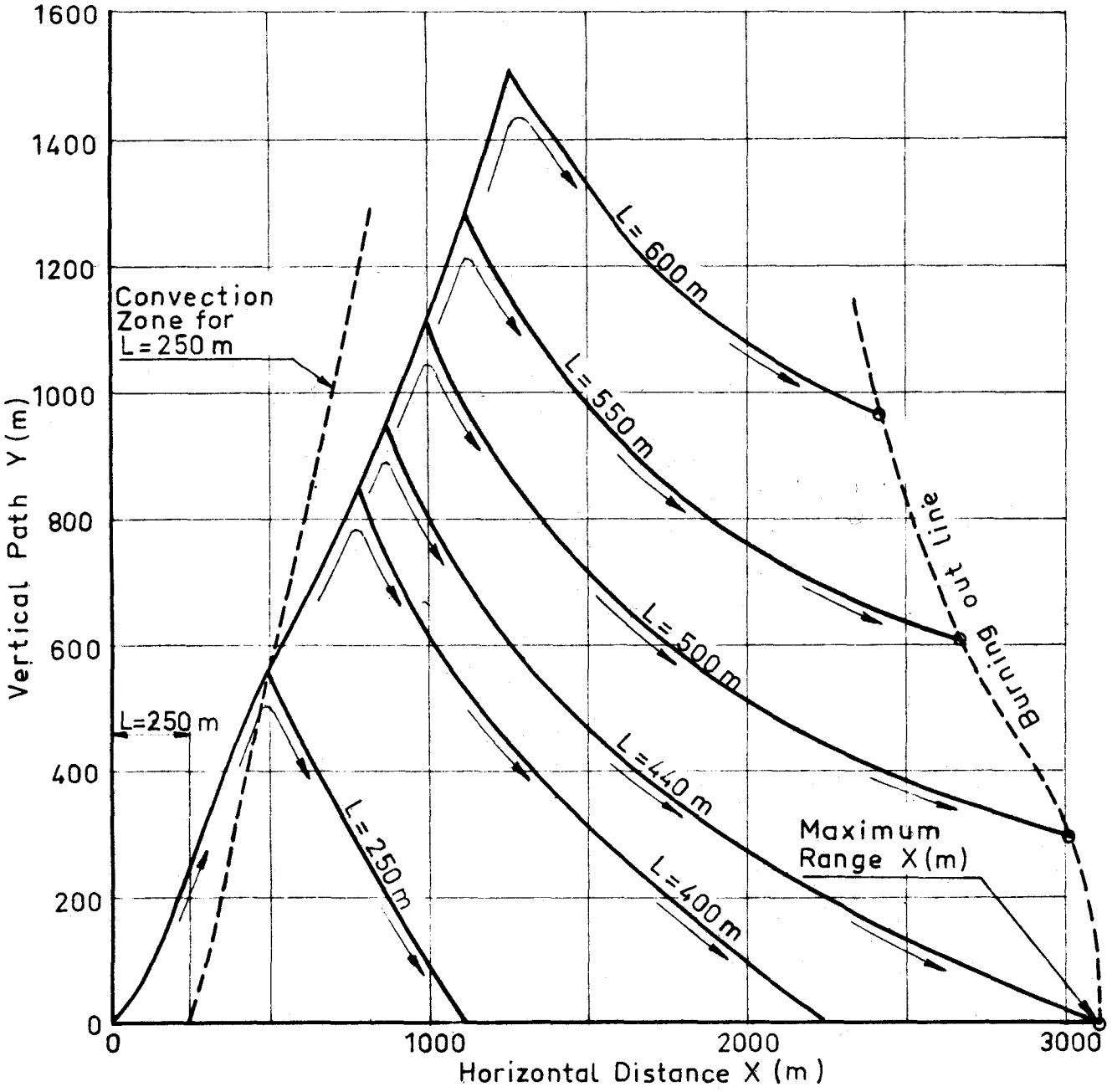

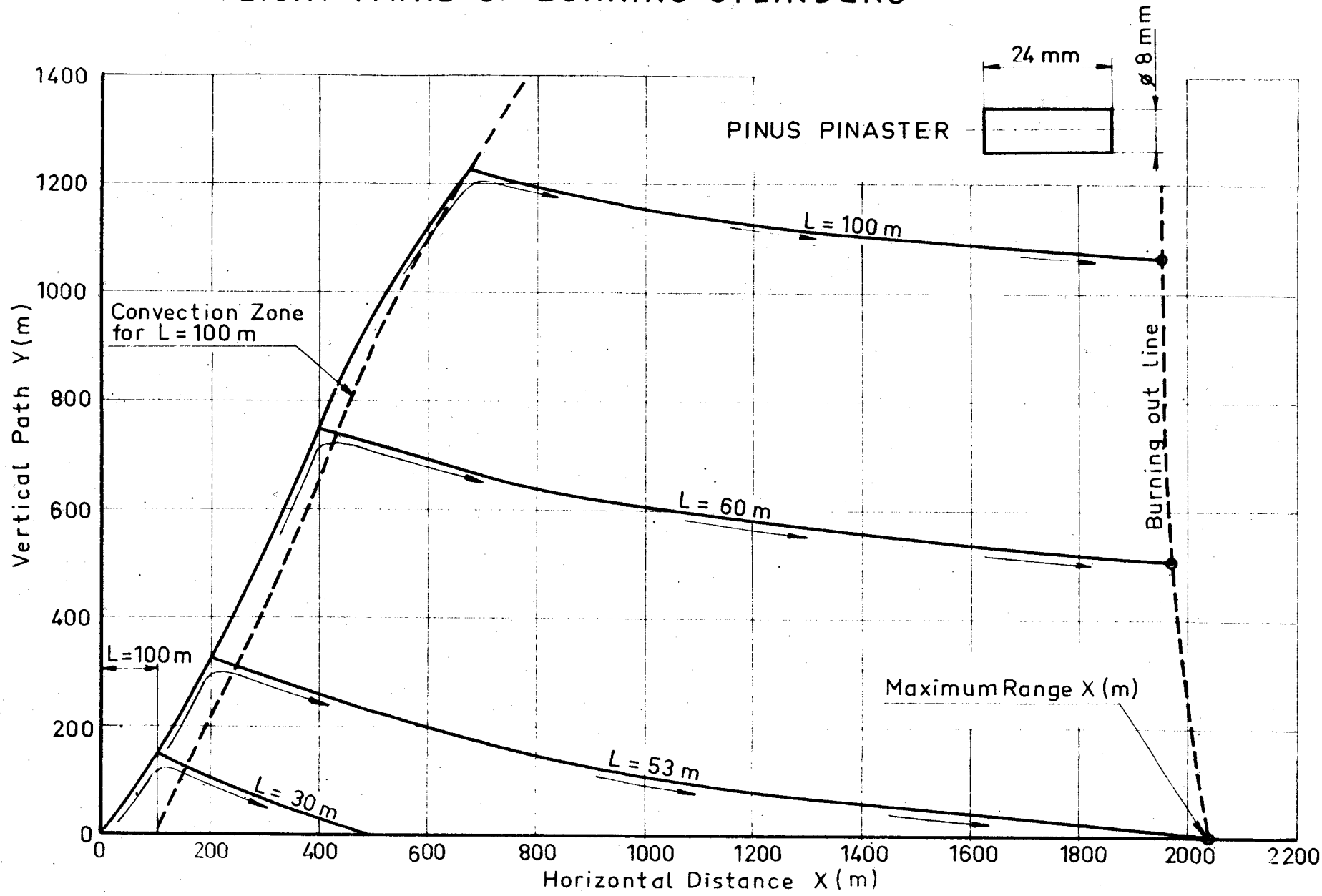
FLIGHT PATHS OF BURNING CYLINDERS
24 mm
ø 8 mm
PINUS PINASTER
L = 100 m
Convection Zone
for L = 100 m
Burning out Line
L = 60 m
L = 100 m
Maximum Range X (m)
L = 53 m
L = 30 m
Vertical Path Y (m)
Horizontal Distance X (m)
0
200
400
600
800
1000
1200
1400
1600
1800
2000
2200

FIG. 51

TIME OF FALL OF CYLINDERS AND SQUARE PLATES OF WOOD AS A FUNCTION OF TIME

PINUS PINASTER

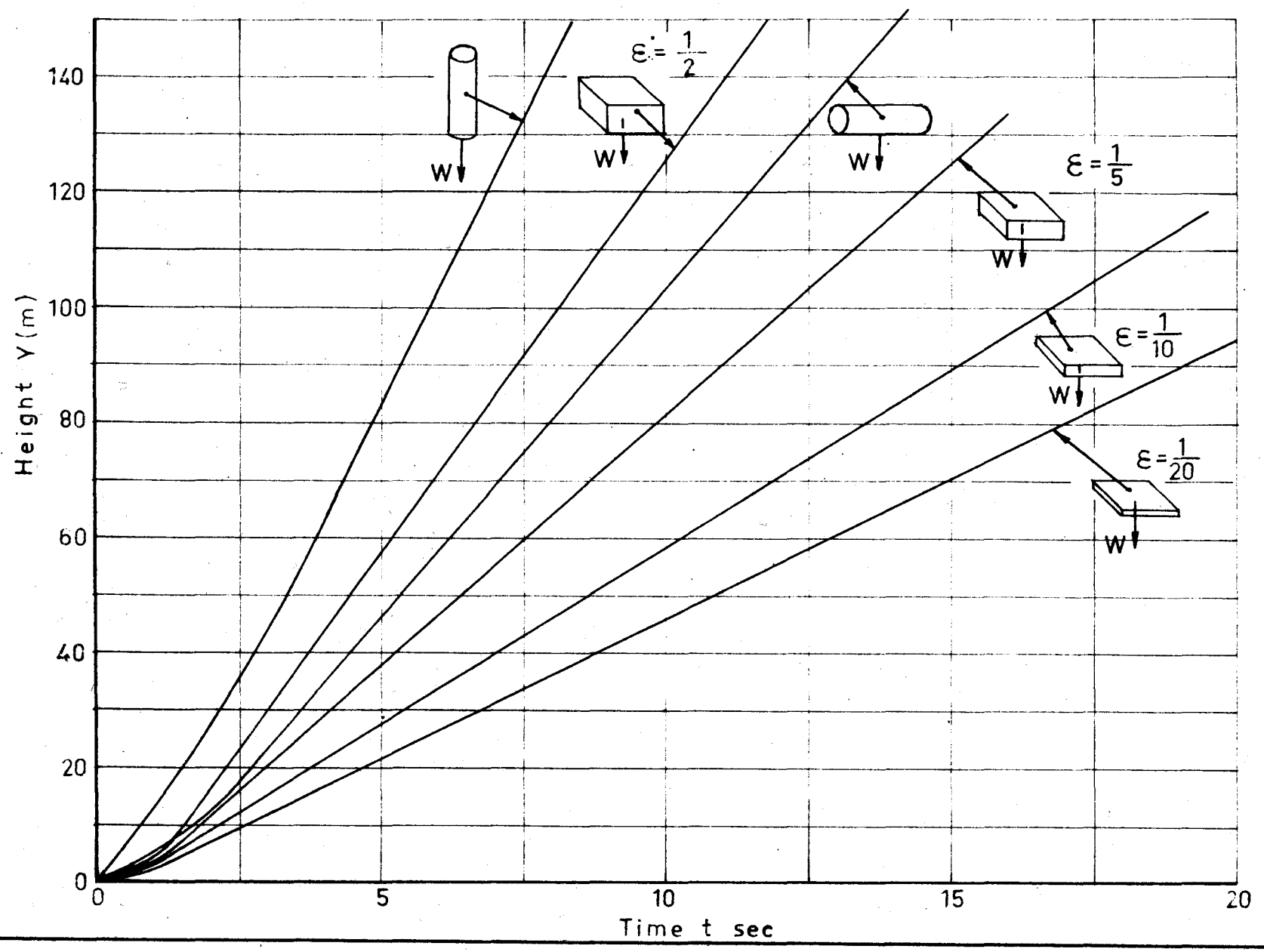

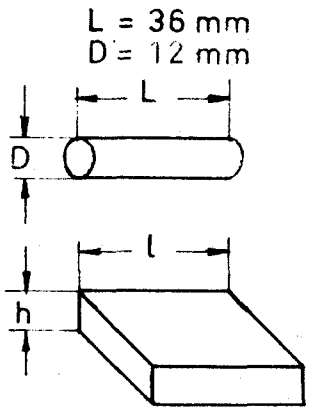

FIG. 52

FIG. 53

MEASURING RING

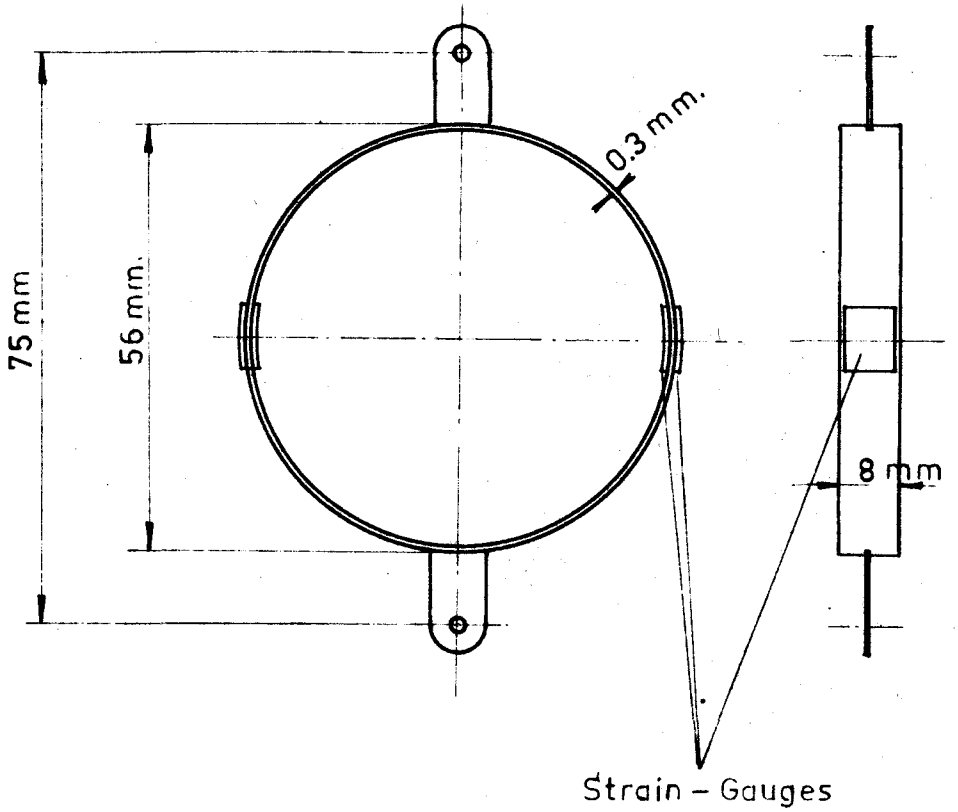

BALANCE SCHEME

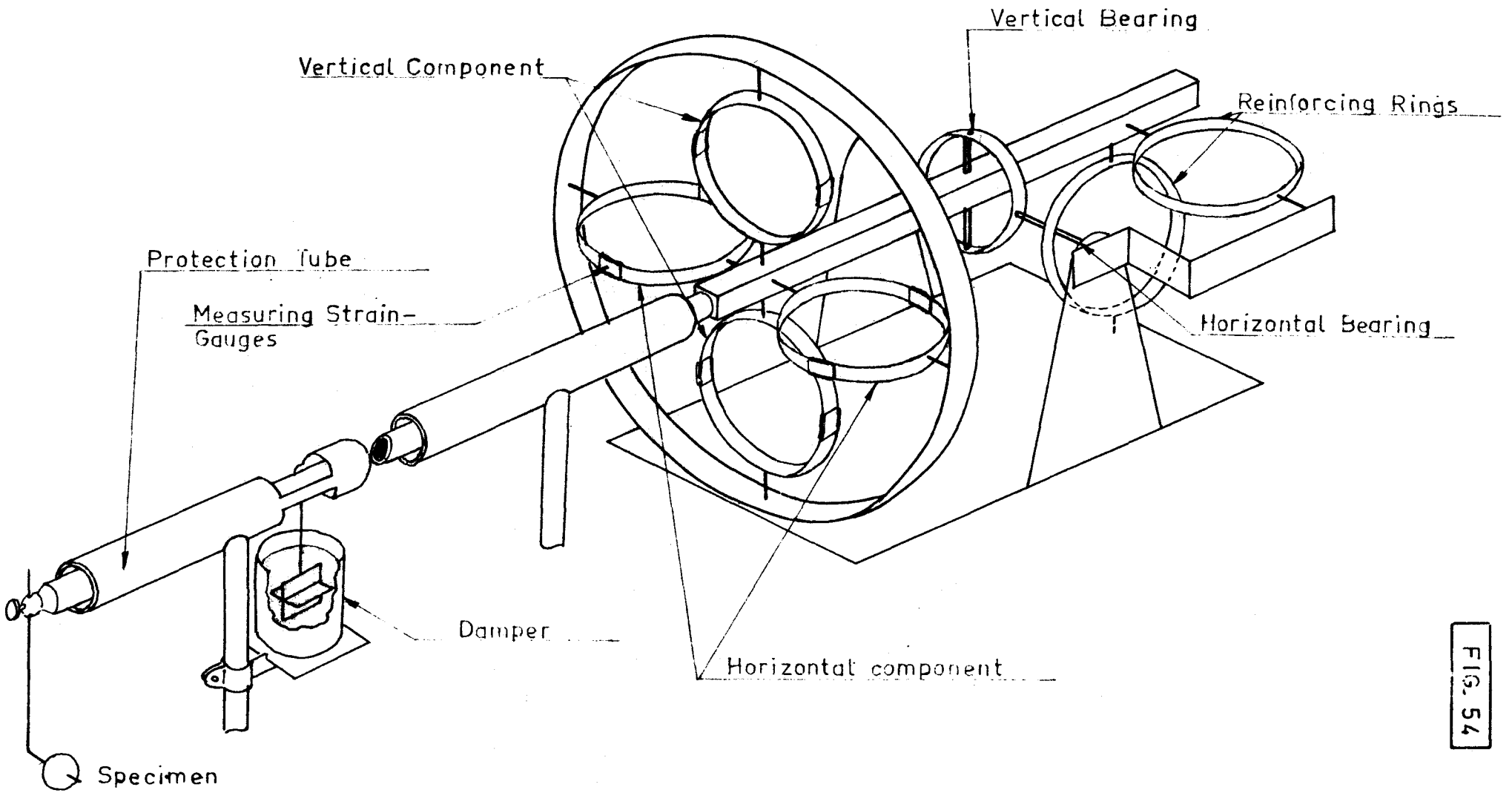

FIG. 54

FIG. 55

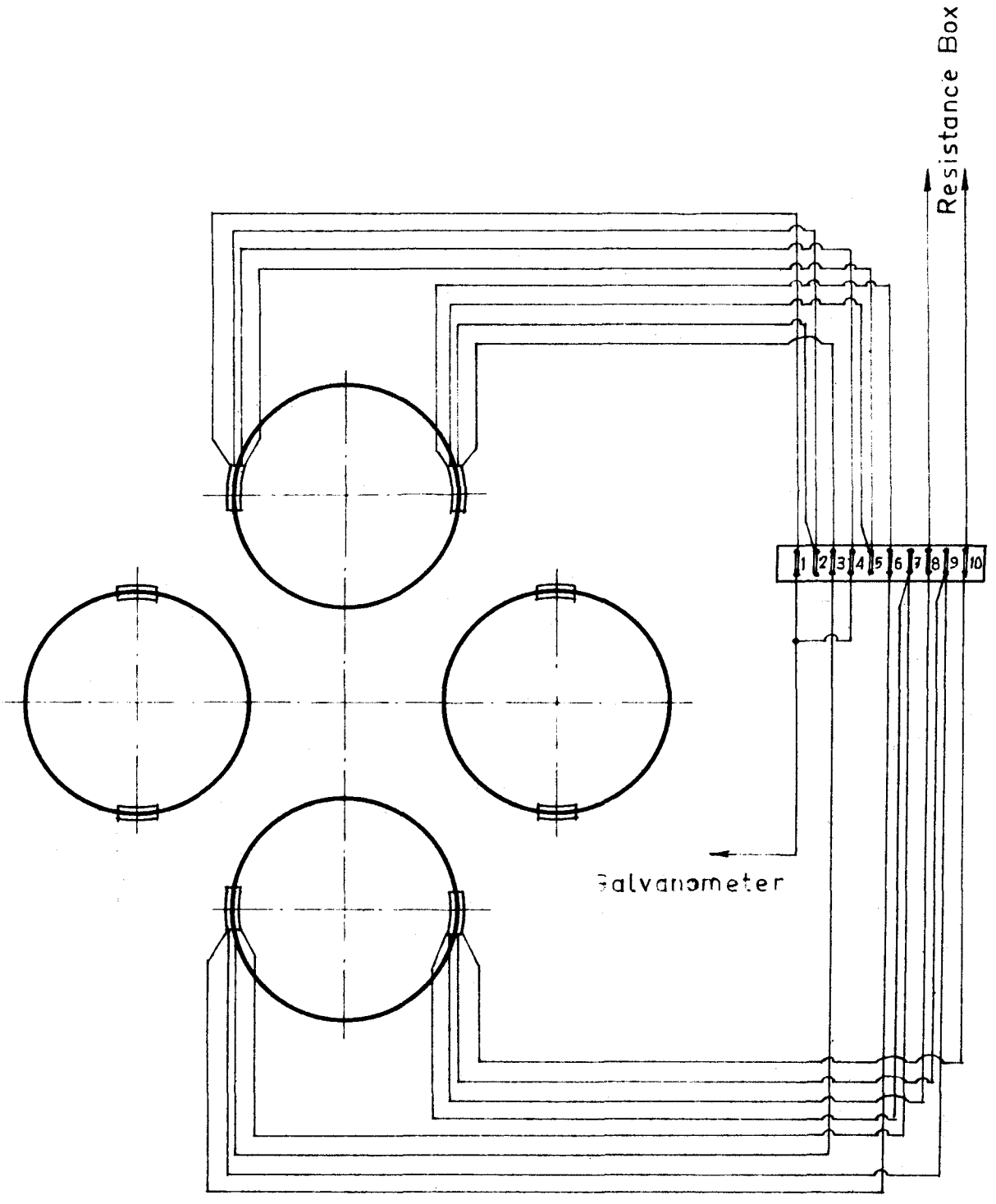

ELECTRICAL CIRCUITS

FIG. 56

FIREBRAND RADIUS AND DENSITY AS A FUNCTION OF TIME
EXPERIMENTAL AND ANALITYCAL RESULTS

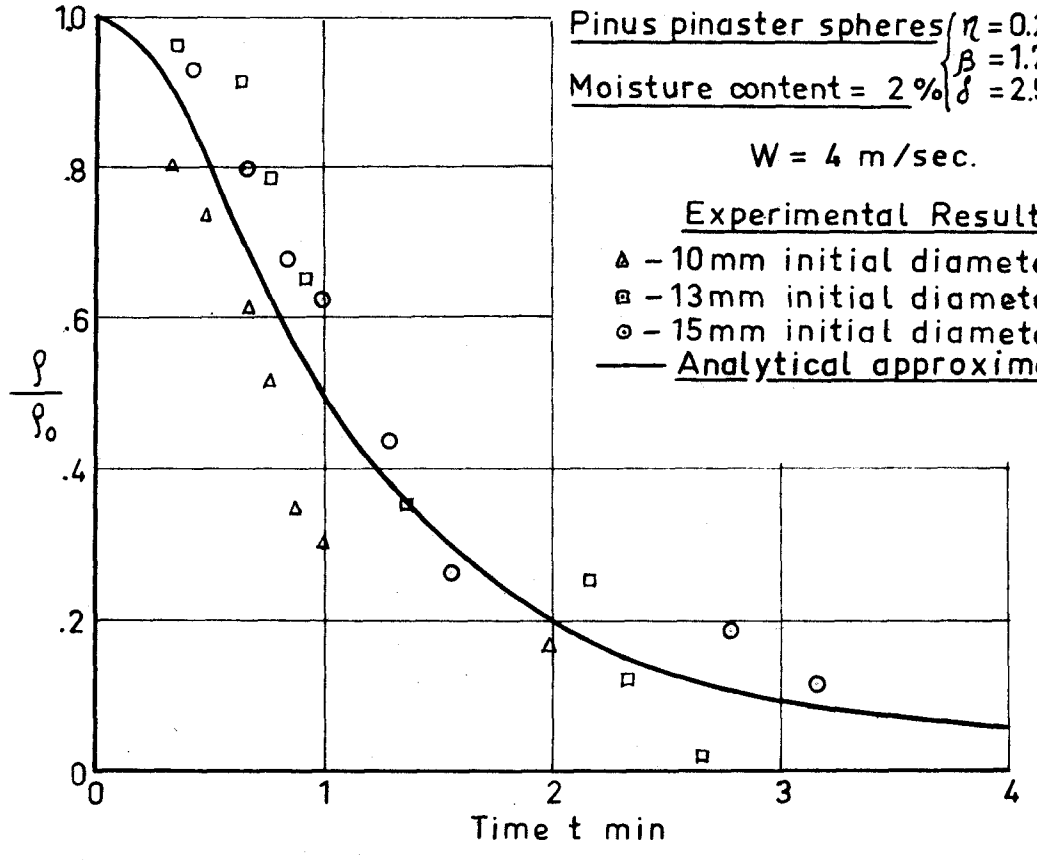

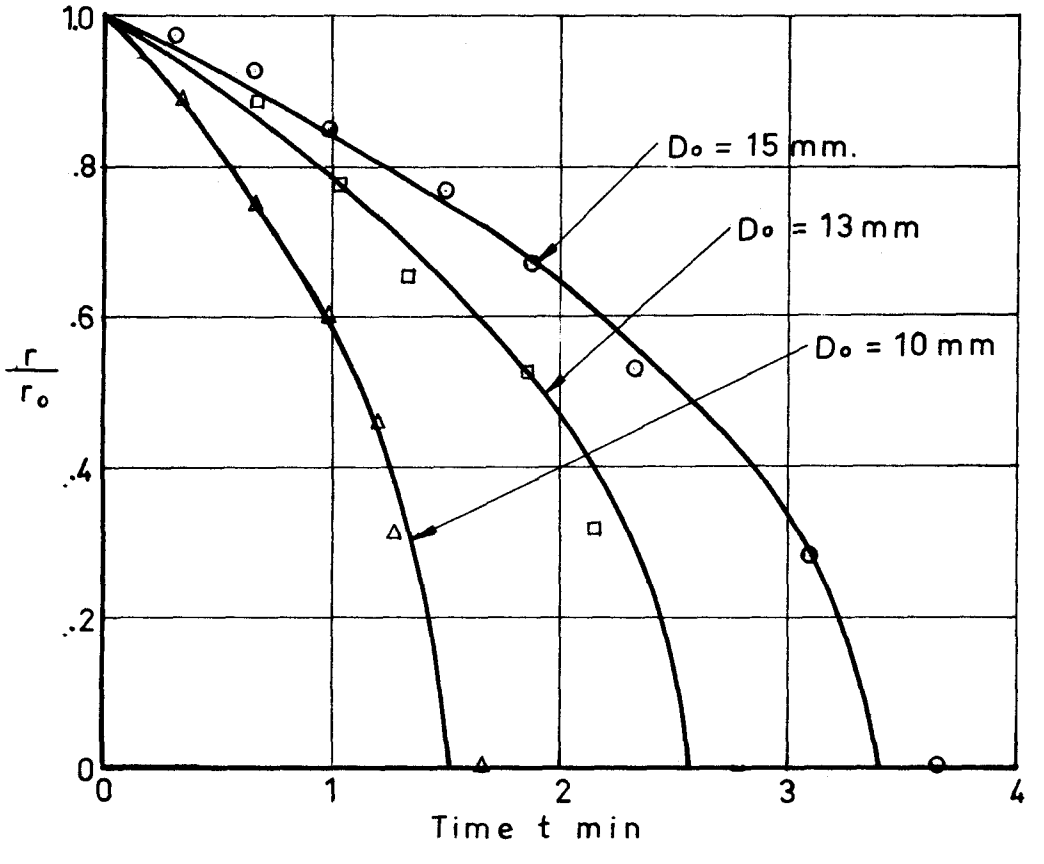

FIG. 57

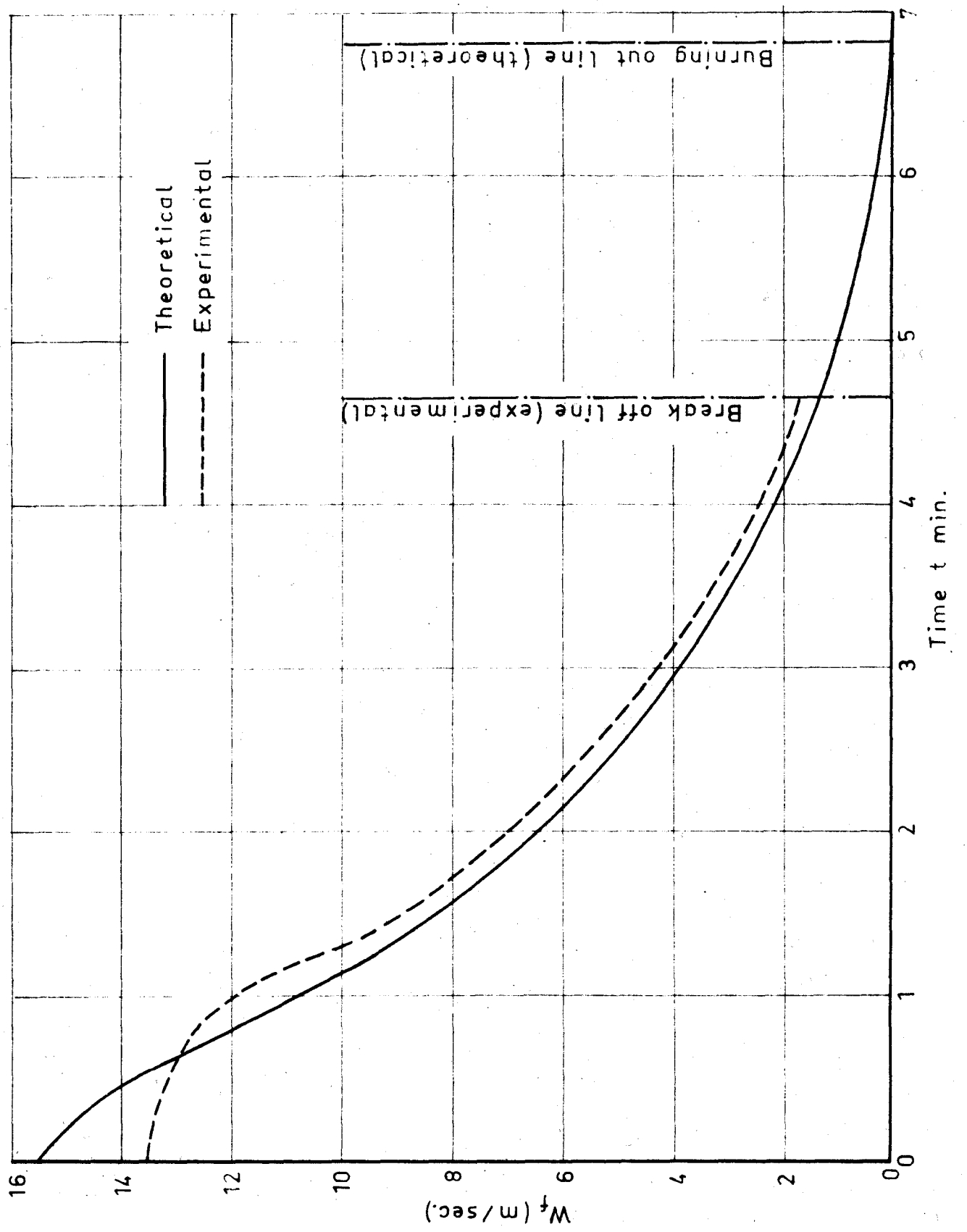
Theoretical
Experimental
Breek off line (experimental)
Burning out line (theoretical)
W_f (m/sec.)
Time t min.
0
2
4
6
8
10
12
14
16
1
3
5
7

FIG. 58

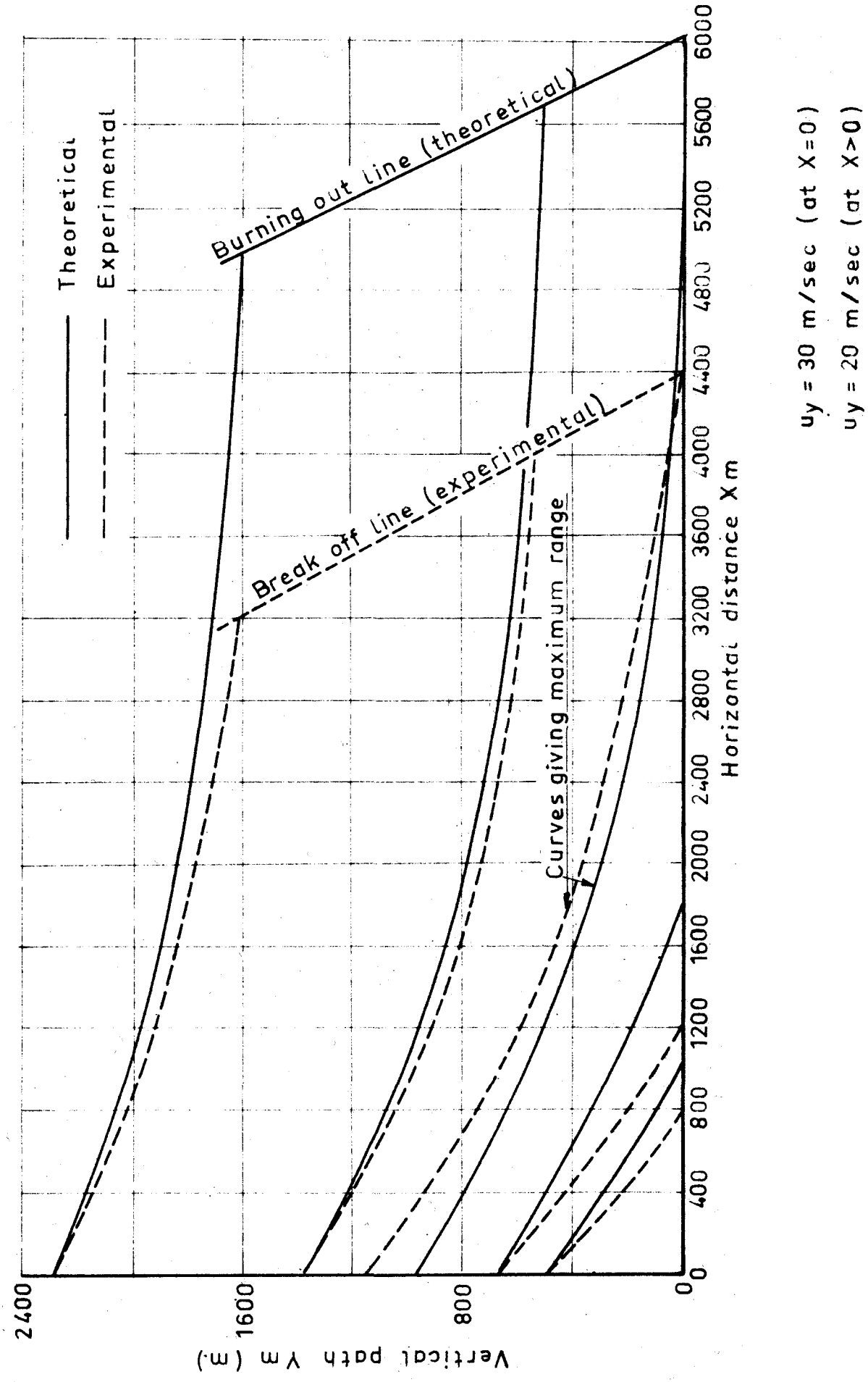
Theoretical
Experimental
Burning out line (theoretical)
Break off line (experimental)
Curves giving maximum range
Vertical path Y m (m)
Horizontal distance X m
2400
1600
800
0
0
400
800
1200
1600
2000
2400
2800
3200
3600
4000
4400
4800
5200
5600
6000
uy = 30 m/sec (at X=0)
uy = 20 m/sec (at X>0)